2022

Nitrite and insulin lower the oxygen cost of ATP synthesis in skeletal muscle cells by pleiotropic stimulation of glycolysis

Donnell, Rosie

UNIVERSITY OF PLYMOUTH

NITRITE AND INSULIN LOWER THE OXYGEN COST OF ATP SYNTHESIS IN SKELETAL MUSCLE CELLS BY PLEIOTROPIC STIMULATION OF GLYCOLYSIS

By

Rosie Donnell

A thesis submitted to the University of Plymouth
in partial fulfilment for the degree of

DOCTOR OF PHILOSOPHY

School of Biomedical Sciences

February 2022

2

Acknowledgements

I would first and foremost like to thank my Director of Studies, Dr Charles Affourtit, without whom, this PhD thesis would not have been possible. I would particularly like to thank him for his invaluable guidance and expertise throughout the formulation of this research, and for allowing me to complete the research in the first place. Finally, I would like to thank him for always having the time to discuss my ideas and the mistakes I may have made during our weekly lab meetings, which always kept me on track. My gratitude also goes to the University of Plymouth, who funded this research.

I would also like to thank the rest of my supervisory team, Professors Paul Winyard and Andrew Jones, who were always available to help and to discuss ideas with me. A special thank you goes to the other members of the Affourtit laboratory, Mr Anthony Wynne and Dr Jane Carré, for their support, advice and friendship. I would like to thank Mat Upton's research group, particularly Matt Koch, for making time for coffee breaks and keeping my head level in my times of despair. My gratitude goes to all of the other PhD students and staff in the JBB and DRF, and I'd particularly like to thank Dr Paul Waines, for his methodological help and friendship.

Finally, this research would not have been possible without the love and support I received from my friends and family. To my Nan, who is my eternal cheerleader and always cared how my cells were and if they were still alive. My Granddad, who could calm me down with a few simple words. My sister, Alice, who listened and pretended to understand me explain scientific "stuff". And finally, to Chris, who did all of the above but had to live with me throughout. I could not have completed this research without you.

Author's Declaration

At no time during the registration for the degree of Doctor of Philosophy has the author been registered for any other University award without prior agreement of the Doctoral College Quality Sub-Committee.

Work submitted for this research degree at the University of Plymouth has not formed part of any other degree either at the University of Plymouth or at another establishment.

This study was financed with the aid of a studentship from the University of Plymouth.

A programme of advanced study was undertaken, which included Postgraduate Research Skills & Methods (BIO5151).

The following external institutions were visited for consultation purposes: University of Exeter

Word count of main body of thesis: **31,702**

Signed: Rosie Donnell

Date: 19/02/2022

Abstract

Dietary nitrate lowers the oxygen cost of submaximal exercise, but precise mechanistic insight into how this occurs is lacking. Research suggests that dietary nitrate may render oxidative ATP synthesis more efficient, but evidence is inconclusive at present. This thesis aimed to establish how nitrite (a reduced form of nitrate) affects the bioenergetics of cultured skeletal muscle cells. Comparison between the acute effects of nitrite and insulin, a hormonal regulator of muscle function that increases mitochondrial efficiency, was explored to assess possible mechanistic overlap. Calculation of real-time intracellular ATP synthesis rates from simultaneous oxygen consumption and medium acidification measurements revealed the effects of sodium nitrite and insulin on intact rat (L6) myoblasts and myotubes. These extracellular flux data were also used to determine how mitochondrial and glycolytic ATP supply is used to fuel ATP-demanding processes. The data presented in this thesis revealed that both nitrite and insulin acutely stimulate glycolytic ATP synthesis. This stimulation occurs without significant mitochondrial ATP supply changes, thus increasing the glycolytic index of myocytes. Consequently, nitrite and insulin lower the oxygen cost of cellular ATP supply. Notably, insulin lowers oxygen consumption linked to mitochondrial proton leak, thus increasing mitochondrial efficiency. Nitrite does not improve coupling efficiency in myoblasts or myotubes. Further investigations revealed that stimulation of glycolytic ATP supply is not secondary to increased glucose availability. In myotubes, glycolytic stimulation persists in the presence of a mitochondrial uncoupler, suggesting that glycolysis is increased directly. In myoblasts, stimulation is annulled by uncoupler, suggesting that glycolysis increases indirectly, via increased ATP consumption. The molecular targets of nitrite and insulin remain unclear, but the data exclude stimulation

of protein synthesis. Together, the data demonstrate that nitrite and insulin lower the oxygen cost of ATP synthesis in skeletal muscle cells by pleiotropic stimulation of glycolysis. The data inform the ongoing debate regarding the mechanism by which dietary nitrate lowers the oxygen cost of exercise, suggesting a push toward a more glycolytic phenotype. Such mechanistic insight is crucial for achieving the full translational potential of dietary nitrate.

Table of contents

List of abbreviations

BAM15: (2-fluorophenyl){6-[(2-fluorophenyl)amino](1,2,5-oxadiazolo[3,4-e]pyrazin-5-yl)}amine

2DG: 2-Deoxy-D-glucose

ATP/O_2 ratio: Amount of ATP generated per oxygen atom consumed

BSA: Bovine serum albumin

FCCP: Carbonyl cyanide p-trifluoromethoxyphenylhydrazone

DMSO: Dimethyl sulfoxide

DMEM: Dulbecco's Modified Eagle Medium

DPSB: Dulbecco's modified phosphate-buffered saline

ECAR: Extracellular acidification rates

FBS: Foetal bovine serum

GLUT4: Glucose transporter 4

KRPH: Krebs-Ringer-Phosphate-HEPES

ANOVA: One-way analysis of variance

OCR: Oxygen consumption rates

NADH: Reduced nicotinamide adenine dinucleotide

SERCA: Sarco-endoplasmic reticulum $Ca2^+$ ATPase

$NaNO_2$: Sodium nitrite

TCA: Tricarboxylic acid

List of Figures

1 Literature review

1.1 Introduction

The function of skeletal muscle, which accounts for 40%–45% of lean body mass (Kim *et al.*, 2016), has been studied extensively. As the largest insulin-sensitive tissue within the body, skeletal muscle is the primary site of insulin-stimulated glucose uptake and accounts for 70-90% of glucose disposal (DeFronzo *et al.*, 1981; Baron *et al.*, 1988). Thus, it is key to glucose homeostasis. Skeletal muscle is crucial to basal energy metabolism and heat production, thus maintaining body temperature homeostasis (Periasamy *et al.*, 2017). Furthermore, it converts chemical energy, in the form of adenosine triphosphate (ATP), to mechanical energy that is used to power force and movement, and to maintain posture (Barclay, 2017). Skeletal muscle is a highly adaptive tissue that responds to physical exercise by increasing muscle mass and quality, leading to improved health (Minetto *et al.*, 2019). Optimising muscle mass and function, through exercise and nutrition, is essential to several populations, such as athletes, whereby increased capacity for exercise and increased exercise performance leads to a competitive edge. Muscle dysfunction is associated with many disease states, such as chronic obstructive pulmonary disease (Mador *et al.*, 2001), cancer cachexia (Penna *et al.*, 2019), diabetes (Perry *et al.*, 2016), heart failure (Keller-Ross *et al.*, 2019), and ageing (Nair, 2005). Thus, strategies for optimal improvements in muscle mass and function, in both clinical and athletic populations, are of great interest.

Insulin, which is released from pancreatic beta cells in response to increased blood glucose (Rutter *et al.*, 2015), is a signalling hormone that stimulates glucose uptake into tissues such as skeletal muscle (Ho, 2011; Rowland *et al.*, 2011; Richter *et al.*, 2013). As well as restoring blood glucose levels to the normal homeostatic range,

insulin also stimulates several anabolic processes that consume ATP. Insulin increases mitochondrial biogenesis (Cheng *et al.*, 2010), protein synthesis (Boirie *et al.*, 2001; Stump *et al.*, 2003; Robinson *et al.*, 2014), and glycogen synthesis (Gaster *et al.*, 2004). Insulin thus stimulates cellular energy demand, which is fulfilled in skeletal muscle by increasing the rate of ATP supply (the synthesis of ATP) (Affourtit, 2016). Indeed, studies have shown that insulin significantly increases the rate of ATP production (Stump *et al.*, 2003; Petersen *et al.*, 2005; Szendroedi *et al.*, 2007) and the activity of cytochrome *c* oxidase and citrate synthase (Stump *et al.*, 2003), which are enzymes involved in oxidative phosphorylation and tricarboxylic acid (TCA) cycle turnover. Finally, insulin also increases the cellular respiratory control ratio and coupling efficiency (see Methods), by decreasing proton leak-linked respiration (Nisr *et al.*, 2014). Thus, insulin plays a diverse role in skeletal muscle energy metabolism.

Nitric oxide is a potent signalling molecule involved in many biological functions within the body (Moncada *et al.*, 2006; Tripathi *et al.*, 2007). In humans, nitric oxide can be produced via two pathways. The first is the endogenous canonical pathway, whereby nitric oxide synthases oxidise L-arginine to form L-citrulline (Moncada *et al.*, 1993). The second is via an oxygen-independent pathway, involving the reduction of nitrate to nitrite and subsequently nitric oxide (Lundberg *et al.*, 2008). Nitrate and nitrite have long been thought of as inert. However, recent evidence suggests that the consumption of nitrate, in the form of nitrate-rich beetroot juice or nitrate salts dissolved in aqueous solutions at daily ingested amounts between 5.1 and 19.5 mmol (Pawlak-Chaouch *et al.*, 2016), has a positive impact on human skeletal muscle function. One of the benefits of consuming nitrate is the lowering of oxygen uptake during submaximal workloads (Larsen *et al.*, 2007; Bailey *et al.*, 2009; Lansley, Winyard, Fulford, *et al.*, 2011). This discovery challenged our understanding of human

exercise, as oxygen consumption was previously believed to be fixed at a given work rate and unresponsive to intervention (Poole *et al*., 1997). Exercise tolerance (Breese *et al.*, 2013; Bailey *et al.*, 2015), time to exhaustion (Bailey *et al.*, 2010; Lansley, Winyard, Fulford, *et al.*, 2011) and exercise performance (Lansley, Winyard, Bailey, *et al.*, 2011; Murphy *et al.*, 2012) can also improve following supplementation with dietary nitrate. However, the positive effects of dietary nitrate on exercise are only apparent in some populations and under certain physiological conditions (Bescós *et al.*, 2012; Peacock *et al.*, 2012; Carriker *et al.*, 2016; Pawlak-Chaouch *et al.*, 2016), which highlights the need to understand the mechanism by which dietary nitrate impacts exercise.

Potential causes for the exercise improvements seen in response to dietary nitrate supplementation include a decreased energetic cost of cellular ATP consuming processes (Bailey *et al.*, 2010) and improved efficiency of mitochondrial ATP synthesis (Larsen *et al.*, 2011) in skeletal muscle. As well as this, nitrogen species also increase mitochondrial biogenesis (Mo *et al.*, 2012; Vaughan *et al.*, 2016), and influence parameters related to glucose homeostasis in rodent models. Nitrogen species have been found to increase insulin secretion (Nyström *et al.*, 2012; Gheibi *et al.*, 2017) and glucose transporter 4 (GLUT4) expression (Lira *et al.*, 2007; Vaughan *et al.*, 2016) and translocation (Jiang *et al.*, 2014). Dietary nitrate supplementation has thus been associated with diverse cellular effects, which further increases interest in the potential therapeutic and exercise focused uses of this common food component.

While the effects of insulin on cellular energy metabolism are relatively well known and understood, comparatively little conclusive knowledge has been gained regarding the effects of nitrogen species on myocyte bioenergetics. However, there is considerable overlap between the effects driven by nitrogen species and insulin on

skeletal muscle function. Thus, there may be overlap between the mechanisms by which insulin and dietary nitrate affect skeletal muscle function. Dietary nitrate benefits on parameters related to exercise likely involve improved skeletal muscle energy metabolism, but precise mechanistic insight on this bioenergetic improvement is lacking at present. Therefore, before nitrogen species can be safely and rationally implemented as ergogenic or therapeutic aids, and to understand whether nitrogen species and insulin act similarly to induce benefit in skeletal muscle, it is fundamental to ascertain the actions of nitrogen species on myocyte bioenergetics. Once this insight is obtained, it may become apparent why some populations are non-responders to observed exercise benefits exerted by nitrogen species. This introductory chapter provides an overview of the literature that reports dietary nitrate and insulin effects related to skeletal muscle energy metabolism.

1.2 Skeletal muscle energy metabolism

Cells require energy to stay alive and to carry out their functions. ATP is the cells' main energy currency: its hydrolysis to adenosine diphosphate (ADP) and inorganic phosphate (Pi) liberates free energy that can be used to drive energy-requiring processes. ADP and Pi are then used to resynthesize ATP by both substrate-level and oxidative phosphorylation (Berg *et al.*, 2002). Energy metabolism can be considered the interaction between ATP demand and ATP supply, via a common intermediate, the cytosolic phosphorylation potential (or ATP/ADP ratio). Cellular ATP levels are kept very high, and, therefore, the ATP/ADP ratio is high. Thus, when cells hydrolyse ATP to form ADP and Pi, the reaction moves spontaneously because the ratio is kept far away from thermodynamic equilibrium. When hydrolysis of ATP occurs, energy is liberated, which can be used by the cell to drive various reactions. In skeletal muscle,

the supply of ATP is usually dictated by the demand for ATP. Thus, when demand for ATP is high, the ATP/ADP ratio drops, and the cell responds by making more ATP (Berg *et al.*, 2002). Skeletal muscle can utilise various nutrients to make ATP, such as fats and glucose. When energy metabolism is driven by glucose, glycolysis and mitochondrial respiration both contribute to ATP supply.

Glycolysis is a metabolic pathway that occurs within the cytosol of the cell and allows the breakdown of glucose to pyruvate, resulting in the liberation of energy that is captured as ATP (Feher, 2017) (Figure 1.1). This type of ATP production does not require oxygen. When glucose enters the cell, it is rapidly phosphorylated to glucose-6-phosphate by hexokinase, requiring two ATP. Following this, the glucose-6-phosphate molecule undergoes a series of enzymatic reactions, resulting in the production of two reduced nicotinamide adenine dinucleotide (NADH), four ATP and two pyruvate molecules. The net production of ATP from glycolysis is two ATP, as the initial step costs two ATP (Feher, 2017). The pyruvate generated from glycolysis can then be reduced to lactate by lactate dehydrogenase (LDH), resulting in the efflux of two lactate anions and two protons from the cell for every glucose molecule broken down (Divakaruni *et al.*, 2014). When pyruvate is reduced to lactate, NADH is oxidised in the LDH reaction, to regenerate the NAD^+ required for the reaction of glyceraldehyde-3-phosphate to 1,3-diphosphoglycerate in glycolysis (Feher, 2017). Glycolytic NADH can also be transferred into the mitochondria by the glycerol-3-phosphate and malate-aspartate shuttles for use in oxidative phosphorylation (Feher, 2017).

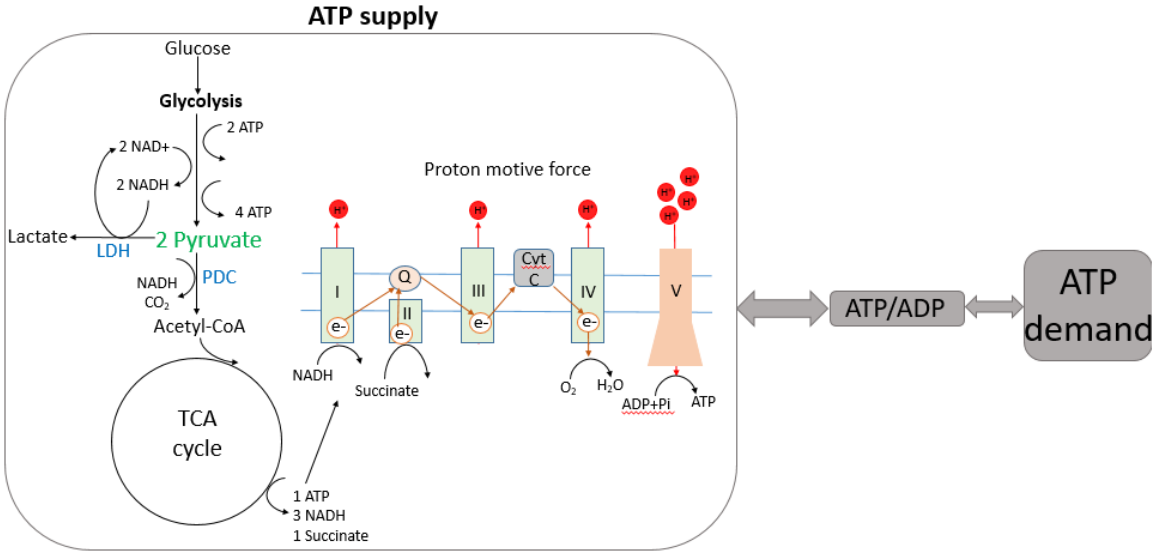

Figure 1.1 – ATP supply during glucose catabolism.
When energy metabolism is driven by glucose, glycolysis and mitochondrial respiration both contribute to ATP supply. Black arrows show the sequence of events and the reactants and products of pathways. Orange arrows show the direction of electron (e-) transfer, and red arrows show the movement of protons (red circles with H^+). The inner mitochondrial membrane is shown as the parallel blue lines, with the mitochondrial matrix below and the intermembrane space above the blue parallel lines. LDH = lactate dehydrogenase, PDC = pyruvate dehydrogenase complex, TCA = tricarboxylic acid cycle, I, II, III, IV = the electron transfer chain, Q = ubiquinone, Cyt C = cytochrome c, V = the ATP synthase.

When pyruvate enters into the mitochondria, it is used to form acetyl-CoA, through oxidative decarboxylation driven by the pyruvate dehydrogenase complex (PDC). This reaction also leads to the production of CO_2 and NADH (Mookerjee *et al.*, 2017) (Figure 1.1). Each acetyl-CoA fuels one TCA cycle turnover, which does not require oxygen, but produces one ATP, and three NADH and one succinate by removing electrons from the acetyl-CoA molecule (Berg *et al.*, 2002). The TCA cycle thus generates the reducing power that fuels oxidative phosphorylation (Figure 1.1).

Oxidative phosphorylation is a process by which the energy generated from burning nutrients is conserved as ATP. NADH and succinate deliver the electrons to the electron transfer chain (ETC), which is a series of protein complexes embedded within the inner mitochondrial membrane (Berg *et al.*, 2002). NADH donates 2 electrons to complex I, whereas succinate donates 2 electrons to complex II. The electrons that become available through oxidation are used to reduce ubiquinone to ubiquinol, which then passes the electrons to complex III. Following this, the electrons are passed on to cytochrome *c*, reducing it, causing it to become a substrate for cytochrome *c* oxidase (complex IV). The electrons are then passed to complex IV, where they are finally used to reduce oxygen to water (Figure 1.1). Mitochondrial electron transfer is a thermodynamically favourable process and an oxidative process, as it is associated with the consumption of oxygen (Berg *et al.*, 2002). These reactions liberate energy, which some complexes use to generate a proton-motive force. As electrons are passed, complexes I, III and IV translocate protons from the mitochondrial matrix, across the membrane and into the intermembrane space. This translocation creates a proton gradient, which is a potential source of energy. Protons then move back across the membrane through the ATP synthase (complex V), causing it to rotate, which catalyses ADP phosphorylation to ATP (Berg *et al.*, 2002).

The coupling between electron transfer and ATP synthesis is not fully efficient. One of the reasons for this is electron leak, which is the escape of electrons from the ETC complexes that can incompletely reduce oxygen, forming reactive oxygen species (Affourtit *et al.*, 2012). Electron leakage from particular sites of the ETC depends on the redox state of the electron donor. For example, an increased respiration rate due to increased substrate supply leads to a more reduced ETC and therefore higher rates of electron leak and reactive oxygen species production, whereas increased respiration rates driven by increased ATP demand leads to a more oxidised ETC, with lower electron leak and reactive oxygen species production (Brand, 2016). Another reason is proton leak, which occurs when protons that make up the proton-motive force move back across the inner mitochondrial membrane, in a fashion that bypasses the ATP synthase, thus lowering the efficiency of oxidative phosphorylation (Brand, 2005). Proton leak may exist to protect cells from oxidative damage resulting from reactive oxygen species generation, which is a by-product of oxidative phosphorylation, by relieving the system of a high proton-motive force (Brand, 2000). The proton-motive force is also used by mitochondrial carriers, such as the adenine nucleotide translocator carrier, to transport Pi and ADP into, and ATP out of the mitochondria (Mookerjee *et al.*, 2017). However, the adenine nucleotide translocator has also been found to contribute to approximately two-thirds of basal proton leak, independent of its function as a reactant exchanger (Brand *et al.*, 2005). Furthermore, proton leak can also be induced by uncoupling proteins (Divakaruni *et al.*, 2011). By preventing the transfer of electrons and dissipating the proton-motive force, electron and proton leak lower the amount of ATP generated by nutrient catabolism, thus lowering the coupling efficiency of oxidative phosphorylation. Therefore, compounds (such as nitrogen species and insulin) that may increase mitochondrial efficiency are of great interest.

Once synthesised, ATP can be hydrolysed to ADP and Pi, which liberates the energy required to drive various endergonic reactions (Berg *et al.*, 2002) (Figure 1.2). An example of an energy-requiring process within skeletal muscle that consumes large amounts of ATP is contraction, due to the need to fuel myosin ATPase and the sodium-potassium and calcium exchange across the cell membrane (Egan *et al.*, 2013). At times of vigorous contraction, such as during high-intensity exercise, skeletal muscle can increase its use of ATP around 300-fold from the resting state (Westerblad *et al.*, 2010). Other cellular processes, such as DNA, RNA and protein synthesis, and cytoskeletal movement, also consume large amounts of ATP (Buttgereit *et al.*, 1995; Nisr *et al.*, 2016; Mookerjee *et al.*, 2017) (Figure 1.2)

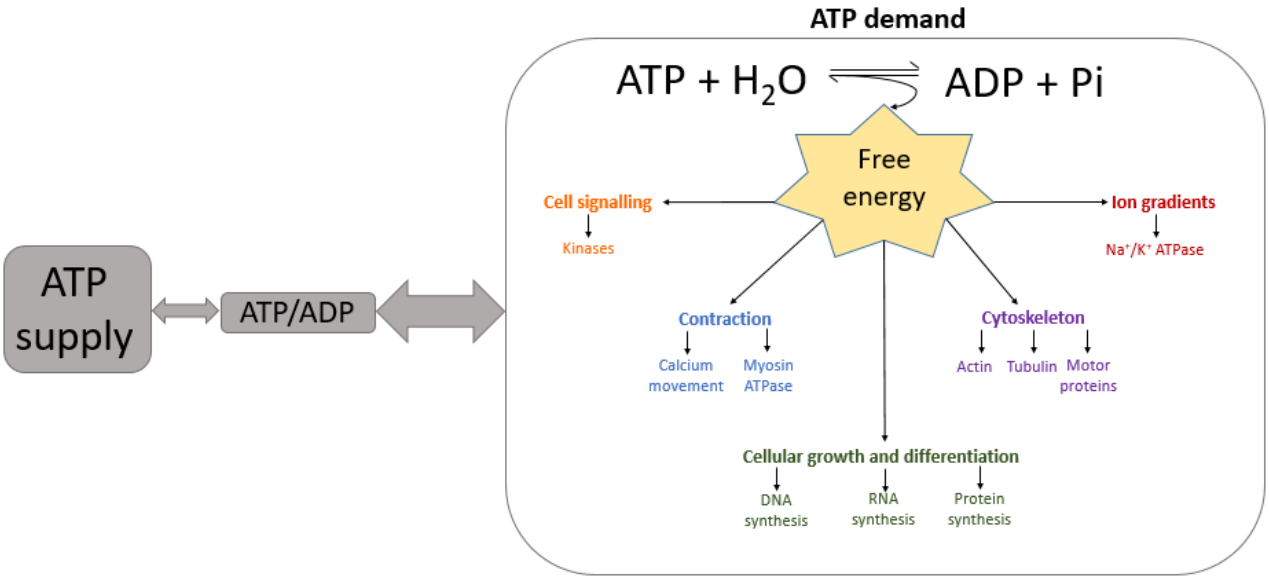

Figure 1.2 – ATP hydrolysis and cellular energy-requiring processes.
Energy metabolism is the communication between ATP demand and ATP supply, via the cytosolic phosphorylation potential (ATP/ADP ratio). In skeletal muscle, the supply of ATP is usually dictated by the demand for ATP. Hydrolysis of ATP results in the liberation of energy, which can be used by the cell to drive various reactions, such as contraction and cellular growth (Berg *et al.*, 2002).

In skeletal muscle, energy metabolism is primarily controlled by ATP demand, which has been likened to a market economy, whereby the flux of ATP is governed by the consumer and not the producer (Affourtit, 2016). This control structure is apparent when ATP-consuming processes are inhibited, which acutely causes decreased mitochondrial respiration linked to ATP synthesis (Buttgereit *et al.*, 1995; Nisr *et al.*, 2016; Mookerjee *et al.*, 2017). Arguably one of the most important parameters in skeletal muscle energy metabolism is the ATP/ADP ratio, or the phosphorylation potential. The cytosolic phosphorylation potential refers to the concentration ratio of free ATP and ADP within the cytosol, which describes the energy status of the cell or the ability of the cell to carry out work (Veech *et al.*, 1979). Within cells, there is an ATP/ADP ratio within the cytosol, which is kept high, and one within the mitochondria, which is kept low, due to the electrogenic exchange of ATP and ADP across the mitochondrial membrane (Heldt *et al.*, 1972). When hydrolysis of ATP occurs within the cytosol through the demand for ATP, the cytosolic ATP/ADP ratio drops, promoting ATP synthesis (Affourtit, 2016). Thus, the phosphorylation potential links ATP supply with ATP demand (Figure 1.2).

1.3 Skeletal muscle insulin sensitivity

Insulin is an anabolic peptide hormone that is made and released by pancreatic beta cells when the blood glucose level rises (Rutter *et al.*, 2015). Insulin provokes organ activity that brings the glucose level back to its homeostatic set point. Skeletal muscle is the primary site of insulin-stimulated glucose uptake and accounts for 70-90% of glucose uptake (DeFronzo *et al.*, 1981; Baron *et al.*, 1988). The signalling pathway leading to glucose uptake by cells has been extensively studied and reviewed (Ho, 2011; Rowland *et al.*, 2011; Richter *et al.*, 2013) and is summarized in Figure 1.3.

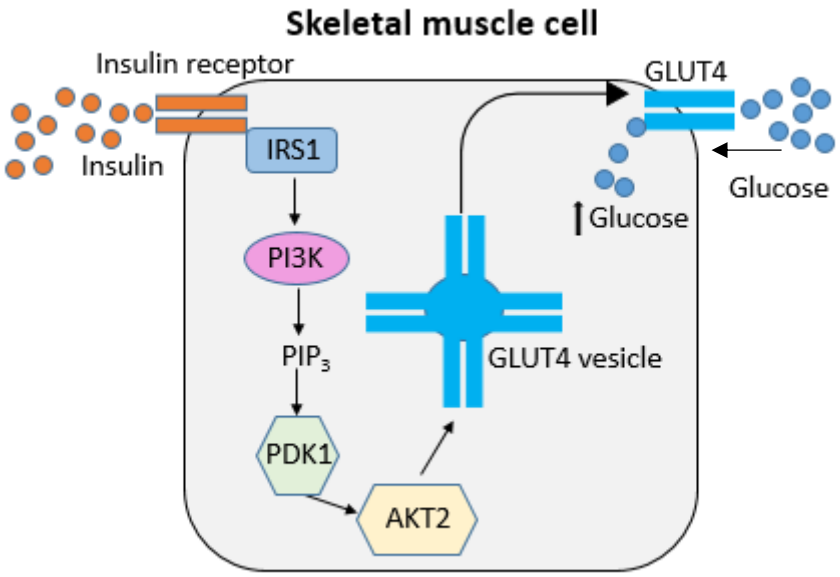

Figure 1.3 – insulin release and skeletal muscle signalling pathway.
Pancreatic beta cells produce and release insulin into the bloodstream (Rutter *et al.*, 2015). *Insulin then binds to the insulin receptor on skeletal muscle, causing transautophosphorylation of the intracellular tyrosine residues, which then act as docking sites for the insulin receptor substrate (IRS1). IRS1 is phosphorylated and recruits and activates phosphatidylinositol-3-kinase (PI3K) at the membrane, which catalyses the formation of phosphatidylinositol (3, 4, 5) triphosphate (PIP_3). PIP_3 formation leads to the activation of 3-phosphoinositide–dependent protein kinase 1 (PDK1) and protein kinase B (AKT2). Activation of this pathway ultimately results in the release of GLUT4 from intracellular vesicles and its translocation into the plasma membrane. Glucose then enters from the blood and into the muscle cell via facilitated diffusion through GLUT4* (Ho, 2011; Rowland *et al.*, 2011; Richter *et al.*, 2013).

As well as restoring blood glucose levels to the normal homeostatic range, activation of the insulin receptor leads to the activation of the protein kinase B and Ras-mitogen-activated protein kinase pathways, resulting in the stimulation of several anabolic processes within the cell (Affourtit, 2016). Insulin promotes cellular growth and differentiation (Li *et al.*, 2013) and mitochondrial biogenesis (Cheng *et al.*, 2010), which are processes that require protein synthesis. Insulin stimulates mitochondrial (Boirie *et al.*, 2001; Stump *et al.*, 2003; Robinson *et al.*, 2014), myofibrillar and sarcoplasmic protein synthesis (Robinson *et al.*, 2014). Protein synthesis represents a major ATP consuming process in many cell types (Buttgereit *et al.*, 1995; Nisr *et al.*, 2016) and accounts for 20-35% of energy expenditure in cultured myocytes (Nisr *et al.*, 2016; Mookerjee *et al.*, 2017). DNA and RNA synthesis are also required for protein synthesis and cellular growth and differentiation, which consume large amounts of ATP (Buttgereit *et al.*, 1995; Nisr *et al.*, 2016). DNA and RNA synthesis accounts for ~16% of oxidative ATP expenditure in cultured rat and human myocytes (Nisr *et al.*, 2016). Insulin also has an impact on small molecule movement within cells. When insulin binds to its receptor, it increases the activity of the sodium-potassium-ATPase by increasing the expression of the pump itself (Ho, 2011). The sodium-potassium-ATPase consumes ~20% of oxidative ATP supply in cultured L6 myocytes (Nisr *et al.*, 2016) and ~6% of total ATP expenditure in C2C12 myocytes (Mookerjee *et al.*, 2017).

Insulin drives glucose uptake by cells, which involves the exocytosis of GLUT4 from intracellular vesicles to the cellular membrane (Ho, 2011; Rowland *et al.*, 2011; Richter *et al.*, 2013) (Figure 1.3). The translocation of GLUT4 to the cell membrane involves the remodelling of actin filaments at the plasma membrane in adipocytes (Omata *et al.*, 2000) and skeletal muscle (Tsakiridis *et al.*, 1994). As well as utilising actin, GLUT4 storage vesicles are moved intracellularly via the motor proteins of

microtubules, kinesin and dynein, which aid in the exocytosis and endocytosis of GLUT4 at the membrane (Tunduguru *et al.*, 2017). Actin remodelling and the movement of vesicles via motor proteins are ATP-consuming processes (Stossel *et al.*, 2006; Kolomeisky, 2014). Cultured C2C12 myocytes dedicate 8% and 16% of their total energy expenditure to tubulin and actin dynamics, respectively (Mookerjee *et al.*, 2017). Furthermore, insulin also stimulates glycogen synthesis (Gaster *et al.*, 2004), which is a process that consumes ATP (Rahmatabady, 2013). As well as stimulating ATP-dependent processes, insulin also prevents protein degradation (Rooyackers *et al.*, 1997) in brain, liver and skeletal muscle cells (Fawcett *et al.*, 2001). However, while insulin inhibits some ATP consuming processes, overall, it has a stimulatory effect on ATP demand (Affourtit, 2016).

Studies have shown that insulin significantly increases the rate of ATP production (Stump *et al.*, 2003; Petersen *et al.*, 2005; Szendroedi *et al.*, 2007), which may occur in response to the stimulatory effect of insulin on energy demand. Studies using ^{31}P magnetic resonance spectroscopy have shown that insulin significantly increases the rate of ATP production in the muscle of healthy individuals (Petersen *et al.*, 2005; Szendroedi *et al.*, 2007). However, whether this increase is due to stimulation of glycolytic or oxidative ATP production is not clear, as ^{31}P magnetic resonance spectroscopy has been found to reveal very little about mitochondrial function and to overestimate oxidative ATP synthesis in resting muscle, due to a glycolytically mediated Pi↔ATP exchange reaction (Kemp *et al.*, 2012). More specifically, insulin stimulates ATP synthesis in mitochondria isolated from healthy human muscle (Stump *et al.*, 2003). This stimulation of oxidative ATP production was attributed to the increased oxidative capacity of mitochondria, through increased mitochondrial protein

synthesis and increases in citrate synthase and cytochrome *c* oxidase activity (Stump *et al.*, 2003).

Indeed, insulin is shown to increase glucose oxidation (Gaster *et al.*, 2004) and to increase basal and maximum respiration in C2C12 myotubes (Yang *et al.*, 2012), supporting the idea that insulin increases mitochondrial capacity (Stump *et al.*, 2003). However, insulin also impacts oxidative metabolism by lowering proton leak-linked respiration, in the absence of increased capacity of oxidative phosphorylation (Nisr *et al.*, 2014). This acute insulin effect increases both the cellular respiratory control ratio (i.e., the ratio between the uncoupled and oligomycin-inhibited respiration) and coupling efficiency of oxidative phosphorylation in cultured rat and human myocytes (Nisr *et al.*, 2014). Increased coupling efficiency occurred without effect on maximum respiration in myocytes subjected to insulin (Nisr *et al.*, 2014). However, differences in insulin exposure may account for the differences in results concerning mitochondrial capacity (20 minutes (Nisr *et al.*, 2014) versus 48 hours (Yang *et al.*, 2012)). Collectively, these results indicate that insulin may improve mitochondrial function and increase oxidative ATP supply by improving both the capacity for, and efficiency of, such production.

In addition to increasing mitochondrial protein synthesis (Stump *et al.*, 2003), insulin increases the expression of the glycolytic enzymes phosphofructokinase and pyruvate kinase (Berg *et al.*, 2002). Thus, insulin may increase glycolytic ATP supply by directly influencing the expression and activity of enzymes involved in this pathway. Indeed, as well as stimulating basal respiration, insulin also significantly increases medium acidification in C2C12 myotubes (Yang *et al.*, 2012), suggesting that it raises both glycolytic and oxidative ATP supply. In contrast, when the bioenergetic behaviour of L6 myocytes exposed to insulin is measured in a buffer lacking a metabolic fuel,

injection of 2mM glucose instantly stimulates acidification of the extracellular medium but leaves oxygen consumption unaffected (Nisr *et al.*, 2014). These results indicate that insulin may increase glycolytic ATP supply and the production of pyruvate that is subsequently reduced to lactate, without increasing oxidative ATP supply. Taken together, insulin has a diverse array of effects on skeletal muscle energy metabolism, by provoking both ATP demand and ATP supply.

1.4 Nitric oxide, nitrate and nitrite effects on skeletal muscle

1.4.1 Background

Nitric oxide is a signalling molecule involved in many physiological processes, such as vasodilation (Moncada *et al.*, 2006) and immunological defence (Tripathi *et al.*, 2007). Nitric oxide is also believed to be responsible for protective effects against cardiovascular disease (Omar *et al.*, 2014) and the metabolic syndrome (Carlström *et al.*, 2010). Production of nitric oxide can occur endogenously during the oxygen-dependent oxidation of L-arginine to form L-citrulline by nitric oxide synthases (Moncada *et al.*, 1993). Nitric oxide can then be oxidised relatively slowly by a multicopper oxidase within the plasma, named ceruloplasmin and by cytochrome *c* oxidase to form nitrite, and relatively quickly by myoglobin and haemoglobin to form nitrate (Shiav, 2013). Recently, an alternative, oxygen-independent pathway for the generation of nitric oxide has been discovered, whereby dietary nitrate is reduced, forming nitrite and subsequently nitric oxide, under low pH and hypoxic conditions (Lundberg *et al.*, 2008).

Nitrate can be obtained via the diet and is abundant in vegetables such as spinach and beetroot (Lidder *et al.*, 2013). Once consumed and absorbed into the blood, ~25% of circulating nitrate is transported into the salivary glands by sialin, the sialic

acid/H^+ and $2NO_3^-/H^+$ cotransporter located in the plasma membrane of salivary gland cells (Qin *et al.*, 2012). Nitrate is then secreted into the saliva (Qin *et al.*, 2012). Anaerobic bacteria expressing nitrate reductases, such as *Veillonella* (Hyde *et al.*, 2014), located on the dorsal surface of the tongue, then reduce nitrate to nitrite (Doel *et al.*, 2005). Pathways involving deoxyhaemoglobin, xanthine oxidase, deoxymyoglobin and mitochondrial enzymes are implicated in reducing nitrite to nitric oxide (Govoni *et al.*, 2008). Nitrate and nitrite have previously been thought of as inert end-products of nitric oxide metabolism. As precursors to N-nitroso compounds, which are potent carcinogens, these anions have been portrayed as compounds to be avoided. However, evidence to suggest that nitrate and nitrite cause cancers is inconclusive and depends on their source, such as whether they come from plant or meat, as plants contain components such as vitamin E and phenolic compounds, which may protect against cancer development (Lidder *et al.*, 2013). Furthermore, recent studies have shown that nitrate and nitrite consumption positively impacts human skeletal muscle function.

1.4.2 Exercise-related benefits of nitrate supplementation

A wealth of recent evidence has shown that dietary nitrate consumption has many physiological benefits, particularly relating to exercise. Several recent reviews cover the physiological effects of nitrogen species on exercise (Jones, 2014; Jones *et al.*, 2016; Domínguez, Cuenca, *et al.*, 2017; Domínguez *et al.*, 2018). Nitrate supplementation lowers the oxygen cost of submaximal exercise by decreasing the respiratory activity required to drive skeletal muscle work at a set rate (Larsen *et al.*, 2007; Lansley, Winyard, Fulford, *et al.*, 2011). However, the lowered oxygen cost of submaximal exercise in response to nitrate is not universal, as individuals with chronic illnesses (Pawlak-Chaouch *et al.*, 2016) and the highly aerobically fit (Carriker *et al.*, 2016) appear to be non-responders to this phenomenon.

Supplementation with nitrate has other benefits on exercise that may not be related to decreases in oxygen consumption. The measurement of exercise tolerance, usually through time to exhaustion protocols, assesses an individual's capacity to complete exercise, while completing a predefined set of exercises in a faster time indicates improved exercise performance (Jones, 2014). Nitrate supplementation has been shown to increase exercise tolerance by ~22% (Breese *et al.*, 2013; Bailey *et al.*, 2015) and improve power output and performance (Lansley, Winyard, Bailey, *et al.*, 2011; Murphy *et al.*, 2012). Again, these effects are not universal, as elite and endurance athletes show no such improvement in exercise performance in response to nitrate supplementation (Bescós *et al.*, 2012; Peacock *et al.*, 2012).

Several factors may explain the differences in responsiveness to the exercise benefits exerted by nitrate supplementation between and within populations, such as genetics, muscle oxygenation and the muscle fibre-type composition of the population being studied. It has been hypothesised that nitrate may specifically target type II muscle fibres (Jones *et al.*, 2016). Furthermore, inconsistent results may also arise due to differences in supplementation protocols between studies. For example, 4 days supplementation with 70ml of a drink containing 6.2 mmol nitrate was given in a study where no effect was found on oxygen uptake during submaximal exercise (Carriker *et al.*, 2016), whereas 500ml of a drink containing 6.2 mmol nitrate was given over 6 days in a study where a lowering of oxygen uptake was observed (Lansley, Winyard, Fulford, *et al.*, 2011). However, it remains to be established why nitrate supplementation does not benefit exercise universally.

Nitric oxide formation is likely responsible for the protective effects of nitrogen species on health (Tripathi *et al.*, 2007; Omar *et al.*, 2014). However, the nitrogen species responsible for driving the positive effects of dietary nitrate on skeletal muscle

and exercise discussed above remains to be convincingly demonstrated. Many studies suggest that the reduction of nitrite to nitric oxide is responsible for the positive effects exerted by nitrate on exercise, such as lowering oxygen uptake (Larsen *et al.*, 2007) and improving exercise performance (Thompson *et al.*, 2016). Within these human studies, it is common to measure nitrate and nitrite levels within the blood, which is suggested to be a marker of nitric oxide bioavailability (Lundberg *et al.*, 2008). Nitrite has also been suggested to be a reservoir for nitric oxide during periods of hypoxia (Lundberg *et al.*, 2008). The measurement of nitric oxide itself in human systems is relatively difficult because nitric oxide has a very short half-life, is present in small concentrations and is highly reactive (Archer, 1993). Nevertheless, following nitrate supplementation, the concentrations of nitrate and nitrite rise in the blood compared to controls (Larsen *et al.*, 2007; Bailey *et al.*, 2009, 2010; Vanhatalo *et al.*, 2010; Shannon *et al.*, 2017; Thompson *et al.*, 2017). In some cases, post-exercise decreases in nitrite concentrations have been observed, and the authors speculate that nitrite is consumed during exercise because of further reduction of nitrite to nitric oxide (Larsen *et al.*, 2007; Shannon *et al.*, 2017). However, the measurement of nitrate and nitrite within the blood are indirect measurements of nitric oxide and do not necessarily reflect the production of nitric oxide itself. Thus, any benefit on exercise observed in response to nitrate supplementation could be in response to nitric oxide, nitrite or nitrate.

The efficiency of oxidative phosphorylation has been shown to increase in response to nitric oxide in isolated mitochondria (Clerc *et al.*, 2007). Nitric oxide also inhibits cytochrome *c* oxidase, competing with oxygen, thus lowering mitochondrial respiration and ATP production (Brown *et al.*, 2007). Nitric oxide-driven cytochrome *c* oxidase inhibition could lower oxygen consumption during exercise, but the lower ATP levels would be expected to decrease muscle performance, which is not reflected in

response to nitrate supplementation (Lansley, Winyard, Bailey, *et al.*, 2011; Murphy *et al.*, 2012). Furthermore, nitrite impacts intracellular actions independently of nitric oxide production. Nitrite has been shown to stimulate mitochondrial biogenesis independently of nitric oxide, as it does not involve activation of soluble guanylate cyclase but rather the activation of adenosine monophosphate-activated kinase through increased activation of adenylate kinase 1, resulting in increased mitochondrial efficiency and respiratory control (Mo *et al.*, 2012). Nitrite activates protein kinase A, stimulating mitochondrial fusion and respiratory control under normoxic conditions in cardiomyocytes (Pride *et al.*, 2014). Nitrite activates protein kinase A and stimulates mitochondrial fusion in adipocytes (Khoo *et al.*, 2014) and increases myocyte proliferation independently of nitric oxide (Totzeck *et al.*, 2014). This challenges the assertion that the effects of nitrate supplementation on exercise are mediated solely by nitric oxide. Furthermore, the extremely low oxygen and pH levels required for nitrite reduction to nitric oxide (Pereira *et al.*, 2013) are unlikely to occur within the muscle of healthy subjects, such as those used during these physiological studies (as discussed in Affourtit *et al.*, 2015).

Skeletal muscle has recently been shown to store nitrate and nitrite (Nyakayiru *et al.*, 2017; Wylie *et al.*, 2019), which are suggested to serve as reservoirs for the production of nitric oxide in hypoxic conditions (Lundberg *et al.*, 2008). Indeed, in rodents, the concentration of nitrate in skeletal muscle is much higher than in the blood (Piknova *et al.*, 2015). Furthermore, concentrations of nitrate and nitrite increase in human skeletal muscle, to a greater extent than that found in the plasma, following supplementation with nitrate (Nyakayiru *et al.*, 2017; Wylie *et al.*, 2019). Sialin is responsible for the transport of nitrate from circulation into the salivary glands when consumed (Qin *et al.*, 2012). Sialin transports nitrate into cells by co-transporting $2NO_3^-$

/H^+ into the cell, which is hypothesised to occur actively, against its concentration gradient (Srihirun *et al.*, 2020), and is linked to the Na^+/H^+ exchanger, using the Na^+/K^+-ATPase (Takahama *et al.*, 2013). Expression of the nitrate transporter, sialin, in human skeletal muscle was recently discovered and likely drives transportation of nitrate and nitrite from the blood and into skeletal muscle, thereby increasing nitrate storage (Wylie *et al.*, 2019). However, while knockdown of sialin in skeletal muscle cells decreased nitrate uptake significantly, it did not inhibit nitrate transport completely, indicating that other transporters of nitrate, such as chloride channel 1, also play a role in skeletal muscle transport and storage of nitrate (Srihirun *et al.*, 2020). The role of such storage is unclear, but it has been suggested that storage of relatively stable nitrate provides fast and local production of unstable nitric oxide through the nitrate-nitrite-nitric oxide pathway (Nyakayiru *et al.*, 2020).

Xanthine oxidoreductase, a nitrate-reducing enzyme (Piknova *et al.*, 2015), is present in human skeletal muscle (Wylie *et al.*, 2019), which suggests human skeletal muscle can reduce nitrate to nitrite. Furthermore, cultured primary human myocytes incubated in 1mM nitrate are shown to rapidly take up nitrate, with myotubes showing further increases in nitrite concentrations, possibly due to the expression of xanthine oxidoreductase and mitochondrial amidoxime-reducing components (Srihirun *et al.*, 2020). Notably, this concentration is much higher than the plasma nitrate levels seen after nitrate supplementation (182μM) (Larsen *et al.*, 2007). Overall, these studies propose that nitrate storage in skeletal muscle is relevant for nitric oxide production. However, as discussed above, it is unknown which nitrogen species drives the positive effects on exercise in response to nitrate supplementation. The observation that nitrate, nitrite and possibly nitric oxide are present in skeletal muscle means relatively little, without knowing the exact mechanism by which enhanced muscle activity is driven.

Overall, nitrate supplementation lowers the oxygen cost of exercise (Larsen *et al.*, 2007) and improves exercise tolerance and performance (Lansley, Winyard, Bailey, *et al.*, 2011; Breese *et al.*, 2013), suggesting that nitrogen species impact myocyte energy metabolism. Therefore, the beneficial effects of nitrogen species on exercise likely arise due to improvements or changes in the way ATP is supplied, or changes in the energetic cost of cellular ATP consuming processes, as oxidative ATP production consumes oxygen and production is driven by demand. The variability in response to nitrate supplementation and a lack of information regarding the nitrogen species that drives such exercise benefits highlights the requirement to understand the actions of nitrogen species on myocyte bioenergetics fully. The effects of nitrogen species on parameters related to ATP supply and ATP demand are discussed in more detail below.

1.4.3 Mitochondrial ATP supply

Mechanistic understanding as to how nitrate improves human skeletal muscle function is incomplete, but most models predict changes in skeletal muscle bioenergetics. Cells can supply the ATP that is needed for energy-demanding processes in various ways. Firstly, via an initial, rapid breakdown of phosphocreatine, which is limited and must then be re-synthesised. Secondly, via glycolysis, which contributes significant amounts of ATP during periods of high-intensity exercise. Finally, via oxidative phosphorylation, which occurs within the mitochondria and takes minutes to become activated but provides a sustained ATP supply, particularly at low activation of muscle (Fiedler *et al.*, 2016). The finding of lowered oxygen uptake during submaximal workloads, in the absence of changes in blood lactate levels, suggests that nitrate supplementation improves the efficiency of mitochondrial oxidative metabolism (Larsen *et al.*, 2007). Nitrate supplementation was shown to improve phosphocreatine

recovery after hypoxic exercise by ~16% (Vanhatalo *et al.*, 2011). This observation indicates improvements in the maximal rate of oxidative ATP synthesis, as phosphocreatine recovery is driven by oxidative phosphorylation (Haseler *et al.*, 1999). Furthermore, it has been suggested that an improved rate of oxidative ATP re-synthesis during severe intensity exercise may account for increased exercise tolerance, further supporting the notion that nitrate supplementation improves oxidative metabolism (Breese *et al.*, 2013).

The lowered oxygen cost of exercise following nitrate supplementation (Larsen *et al.*, 2007) has been attributed to improved mitochondrial efficiency (Larsen *et al.*, 2011). Mitochondria isolated from sodium-nitrate-supplemented individuals were found to make more ATP per oxygen atom consumed than mitochondria from non-supplemented control individuals (i.e., the mitochondria exhibited an increased P/O ratio [Brand and Nicholls, 2011]), which is consistent with the relatively low oxygen uptake during exercise (Larsen *et al.*, 2011). This increased efficiency of oxidative ATP production occurred without changes in mitochondrial content and arose from a 45% decrease in proton-leak-linked respiration (Larsen *et al.*, 2011). The lowered proton leak was attributed to decreased adenine nucleotide translocator expression and slightly decreased expression of uncoupling protein 3 (Larsen *et al.*, 2011).

In support of nitrate‘s ability to improve mitochondrial efficiency, C2C12 myocytes exposed to nitrate-containing beetroot juice show increased mitochondrial biogenesis and increased basal respiration without proton leak changes (Vaughan *et al.*, 2016). These results suggest that respiration used toward ATP synthesis must have increased, indicating improved coupling efficiency. However, beetroot juice is of ill-defined composition containing protein, carbohydrates, fats and vitamins. Therefore, the results could have been the response to any of these factors, as the study lacked an

appropriate nitrate-depleted beetroot juice control. In support of this, the application of 25μM nitrite to rat smooth muscle cells under hypoxic conditions resulted in increased mitochondrial content and the generation of mitochondria that exhibited greater mitochondrial efficiency (Mo *et al.*, 2012). This improvement in efficiency also arises due to increased respiration linked with ATP synthesis rather than decreased proton leak (Mo *et al.*, 2012). Finally, adipocytes exposed to nitrite for 24 hours also display increased mitochondrial efficiency due to increased basal respiration (Khoo *et al.*, 2014). The results described here differ from those previously obtained (Larsen *et al.*, 2011), as coupling efficiency improvements in these studies arise due to increases in respiration linked with ATP synthesis, rather than a decrease in proton leak (Larsen *et al.*, 2011).

The hypothesis that nitrogen species impact oxidative metabolism is controversial (Whitfield *et al.*, 2016; Ivarsson *et al.*, 2017; Axton *et al.*, 2019; Ntessalen *et al.*, 2020). Using muscle fibres and mitochondria from *Vastus lateralis* biopsies, taken before and after supplementation with beetroot juice, it has been demonstrated that decreased oxygen uptake during submaximal exercise can occur without improved mitochondrial efficiency (Whitfield *et al.*, 2016). For instance, Whitfield and colleagues (2016) found that beetroot juice had an exercise benefit without a change in proton-leak-linked respiration, the P/O ratio, or the expression of adenine nucleotide translocator proteins. They found no correlation between the P/O ratio and oxygen uptake, and suggest that decreased ATP turnover during contraction contributes to the observed decreased oxygen uptake during submaximal exercise in response to nitrate supplementation (Whitfield *et al.*, 2016). Furthermore, while acknowledging the limitation of physiological relevance, a study exploring the effects of sodium nitrate in

mice discovered that the P/O ratio was decreased (rather than increased) following sodium nitrate supplementation (Ivarsson *et al.*, 2017).

Adding to the argument that nitrogen species do not improve mitochondrial efficiency, no differences were found for oxidative phosphorylation, proton leak or the P/O ratio between mitochondria isolated from zebrafish given sodium nitrate or sodium nitrite in their water and control mitochondria (Axton *et al.*, 2019). This group also found no change in mitochondrial abundance between experimental groups (Axton *et al.*, 2019), which agrees with the lack of effect of sodium nitrate on mitochondrial content in humans (Larsen *et al.*, 2011) but disagrees with the reported increase in mitochondrial biogenesis found elsewhere (Mo *et al.*, 2012; Vaughan *et al.*, 2016). Furthermore, extracellular flux (XF) analysis of mitochondria isolated from sodium nitrate and sodium nitrite supplemented mice also revealed no effect of these molecules on mitochondrial efficiency (Ntessalen *et al.*, 2020). Sodium nitrite supplementation lowered overall mitochondrial respiration compared to the control, which could translate to the human exercise phenotype. However, because the decrease in proton leak was matched by a proportionally decreased respiratory activity linked to ATP synthesis, this did not affect coupling efficiency (Ntessalen *et al.*, 2020). This study found that expression of uncoupling protein 3 and ADP/ATP carriers in human and murine skeletal muscle were also not altered in response to dietary nitrate or nitrite supplementation (Ntessalen *et al.*, 2020), which further disputes previous findings (Larsen *et al.*, 2011). However, it should be noted that the human plasma concentrations of nitrate and nitrite at the time of biopsy were not increased compared to baseline measurements (Ntessalen *et al.*, 2020).

Overall, evidence to suggest that nitrogen species improve mitochondrial function by increasing mitochondrial efficiency is inconclusive. Although nitrogen

species have been shown to improve mitochondrial efficiency (Larsen *et al.*, 2011), the mechanism by which this occurs is not consistent across studies, which could reflect the different form of nitrogen species used and cell model explored across experiments. Importantly, improvements in coupling efficiency arising from increased ATP-linked respiration (Mo *et al.*, 2012; Vaughan *et al.*, 2016) do not seem to relate to the exercise phenotype exerted by nitrate supplementation, where a decrease in oxygen consumption is expected.

1.4.4 Glycolytic ATP supply

Dietary nitrate could, in principle, lower the oxygen cost of ATP supply by increasing the proportion of ATP that is obtained from glycolysis. This possibility was initially discarded based on the observation that nitrate lowered the oxygen cost of sub-maximal-intensity exercise without increases in circulating lactate concentrations (Larsen et al., 2007). However, the 'lactate phenotype' of dietary nitrate is highly variable and depends on exercise intensity. For example, sodium nitrate given to trained cyclists or triathletes (Larsen *et al.*, 2007) and beetroot juice given to recreationally active males (Betteridge *et al.*, 2016) during submaximal workloads provoked no change in blood lactate levels compared to control groups.

In support of these effects in humans, supplementation with beetroot juice in rats also provoked no change in blood lactate levels at rest, but a significant decrease following submaximal exercise compared to a control was observed (Ferguson *et al.*, 2013). However, this study failed to provide a nitrate-depleted beetroot juice control. Metabolomic analysis of whole zebrafish provided with sodium nitrate or sodium nitrite in their water showed significant decreases in the number of glycolytic intermediates and decreased lactate accumulation following exercise, compared to their rested counterparts (Axton *et al.*, 2019). Furthermore, XF analysis of C2C12 myocytes treated

with beetroot juice showed significantly lower basal and peak medium acidification, indicating decreased glycolysis and lactate production (Vaughan *et al.*, 2016). However, this decrease in medium acidification could have occurred in response to the increased oxidative ATP production observed (discussed above), potentially resulting from several of the extra components contained within the beetroot juice, which were not matched in the control condition. This evidence suggests that glycolysis leading to lactate production is decreased in response to nitrogen species supplementation.

As exercise intensity increases, the effect of dietary nitrate supplementation on lactate production changes. The blood lactate concentration increased in response to beetroot juice supplementation during high-intensity intermittent cycling, compared to a nitrate-depleted beetroot juice control (Wylie *et al.*, 2016). Beetroot juice increased blood lactate levels and performance during short-duration, high-intensity time trial experiments but did not impact these parameters when longer duration, lower intensity exercise was performed (Shannon *et al.*, 2017). Furthermore, during a 30-second maximal intensity test on a cycle ergometer, blood lactate significantly increased in response to beetroot juice (Domínguez, Garnacho-Castaño, *et al.*, 2017). These studies suggest that dietary nitrate increases glycolytic ATP supply under a high-intensity workload. Interestingly, blood lactate in humans tended to increase at rest in response to beetroot juice ($p = 0.059$) (Domínguez, Garnacho-Castaño, *et al.*, 2017). Consistently, sodium nitrate and sodium nitrite treatment in zebrafish significantly increased the abundance of several glycolytic intermediates and lactate at rest (Axton *et al.*, 2019). Overall, the effects of dietary nitrate on blood lactate are variable.

At present, it is unclear why nitrogen species may increase lactate at rest, have no effect on lactate production during submaximal workloads, and then increase lactate release during high-intensity exercise. In this respect, it should be noted that steady-

state blood lactate levels do not necessarily reflect the rate by which skeletal muscle releases lactate, as this lactate level is also controlled by other processes (Billat *et al.*, 2003; Phypers *et al.*, 2006; Jones *et al.*, 2019). Overall, it is unclear if and how nitrogen species affect glycolytic ATP supply.

1.4.5 ATP expenditure

One of the main functions of skeletal muscle is to enable locomotion (Barclay, 2017), which requires repeated contraction and relaxation. Both the contraction and relaxation of muscle fibres requires much ATP, which is largely due to the involvement of myosin and calcium ATPases in these processes (Allen *et al.*, 2008; Kuo *et al.*, 2015). The lowered oxygen cost of exercise in response to dietary nitrate could, in principle, be explained by a lowered ATP cost of contraction. Nitrate was shown to decrease ATP turnover during contraction (Bailey *et al.*, 2010), indeed suggesting a lowered ATP cost of contraction. Furthermore, a recent meta-analysis revealed that nitrate and nitrite do not affect resting metabolic rate (Pawlak-Chaouch *et al.*, 2016), indicating that contraction may be required to disclose benefit.

Murine studies have shown that chronic exposure to sodium nitrate increases force production at low stimulation frequencies in fast-twitch muscle fibres, due to increased calcium release from the sarcoplasmic reticulum, coupled with an increased expression of calcium handling proteins (Hernández *et al.*, 2012; Ivarsson *et al.*, 2017). Human studies in healthy, untrained men also show increased force production at low stimulation frequencies in response to beetroot juice (Haider *et al.*, 2014; Whitfield *et al.*, 2017), which appears to occur in the absence of increased expression of calcium handling proteins (Whitfield *et al.*, 2017). However, the latter human study failed to differentiate between muscle fibre types and used two different cohorts for force production and expression experiments. These limitations make it difficult to ascertain

if the increased force production cohort experienced this effect coupled with increased calcium handling protein expression within fast-twitch fibres, as seen in murine studies.

Improvements in force production in response to dietary nitrate are not universal, as a study exploring the effect of beetroot juice in humans found no change in force production at low stimulation frequencies (Hoon *et al.*, 2015). The differences in results may be attributed to differences in supplementation protocol (3 days (Hoon *et al.*, 2015) versus 7 days (Haider *et al.*, 2014; Whitfield *et al.*, 2017)). However, nitrate supplementation lowers the oxygen cost of exercise and improves skeletal muscle function during acute exposure (Vanhatalo *et al.*, 2010). In contrast to this, a study in women found that acute (2.5 hours) supplementation with beetroot juice had no effect on oxygen uptake during exercise but significantly increased the force applied by the muscles (torque) at low stimulation frequencies (Wickham *et al.*, 2019). This finding indicates that nitrate supplementation may impact skeletal muscle function differently depending on sex. Overall, these results highlight the variability in response regarding nitrogen species' actions under different experimental design and physiological setting.

Mechanistic models as to how dietary nitrate may increase force production have been proposed. Higher levels of free cytosolic calcium and sarcoplasmic reticulum calcium content were observed in response to sodium nitrate, along with increased force production (Hernández *et al.*, 2012). These results were attributed to an increased expression of the calcium handling proteins calsequestrin and Dihydropyridine receptors, which increase the storage of calcium within the sarcoplasmic reticulum and aid in calcium release into the myoplasm following depolarisation, respectively, leading to increased force production (Hernández *et al.*, 2012). However, increased expression of calcium handling proteins alone are unlikely the cause of increased calcium release and, therefore, force production. Increased expression of calcium handling proteins also

does not translate to human studies, where increased force production was observed (Whitfield *et al.*, 2017).

A more likely explanation as to how dietary nitrate increases force production is the quick and direct modulation of enzymes involved in the contraction pathway. Skeletal muscle contraction is a highly energetic process, with large amounts of ATP consumed by sarco-endoplasmic reticulum Ca^{2+} ATPase (SERCA) activity (Barclay *et al.*, 2007). An improvement in the efficiency, or inhibition, of SERCA in response to nitrogen species could account for the apparent decrease in the ATP cost of contraction (Bailey *et al.*, 2010), which could also account for the lowered oxygen cost of exercise. Indeed, sarcoplasmic reticulum isolated from rabbit fast-twitch fibres, exposed for 25 minutes to the nitric oxide donor, NOR3, exhibited a decrease in the activity of SERCA1 in a concentration and time-dependent manner (Ishii *et al.*, 1998). The inhibition of SERCA by nitrogen species may result in an increase in calcium within the cytosol and may, over time, prompt the requirement for increased expression of calcium handling proteins (such as in Hernández *et al.*, 2012).

The potential inhibitory effects of nitrogen species on SERCA may slow the relaxation rate of muscle and may potentially result in depletion of calcium in the sarcoplasmic reticulum, leading to a lower amount of calcium release during subsequent contractions. This interaction with SERCA would not explain how increased calcium content within the cytosol *and* sarcoplasmic reticulum were observed (Hernández *et al.*, 2012). However, other mechanisms exist within skeletal muscle to replenish sarcoplasmic reticulum calcium content during contraction. One such mechanism is store-operated calcium entry, which involves the activation of the stromal interaction molecule and Orai, allowing extracellular calcium entry into the sarcoplasmic reticulum (Avila-Medina *et al.*, 2018). Store-operated calcium entry activates in skeletal muscle

following contraction and remains active following SERCA inhibition (Koenig *et al.*, 2018). During contraction, the concentration of calcium within the sarcoplasmic reticulum decreases from ~390μM to ~8μM (Ziman *et al.*, 2010), and extracellular calcium ranges from 1.1mM to 1.4mM (Breitwieser, 2008), providing a strong chemical gradient as a driving force for calcium entry. Thus, the refilling of the sarcoplasmic reticulum through store-operated calcium entry may require less ATP compared to the use of SERCA, which requires large amounts of ATP as it moves calcium against its concentration gradient, and may thus result in a decreased ATP cost of contraction (Bailey *et al.*, 2010).

Besides lowering the ATP cost of contraction, nitrate may lower the oxygen cost of exercise by targeting contraction within specific muscle fibres. Indeed, the effect of nitrate on contraction and calcium handling may occur within fast-twitch fibres (Hernández *et al.*, 2012; Ivarsson *et al.*, 2017), which are primarily glycolytic (Spangenburg *et al.*, 2003). Increasing force production in glycolytic muscle at low stimulation frequencies could decrease the use of slow-twitch fibres at submaximal workloads, which are mainly oxidative (Spangenburg *et al.*, 2003), thus lowering oxygen uptake. These fibre type-specific effects of nitrate may account for the fact that endurance athletes are mostly non-responders to the exercise benefits of nitrate (Bescós *et al.*, 2012; Peacock *et al.*, 2012; Christensen *et al.*, 2013), as this population tends to have a higher composition of slow-twitch fibres (Rodriguez *et al.*, 2002).

1.4.6 Glucose homeostasis

Skeletal muscle is the largest insulin-sensitive tissue within the body and contributes to glucose homeostasis by accounting for 70-90% of glucose disposal following a meal (DeFronzo *et al.*, 1981; Baron *et al.*, 1988). Insulin sensitivity and glucose disposal may improve in response to nitrogen species. Nitric oxide-insufficient diabetic mouse

models given sodium nitrite through drinking water displayed a 35% reduction in fasting blood glucose levels, less weight gain, and lower insulin levels compared to a control (Jiang *et al.*, 2014). However, more nitrite and nitrosothiols were found in the liver and fat compared to skeletal muscle (Jiang *et al.*, 2014). Nitrite has also been shown to increase whole-body glucose uptake by 31% in diabetic mouse models, which was attributed to increased mitochondrial uncoupling and reduced muscular ATP production (Singamsetty *et al.*, 2015). Mitochondrial uncoupling mimics ATP demand by dissipating the proton-motive force (Brand *et al.*, 2011), which in turn could provoke increased glucose uptake and oxidation to defend the lowered proton-motive force. These results could indicate improved insulin sensitivity, although not universally, as glucose tolerance was shown to be unaffected by sodium nitrite in rats (Nyström *et al.*, 2012) and nitrate was found to have no effect on glucose homeostasis in humans (Ashor *et al.*, 2016; Betteridge *et al.*, 2016; Beals *et al.*, 2017).

The mechanism by which nitrogen species may improve insulin sensitivity has been explored by assessing the effect of nitrogen species on parameters involved in insulin-stimulated glucose uptake. GLUT4 mRNA expression was increased following a 16-hour exposure to a nitric oxide donor (Lira *et al.*, 2007), and 30-minute exposures to 10μM and 100μM sodium nitrite provoked significant increases in GLUT4 translocation into the plasma membrane (Jiang *et al.*, 2014) in L6 myotubes. Similarly, a 24-hour exposure to beetroot juice applied to C2C12 myocytes induced increased GLUT4 gene and protein expression (Vaughan *et al.*, 2016). Increased GLUT4 translocation in response to sodium nitrite was attributed to a nitric oxide-driven nitrosylation of 2 cysteine residues present on GLUT4, which affected GLUT4 localisation and translocation (Jiang *et al.*, 2014). However, nitrogen species have also been shown to impact upstream substrates of the insulin signalling pathway. Dietary

nitrite has been found to slightly increase the phosphorylation of the regulatory subunit present on phosphatidylinositol-3-kinase, which helps to facilitate its activation, and significantly increases subsequent phosphorylation of protein kinase B, resulting in increased GLUT4 translocation within skeletal muscle (Ohtake *et al.*, 2015). Others have demonstrated that the production of nitric oxide inhibits protein-tyrosine phosphatases, resulting in higher phosphorylation rates of the tyrosine residues on the insulin receptor, which also remain phosphorylated for a longer length of time (Hsu *et al.*, 2010). From these results, it can be hypothesised that nitrogen species may increase glucose transport in skeletal muscle cells through interaction with the insulin signalling pathway components. Whether the effects of nitrogen species on glucose homeostasis are additive to the effects of insulin is currently unknown but could be tested by assessing glucose uptake directly, when nitrogen species or insulin are applied alone, and when nitrogen species and insulin are applied together to a skeletal muscle cell model.

In exercising muscle, glucose uptake occurs in an insulin-independent manner via contraction-dependent mechanisms (Richter *et al.*, 2013). Thus, increases in GLUT4 expression and insertion into the plasma membrane of cells exposed to nitrogen species may arise due to increases in contraction. As discussed, nitrogen species impact parameters related to contraction (Hernández *et al.*, 2012; Haider *et al.*, 2014; Ivarsson *et al.*, 2017; Whitfield *et al.*, 2017), and increase calcium content and release within skeletal muscle cells (Hernández *et al.*, 2012). This increase in calcium may result in the activation of calcium/calmodulin-dependent protein kinase and adenosine monophosphate-activated kinase, leading to increased contraction-dependent GLUT4 insertion (Li *et al.*, 2014). As well as impacting insulin sensitivity, nitrogen species may also increase insulin output from pancreatic beta cells. Dose-dependent increases of

insulin secretion were observed in isolated pancreatic islets from mice at basal (Nyström *et al.*, 2012) and stimulatory (Gheibi *et al.*, 2017) concentrations of glucose following exposure to sodium nitrite. At basal concentrations of glucose, the results were attributed to the formation of nitric oxide from sodium nitrite, which may carry out its effects via the nitric oxide/guanylyl cyclase/cyclic guanosine monophosphate pathway (Nyström *et al.*, 2012). At stimulatory concentrations of glucose, the results were attributed to increased insulin content within islets (Gheibi *et al.*, 2017).

Overall, there is a clear benefit to increasing insulin output and potentially glucose uptake in response to nitrogen species, as this is likely to increase substrate supply within skeletal muscle cells. Substrate supply can impact basal and ATP-synthesis-linked respiration, and substrate oxidation capacity (Divakaruni *et al.*, 2014), which all influence or positively correlate with the coupling efficiency of oxidative phosphorylation (Affourtit *et al.*, 2009). Although research to support the idea that nitrogen species improve coupling efficiency is inconclusive (Larsen *et al.*, 2011; Whitfield *et al.*, 2016), the effect of nitrogen species on glucose homeostasis could, in principle, explain potential effects on coupling efficiency.

1.4.7 Similarities between nitrate and insulin effects on skeletal muscle function

There is considerable overlap between the effects of nitrogen species and insulin on skeletal muscle function. For example, both insulin (Cheng *et al.*, 2010) and nitrogen species (Mo *et al.*, 2012; Vaughan *et al.*, 2016) have been shown to increase mitochondrial biogenesis. The proton-leak-lowering effect of sodium nitrate on skeletal muscle mitochondria reported by Larsen et al. (2011) is reminiscent of the acute effect of insulin on mitochondrial proton leak reported by others (Nisr *et al.*, 2014). Insulin

has also been shown to provoke increases in medium acidification (Yang *et al.*, 2012; Nisr *et al.*, 2014), indicating increases in glycolytic ATP production. Nitrogen species have been shown to increase the expression of glycolytic intermediates and the production of lactate at rest (Axton *et al.*, 2019) and during exercise (Wylie *et al.*, 2016; Domínguez, Garnacho-Castaño, *et al.*, 2017; Shannon *et al.*, 2017). Finally, nitrogen species have been shown to impact parameters of the insulin signalling pathway (Hsu *et al.*, 2010; Ohtake *et al.*, 2015), leading to increased GLUT4 expression and insertion into the membrane of the cell (Lira *et al.*, 2007; Jiang *et al.*, 2014; Vaughan *et al.*, 2016). Thus, the mechanism by which dietary nitrate lowers the oxygen cost of exercise may be better understood by comparing the effects of nitrogen species and insulin on skeletal muscle energy metabolism.

1.5 Aims and objectives

Both insulin and nitrogen species have a positive effect on myocyte energy metabolism. However, the effects of nitrogen species on muscle energy metabolism are not universal (Pawlak-Chaouch *et al.*, 2016), and it is not yet fully understood how these positive effects arise (Larsen *et al.*, 2011; Whitfield *et al.*, 2016). Many earlier studies offering mechanistic insight into the actions of nitrogen species on myocyte energy metabolism have been challenged with more recent research, further clouding our understanding. To address gaps in our knowledge and ascertain whether insulin and nitrogen species impact bioenergetics in the same way, detailed characterisation of the bioenergetic behaviour of skeletal muscle cells in response to insulin and nitrogen species is required.

The overarching aim of this research project was to establish how nitrite (the reduction intermediate between nitrate and nitric oxide) affects the bioenergetics of cultured rat (L6) skeletal muscle cells. It is hypothesised that nitrite increases the efficiency of both ATP production and ATP consumption in skeletal muscle. More specifically, it is predicted that nitrite allows more ATP to be made at a given respiratory activity by either increasing coupling efficiency of oxidative phosphorylation or the rate at which ATP is supplied through glycolysis. Nitrite may also lower the amount of ATP required to perform ATP consuming processes.

To achieve this aim, a detailed bioenergetic analysis of static L6 myoblasts and fully differentiated myotubes in the absence of nitrite and insulin is offered in Chapter 3. This chapter explores and compares the bioenergetics of myocytes under conditions where glucose is available, where glucose is restricted, and where glucose is reintroduced to the system following glucose restriction, which sets the scene for the following chapters. To explore how nitrite impacts myocyte bioenergetics, acute effects of nitrite on the energy metabolism of skeletal muscle cells was measured using XF analysis in Chapter 4, which also explored possible mechanistic overlap between the effects of nitrite and insulin on energy metabolism. This analysis revealed that both nitrite and insulin increased the rate of glycolytic ATP supply and thus pushed myocytes into a more glycolytic phenotype.

The aim of Chapter 5 was to establish the mechanism by which these molecules increase glycolytic ATP supply by assessing whether it occurs secondary to increased glucose uptake. The aim of Chapter 6 was to continue the search for the mechanism by which nitrite and insulin increase glycolytic ATP supply, by assessing their effects on bioenergetics in the combined presence of oligomycin (to inhibit mitochondrial ATP synthesis) and BAM15 (to uncouple oxidative phosphorylation), allowing direct and

indirect stimulation of glycolytic ATP supply to become evident (see Chapter 6). The effect of nitrite and insulin on myoblasts energy expenditure was explored in Chapter 6, specifically on protein synthesis.

Together, the data demonstrate that nitrite and insulin stimulate glycolytic ATP supply irrespective of glucose availability. This effect also arises in both coupled and uncoupled conditions. Thus, nitrite and insulin lower the oxygen cost of ATP synthesis in skeletal muscle cells by pleiotropic stimulation of glycolysis. The data inform the ongoing debate regarding the mechanism by which dietary nitrate lowers the oxygen cost of exercise, suggesting a push toward a more glycolytic phenotype. The reported findings contribute to the mechanistic insight that will be crucial for achieving the full translational potential of dietary nitrate.

2 Materials and methods

2.1 Cell Culture

L6 *Rattus norvegicus* skeletal muscle myoblasts were obtained from the European Collection of Cell Culture (L6.C11). Myoblasts were maintained in Dulbecco's Modified Eagle Medium (DMEM) containing 5mM glucose, 4mM glutamine and 2mM sodium pyruvate, which was supplemented with 10% (v/v) heat-inactivated foetal bovine serum (FBS). The culture was maintained in a humidified incubator at 37ºC, in an atmosphere of 95% air and 5% CO_2. Cells were grown in 75cm^2 canted neck BD Falcon^{TM} flasks to 70-80% confluence and were routinely passaged via trypsinisation. During passage, cells were washed twice with 10ml Dulbecco's modified phosphate-buffered saline (DPBS), followed by application of 2ml 0.25% trypsin EDTA, which was then removed. Cell detachment occurred via gentle agitation, and cells were then re-suspended in 4ml fully supplemented DMEM. Cells were then counted using a haemocytometer and seeded into a new 75cm^2 tissue culture flask at 15 x 10^4 or 25 x 10^4, in a total volume of 12ml fully supplemented DMEM, as specified above. Medium was refreshed every 3 days until cells reached 70-80% confluence. Cells between passages 10 and 24 were used for experimentation.

2.2 Seahorse XF24

2.2.1 Overview

Extracellular fluxes can be measured simultaneously and in real-time in Seahorse XF analysers (Agilent, 2018). XF analysers are plate-based platforms that allow multiple conditions to be run in a single assay (Agilent, 2018). The data reported in this thesis were obtained from experiments with an XF24 analyser that accommodates 24-well plates with complementing sensor cartridges. These sensor cartridges contain fluorescent probes that measure the concentration of dissolved oxygen and free protons (pH) in time, thus allowing simultaneous determination of the oxygen consumption rate (OCR) and extracellular acidification rate (ECAR) (Agilent, 2018). These rates are reported in pmol O_2/min/well for OCR and in mpH/min/well for ECAR. The sensor cartridges also contain injection ports, allowing for sequential injection of up to 4 separate effectors, such as mitochondrial inhibitors and pharmaceutical agents, which allows the user to observe the effect of these compounds on cellular metabolism in real-time (Agilent, 2018). Figure 2.1 shows an example of an XF well with the sensor cartridge situated above.

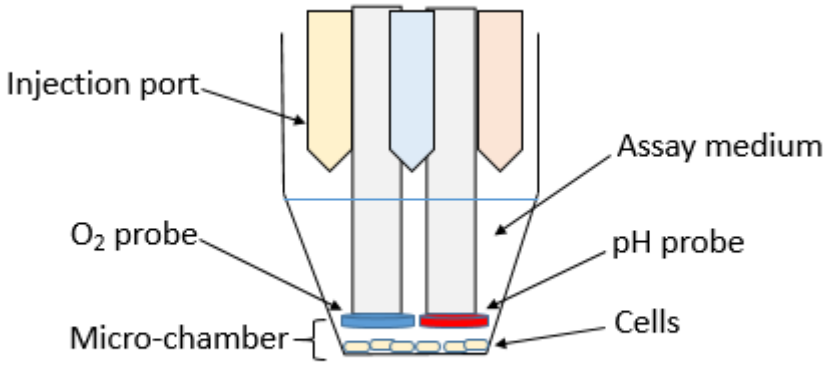

Figure 2.1 – the machinery of the cell microplate and sensor cartridge, used for Seahorse XF Analysis.
Cells are seeded into the microplate in an evenly spread monolayer prior to the assay. The wells are filled with a buffer medium and during the assay, the sensor probes are lowered to 200µm above the bottom of the well, creating a 7µL micro-chamber. The sensor cartridge also contains four injection ports, for sequential addition of mitochondrial effectors.

L6 myoblasts were seeded at 3×10^4 cells/well onto a Seahorse XF24 plate (Seahorse Bioscience). Cells were grown for 24h in fully supplemented, cell-specific DMEM, as specified above. Myoblast experiments took place the morning after this 24h growth. For myotube growth, following the 24h growth in fully supplemented DMEM, cells were cultured in DMEM with reduced FBS at 2% (v/v). This medium was refreshed every 2 days until myoblasts had differentiated into myotubes. Visual inspection using a light microscope indicated that after 8 days growth, 80-90% of cells had differentiated.

On the morning of the experiment, cells were washed 3x in KRPH, containing 2mM HEPES, 0.5mM NaH_2PO_4, 0.5mM $MgCl_2$, 1.5mM $CaCl_2$, 135mM NaCl, and 3.6mM KCl (pH 7.4). Depending on the experimental condition, KRPH was made with or without 5mM glucose. Cells were then incubated in KRPH at 37°C, under air, for 60 minutes. Following this, cells were incubated for 30 minutes in the presence or absence of 1µM sodium nitrite ($NaNO_2$) at 37ºC. 1µM $NaNO_2$ was chosen as response had been seen by previous members of the laboratory at this concentration, with higher concentrations provoking no further response (Wynne and Affourtit, unpublished). The 1µM $NaNO_2$ was then removed, and some of the cells were exposed to 100nM human insulin. The Seahorse plate was then placed into the Seahorse XF24 for a 10-minute equilibration cycle and 3 basal measurements. Overall, 4 measurement cycles were obtained after injection of port A, which contained KRPH with or without 5mM glucose. Finally, for all experiments, oligomycin (5µg/mL), BAM15 (0.7µM), and a mixture of rotenone (1µM) plus antimycin A (1µM) were then added sequentially for 3 measurements cycles each, lasting 8 minutes per cycle. Concentrations of applied effectors were chosen as either the saturating amounts calculated previously in our

laboratory, or by titration (BAM15, data not shown). Injector port solutions were diluted from effector stocks prepared and stored in dimethyl sulfoxide (DMSO).

Mitochondrial and glycolytic ATP production, as well as ATP demand, can be calculated from cellular oxygen consumption and medium acidification (Mookerjee *et al.*, 2017). In response to the addition of mitochondrial effectors, OCR, calculated using the 'Akos' algorithm (Gerencser *et al.*, 2009), can be used to calculate mitochondrial respiration and mitochondrial ATP supply. This is because oxidative phosphorylation is the coupling between ATP synthesis and electron transfer, which consumes oxygen (Mookerjee *et al.*, 2015). During cellular metabolism, medium acidification arises primarily from the pyruvate that is generated from glycolysis, which can be reduced to lactate resulting in the efflux of two lactate anions and two protons from the cell (Divakaruni *et al.*, 2014). Thus, lactate production, which is proportional to anaerobic glycolysis, is a major contributor to ECAR. However, pyruvate can also be oxidised, resulting in the generation of CO_2, which further contributes to ECAR (Mookerjee *et al.*, 2015) (See "Extracellular Acidification"). Therefore, ECAR itself cannot solely be used to determine glycolytic ATP supply, as corrections must first be applied to this measurement. Specifically, ECARs (mpH/min/well) can be converted to proton expulsion rates (pmol H^+/min/well) when the buffering capacity of the assay medium is known, allowing for correction of CO_2 derived acidification and calculation of specific glycolytic ATP supply rates (Mookerjee *et al.*, 2015).

2.2.2 Oxygen consumption

OCR reflects mitochondrial and non-mitochondrial respiration. Non-mitochondrial respiration includes oxygen consumption from non-mitochondrial oxidases, desaturase and detoxification enzymes (Brand *et al.*, 2011; Divakaruni *et al.*, 2014), while

mitochondrial respiration is mostly used to make ATP through oxidative phosphorylation. Notably, a significant proportion of mitochondrial respiration is not coupled to ATP synthesis but is accounted for by mitochondrial proton leak (Divakaruni *et al.*, 2014). Figure 2.2 gives an overview of what is usually observed during a typical XF experiment in terms of OCR. As can be seen, cells generally respond to inhibition of ATP synthase by oligomycin by decreasing their respiration. Uncoupling of oxidative phosphorylation by BAM15 stimulates OCR and inhibition of the ETC by rotenone and antimycin A completely diminishes mitochondrial OCR.

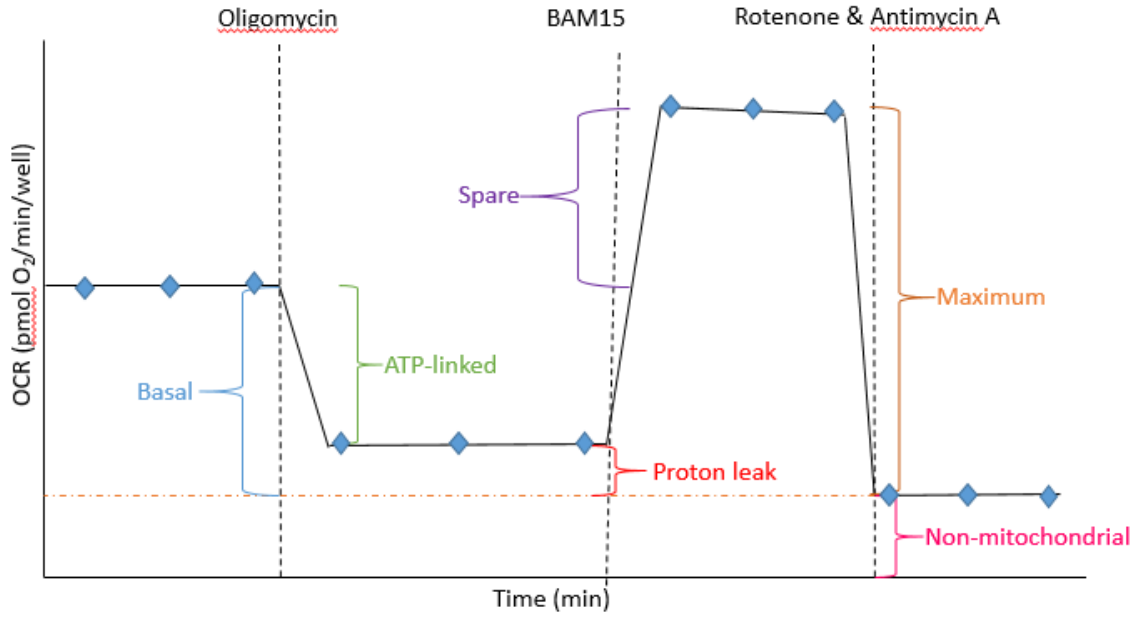

Figure 2.2 – an illustrative representation of what is usually observed during a typical Seahorse XF experiment in terms of OCR.
The graph shows OCR (pmol O_2 / min / well) as a function of time (min). The rates depicted here show basal respiration, in the absence of any effector, or rates in the cumulative presence of oligomycin (injection 1, dashed line), BAM15 (injection 2, dashed line), and a mixture of rotenone and antimycin A (injection 3, dashed line).

Respiration that is used to drive ATP synthesis, together with small contributions from proton leak, are the elements that drive basal (mitochondrial) respiration (Brand *et al.*, 2011; Divakaruni *et al.*, 2014). Generally, ATP supply (and thus mitochondrial respiration) is mostly controlled by ATP demand (Affourtit, 2016), but substrate availability also exerts control (Divakaruni *et al.*, 2014). Basal respiration is usually calculated by subtracting the average value of non-mitochondrial respiration from the average of the first 3 stable basal respiration points, before injection of any effectors (Figure 2.2). In this Thesis, basal respiration was taken as the 3rd measurement on the OCR trace, at which time the cells had been exposed to insulin for ~34 minutes.

The addition of oligomycin, which inhibits the ATP synthase by blocking its proton channel within the Fo portion (Hong *et al.*, 2008), allows for the calculation of respiration used to drive mitochondrial ATP synthesis and proton leak. As can be seen in Figure 2.2, the addition of oligomycin causes cellular respiration to decrease. This is because inhibition of the ATP synthase causes a build-up of protons within the intermembrane space, as these protons are no longer used to make ATP. This build-up of protons causes back pressure on the ETC and thus lowers oxygen consumption (Berg *et al.*, 2002). ATP-synthesis-linked respiration is estimated as the difference between basal respiration and oligomycin-insensitive respiration (Divakaruni *et al.*, 2014).

The addition of oligomycin also shows proton leak-linked respiration, which is calculated by subtracting non-mitochondrial respiration from the oligomycin-resistant rate, taken as the average of the three points (Figure 2.2). Oxidative phosphorylation is not a fully efficient process and one of the reasons for this is proton leak. Proton leak occurs when protons that make up the proton-motive force move back across the inner mitochondrial membrane, in a fashion that bypasses the ATP synthase. Thus, protons that are pumped across the inner mitochondrial membrane via the ETC to generate the

proton-motive force are not exclusively used to drive ATP synthesis (Jastroch *et al.*, 2010). As proton leak depletes some of the proton-motive force, the ETC continues to pass electrons and reduce molecular oxygen to water, to maintain the proton-motive force. Thus, some mitochondrial respiration is still observed in the presence of oligomycin (Divakaruni *et al.*, 2014) (Figure 2.2).

Following the addition of oligomycin, protonophores or chemical uncouplers of oxidative phosphorylation are added to calculate maximum respiration by cells (Figure 2.2). Mitochondrial uncouplers, such as carbonyl cyanide p-trifluoromethoxyphenylhydrazone (FCCP) and (2-fluorophenyl){6-[(2-fluorophenyl)amino](1,2,5-oxadiazolo[3,4-e]pyrazin-5-yl)}amine (BAM15), uncouple nutrient oxidation from ATP synthesis by allowing protons to move across the inner mitochondrial membrane, bypassing the ATP synthase (Divakaruni *et al.*, 2014). By dissipating the proton-motive force in this way, nutrient oxidation can occur beyond control of the ATP/ADP ratio and thus energy demand, usually leading to increased mitochondrial oxygen consumption, due to maximum activity of the ETC to maintain the proton-motive force (Kenwood *et al.*, 2014). Maximum respiration was calculated by subtracting non-mitochondrial respiration from the first point observed in the presence of BAM15. BAM15 was chosen over FCCP as FCCP has been shown to have off-target effects that can interfere with respiratory measurements, such as plasma membrane depolarisation (Kenwood *et al.*, 2014). Spare or reserve respiratory capacity is calculated by subtracting basal respiration from maximal respiration, and is an indicator of the cells' ability to respond to increased ATP demand (Brand *et al.*, 2011; Divakaruni *et al.*, 2014) (Figure 2.2).

Rotenone and antimycin A, which inhibit complex I and III respectively in the ETC, are added to prevent electron transfer and thus mitochondrial respiration

(Divakaruni *et al.*, 2014) (Figure 2.2). In this Thesis, non-mitochondrial respiration was calculated from the average of 3 rates in the presence of rotenone and antimycin A, which was subtracted from all other rates to correct for non-mitochondrial respiration. The coupling efficiency and cell respiratory control ratio are two further bioenergetic parameters that can be calculated from OCRs. The coupling efficiency of oxidative phosphorylation is defined as the percentage of basal respiration used to generate ATP and is calculated by dividing ATP-synthesis-linked respiration by basal respiration (Brand *et al.*, 2011). The cell respiratory control ratio is calculated by dividing maximum respiration in the presence of an uncoupler by oligomycin insensitive respiration and thus detects changes in proton leak and substrate oxidation (Brand *et al.*, 2011).

2.2.3 Extracellular acidification

Generally, in response to the mitochondrial effectors discussed above, ECAR increases (Figure 2.3). For example, inhibition of the ATP synthase by oligomycin causes a build-up of pyruvate within the cell, as the reducing power formed from pyruvate by the TCA cycle is not used for oxidative ATP production. This build-up forces the pyruvate into lactate, resulting in an increase in medium acidification (Mookerjee *et al.*, 2017) (Figure 2.3). Increases in ECAR also occur to compensate for the lack of ATP production via oxidative means in response to these effectors. The cells increase their glycolytic ATP production, which is reflected by an increase in extracellular acidification, to meet the energetic demand of the cells (Brand *et al.*, 2011) (Figure 2.3). Basal ECAR was taken from the 3rd point on the ECAR trace, at which time the cells had been exposed to insulin for ~34 minutes.

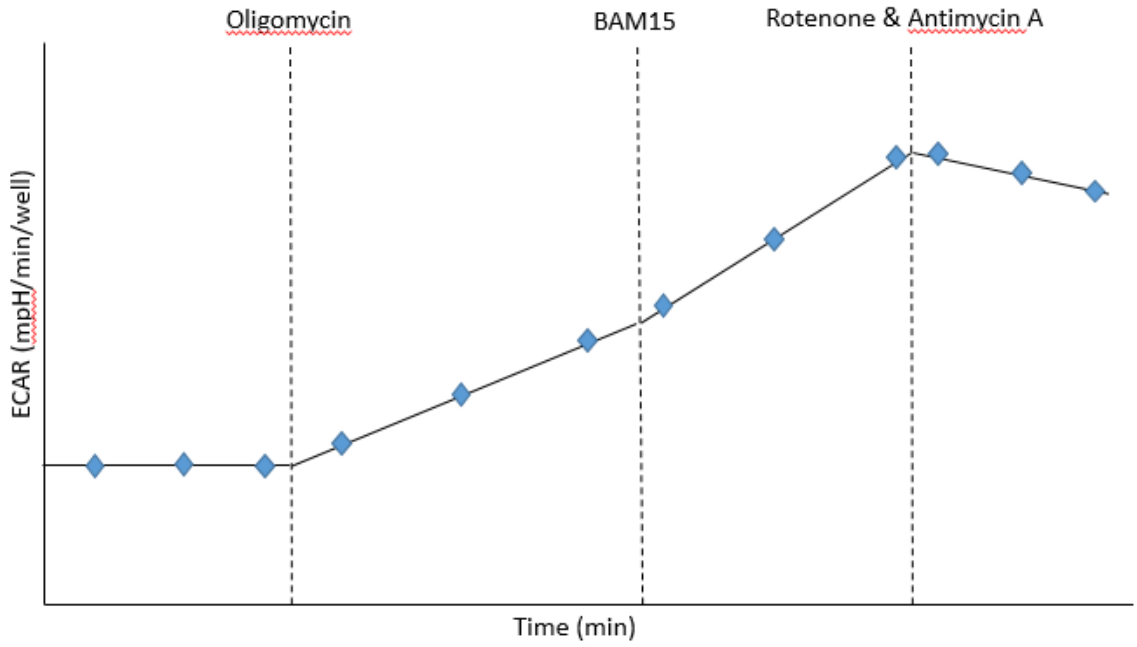

Figure 2.3 – an illustrative representation of what is usually observed during a typical Seahorse XF experiment in terms of ECAR.
The graph shows ECAR (mpH / min / well) as a function of time (min). The rates depicted here show basal medium acidification, in the absence of any effector, or rates in the cumulative presence of oligomycin (injection 1, dashed line), BAM15 (injection 2, dashed line), and a mixture of rotenone and antimycin A (injection 3, dashed line).

ECAR itself cannot solely be used to determine glycolytic ATP supply, as several corrections must first be applied. It is important to acknowledge that lactate production is not the only source of medium acidification. The breakdown of one glucose molecule via glycolysis results in the generation of a net 2 ATP, 2 NADH and 2 pyruvates (Feher, 2017). The pyruvate generated can be reduced to lactate by LDH and this results in the efflux of two lactate anions and two H^+ into the medium (Divakaruni *et al.*, 2014). This then results in medium acidification and an increase in ECAR.

Pyruvate can also enter into the mitochondria, where it is oxidised to form acetyl-CoA, which feeds into the TCA cycle, generating the reducing power that fuels oxidative phosphorylation (Mookerjee *et al.*, 2017). When pyruvate is oxidised in this way, CO_2 is produced, largely from the TCA cycle, and is hydrated to H_2CO_3, which can then dissociate to 6 HCO_3^- and 6 H^+ in the assay medium, again resulting in medium acidification (Divakaruni *et al.*, 2014). Importantly, when pyruvate is oxidised, up to 3 times as many protons can be released into the medium compared to when it is reduced to lactate. Thus, during XF analysis where glucose fuels metabolism, both glycolysis and respiration account for the ECAR. Analysis of a variety of cell lines found that the contribution of CO_2-derived acidification ranged from 3-100% of total ECAR (Mookerjee *et al.*, 2015), highlighting the requirement to correct for this contribution. Without such correction, ECAR cannot be used as a quantitative measure of glycolytic ATP production.

ECARs (mpH/min/well) can be converted to proton expulsion rates (pmol H^+/min/well) when the buffering capacity of the assay medium is known, allowing for correction of CO_2 derived acidification and calculation of specific glycolytic ATP supply rates (Mookerjee *et al.*, 2015). The buffering power is defined as the amount of H^+ added to cause a change in pH by 1 pH unit (Technologies, 2018), and was measured

using KRPH containing 2mM HEPES by filling the wells of an XF microplate with 250 µL KRPH and sequentially injecting known concentrations of HCl via the injection ports into the microplate. The change in pH was then plotted against the amount of H^+ contained in the micro-chamber. The linear slope obtained from this plot is the buffering power of the medium in mpH/pmol H^+ (Mookerjee *et al.*, 2015). The buffer power determined on XF24 plates was used to convert ECAR to proton efflux rates, assuming an effective measuring volume of 22.7uL (Gerencser *et al.*, 2009). This experiment was carried out in triplicate and final buffering power was calculated as 0.03 mpH/pmol H^+.

2.2.4 ATP supply

Simultaneous measurement of oxygen consumption and medium acidification by cultured cells using a Seahorse Extracellular Flux Analyser offers valuable insight into cellular energy metabolism. XF data may be used, by applying biochemistry textbook knowledge, to fully quantify cellular ATP supply that accounts for glycolytic and mitochondrial ATP supply fluxes (Mookerjee *et al.*, 2017). Furthermore, XF analysis can be utilised to show how these ATP supply fluxes are distributed between ATP demanding processes (Nisr *et al.*, 2016; Mookerjee *et al.*, 2017). By extension, XF analysis can be applied to identify the sites at which pharmacological or other agents act on cellular metabolism. XF analysis thus offers complete, quantitative, bioenergetic phenotyping, which is used in this thesis to reveal novel effects of insulin and nitrogen species on skeletal muscle function.

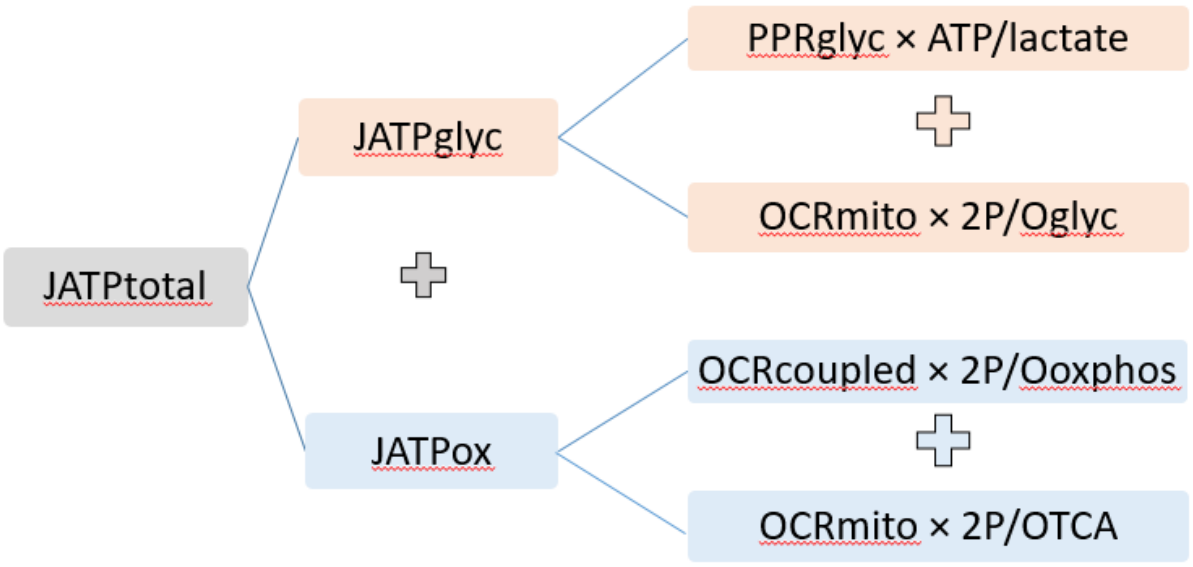

Figure 2.4 – schematic overview of the calculations involved in converting raw OCR and ECAR data into ATP supply fluxes.
Total ATP supply (JATPtotal) is the sum of both mitochondrial (JATPox) and glycolytic (JATPglyc) ATP supply fluxes. JATPox is the sum of coupled respiration (OCRcoupled) multiplied by the P/O ratio for oxidative phosphorylation (P/Ooxphos), and mitochondrial respiration (OCRmito) multiplied by the P/O ratio for the TCA cycle (P/OTCA). JATPglyc is the sum of acidification caused by protons produced via pyruvate that runs to lactate (PPRglyc) multiplied by the amount of ATP produced per lactate produced (ATP/lactate), and mitochondrial respiration (OCRmito) multiplied by the P/O ratio for glycolysis (P/Oglyc).

Total ATP production (JATPtotal) is the sum of glycolytic (JATPglyc) and mitochondrial (JATPox) ATP production (Figure 2.4; Mookerjee *et al.*, 2017). Mitochondrial ATP supply is the sum of two parts, as it accounts for ATP that is produced during substrate-level phosphorylation from the TCA cycle and during oxidative phosphorylation (Mookerjee *et al.*, 2017). To account for ATP production from substrate-level phosphorylation, mitochondrial respiration (OCRmito) is multiplied by the P/O ratio for the TCA cycle (0.121) (Mookerjee *et al.*, 2017). ATP supply from oxidative phosphorylation is calculated from oligomycin-sensitive respiration, which is the portion of mitochondrial respiration that is used to drive respiration coupled to ATP synthesis (OCRcoupled) (Mookerjee *et al.*, 2017). However, oligomycin provokes hyperpolarization of the mitochondrial inner membrane, causing a slight underestimation of this rate (~10%), which must be corrected for (Affourtit *et al.*, 2009). The rate is then multiplied by the P/O ratio for oxidative phosphorylation (2.486) (Mookerjee *et al.*, 2017).

Glycolytic ATP supply is defined as total flux through glycolysis leading to pyruvate. It encapsulates both the pyruvate derived from glycolysis that is reduced to lactate and the pyruvate derived from glycolysis that has an oxidative fate (Mookerjee *et al.*, 2017). ECAR is converted into the total proton production rate using the buffering capacity of the assay medium (Mookerjee *et al.*, 2015). Correction for CO_2 derived acidification occurred using mitochondrial respiration, with a respiratory quotient (RQ; CO_2 produced/O_2 consumed) of 1 and a maximum H^+ released per O_2 consumed (max H^+/O_2) of 1 (Mookerjee *et al.*, 2015). The respiratory proton production rate is then subtracted from the total proton production rate, leaving protons derived from pyruvate reduction to lactate. The glycolytic ATP supply rate was thus calculated from medium acidification to account for pyruvate reduced to lactate plus H^+ (ATP:lactate = 1:1) and

from mitochondrial respiration to account for the pyruvate oxidised to bicarbonate using the P/O ratio for glycolysis (0.167) (Mookerjee *et al.*, 2017). Glycolytic ATP synthesis was also calculated as a percentage of total ATP supply, giving the glycolytic index (GI). Total ATP supply was normalised to total *cellular* respiration (basal respiration not corrected for non-mitochondrial respiration), giving the ATP/O_2 ratio.

2.2.5 ATP consumption

The amount of ATP supply used toward ATP demanding processes can be calculated during XF analysis, through the application of specific ATP demand inhibitors (Divakaruni *et al.*, 2014; Nisr *et al.*, 2016; Mookerjee *et al.*, 2017). Inhibition of ATP demand during XF analysis results in declined ATP synthesis, which is reflected by decreases in OCR and ECAR, from which the change in ATP supply can be calculated (Mookerjee *et al.*, 2017). This indirect approach assumes that ATP supply is predominantly controlled by ATP demand. In experiments where ATP demand inhibitors were applied, cells were incubated in KRPH with 5mM glucose, +/- 1μM $NaNO_2$, +/- 100nM insulin at 37°C, under air, as described previously, before being placed into the Seahorse XF24 Analyser. After a 10-minute equilibration cycle, 3 basal measurements were recorded. 4 measurements cycles were then obtained after injection of port A, which contained either KRPH or varying concentrations of ATP demand inhibitors. Final inhibitor concentrations were chosen as the lowest concentration that gave the maximum inhibition of respiration, without impacting the BAM15-uncoupled rate. Oligomycin (5μg/mL), BAM15 (0.7μM), and a mixture of rotenone (1μM) plus antimycin A (1μM) were then added sequentially for 3 measurements cycles each, lasting 8 minutes per cycle. The activity of an ATP-demanding process was estimated from the response of ATP supply to a specific inhibitor of that process. These responses

were expressed as a percentage of uninhibited glycolytic, mitochondrial or total ATP supply rates. Inhibitor effects were corrected for addition artefacts by subtracting buffer effects.

2.3 Glucose uptake

L6 myoblasts were seeded onto a 96 well plate (Corning®, Costar®, USA) at 3 × 10^4 cells/well. Cells were grown for 24 hours in fully supplemented DMEM, as specified above. Myoblast experiments took place the morning after this 24-hour growth. For myotube growth, following the 24-hour growth in fully supplemented DMEM, cells were cultured in DMEM with reduced FBS at 2% (v/v). This medium was refreshed every 2 days until myoblasts had differentiated into myotubes. Visual inspection using a light microscope indicated that complete differentiation took 8 days.

Glucose uptake was measured in myocytes using a 2DG assay (Yamamoto *et al.*, 2006, 2010). When differentiated, L6 cells express both GLUT4 and GLUT1 and increase glucose transport via insulin stimulation by translocation of GLUT4 and GLUT1 from intracellular vesicles to the plasma membrane (Yamamoto *et al.*, 2006, 2010). Uptake of 2DG by L6 cell monolayers has been found to be linear for at least 20 minutes (Klip *et al.*, 1982), which agrees with the method stated (Yamamoto *et al.*, 2006, 2010) and used in this thesis.

Cells were incubated for 1 hour at 37ºC in glucose-free DMEM, then washed into glucose-free KRPH supplemented with 0.1% (w/v) bovine serum albumin (BSA), and incubated in this medium +/- 1µM $NaNO_2$ for 30 minutes at 37ºC. Cells were incubated for another 20 minutes at 37ºC in fresh glucose-free KRPH +/- 100nM insulin, at which point 5mM 2DG was added. Following another 20 minute incubation at 37ºC, cells were washed with glucose-free KRH, lysed in 0.1 N NaOH (10 min

agitated incubation at 65ºC and 50 min at 85ºC), and neutralised with 0.1 N HCl in triethanolamine (200mM, pH 8). The amount of 2DG was determined from resorufin production during a 50-minute incubation at 37ºC in an assay mixture comprising 50mM triethanolamine (pH 8), 50mM KCl, 15 U/ml glucose-6-phosphate dehydrogenase, 0.2 U/ml diaphorase, 0.1mM $NADP^+$, 0.02% (w/v) BSA and 2µM resazurin. Resorufin was detected by fluorescence (λex/em = 540/590 nm) in a PHERAstar FS plate reader (BMG Labtech). 2DG uptake by myocytes was calculated using standard curves that were generated for each biological repeat, using an assay medium composed of the same constituents as specified above, with the addition of 0.5mM MgCl2, 0.5mM ATP, and 2 U/ml hexokinase (Yamamoto *et al.*, 2006, 2010). An overview of the principle of the 2DG assay can be seen in Figure 2.5.

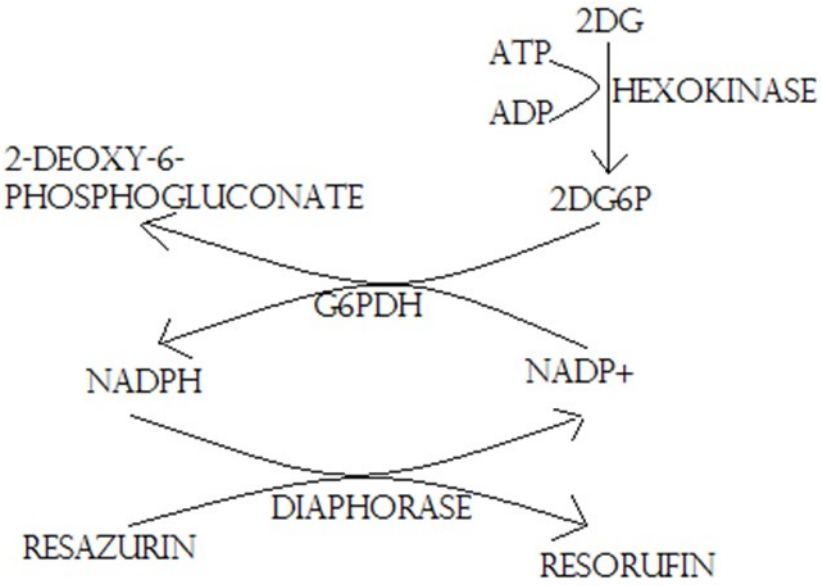

Figure 2.5 – 2DG assay overview.
Cells take up 2DG via glucose transporters, which is then phosphorylated via hexokinase to a derivative; 2-deoxyglucose-6-phosphate (2DG6P). 2DG6P accumulates within the cell because, unlike glucose, it cannot be further metabolised. Glucose-6-phosphate dehydrogenase catalyses the conversion of 2DG6P to 2-deoxy-6-phosphogluconate, which is coupled with the conversion of $NADP^+$ to NADPH. Resazurin is then converted to resorufin, a potent fluorescent substance, via diaphorase, which is coupled to the conversion of NADPH to NADP+, thus recycling these constituents. This reaction continues until the 2DG6P is consumed, and the resorufin fluorophore generated should be equivalent to the amount of 2DG6P present within the cell (Yamamoto *et al.*, 2006)*. Thus, the higher the fluorescence, the more 2DG has entered the cell, which is a reflection of glucose uptake.*

2.4 Lactate release

Lactate release was measured enzymatically in myocytes as described previously (Mookerjee *et al.*, 2015). Cells were seeded onto a 96 well plate (Corning®, Costar®, USA) at 3×10^4 cells/well and grown as described above for myoblasts and myotubes (see "Glucose uptake"). Cells were washed into KRPH with 5mM glucose and incubated under air at 37ºC without or with either 1µM $NaNO_2$ or 100nM insulin. The supernatant was removed at various time points and stored at room temperature until assay. Lactate concentration was determined from the initial rate of NADH production in an assay mixture comprised of 0.5M Tris/HCl (pH 9.8), 10mM EDTA, 200mM hydrazine (pH 9.8), 2mM NAD^+ and 20 U/mL lactate dehydrogenase. NADH was detected by fluorescence (λex/em = 340/460 nm) in a PHERAstar FS plate reader (BMG Labtech). Released lactate amounts were calculated from standard curves that were generated for each biological repeat by assaying varying known amounts of sodium lactate in the same manner as stated above.

2.5 Protein estimation

Experimental results were normalised to total protein content, which was estimated using a Pierce bicinchoninic acid (BCA) Protein Assay Kit (ThermoFisher Scientific). Following experimentation, any remaining assay medium was removed from each well of the assay plate, and cells were then gently washed three times with 250µl BSA-free KRPH. 50µl RIPA lysis medium containing 150mM NaCl, 1mM EDTA, 1% v/v Triton X-100, 0.1% v/v SDS, 50mM Tris, 1mM EGTA and 0.5% w/v sodium deoxycholate pH 7.4 at 22 °C with HCl, was added to each well. Following this, the assay plate was incubated on ice for 30 minutes and then agitated on a plate shaker at 1,200 rpm for 5

minutes. 400ul of the working reagent was then added to each well and mixed via a pipette. The plate was then incubated for 30 minutes at 37ºC in a non-CO_2 incubator. 200µl of the mixture was removed from the original plate and placed into a clear flat bottomed 96-well plate (Greiner bio-one) and absorbance was measured at 562nm using a Well Plate PHERAstarFS (BMG Labtech, UK). Standard curves were generated during each protein estimation, and the amount of protein present within each sample was calculated using this standard curve.

2.6 Data Analysis

All OCR, ECAR and ATP supply rates were calculated in Microsoft Excel 2016 as described above and previously (Mookerjee *et al.*, 2017). Differences between myocellular differentiation state and possible nitrite and insulin effects on bioenergetics, glucose uptake and lactate release were evaluated for statistical significance using GraphPad Prism software (version 8.3.0), applying tests that are specified in the figure legends.

3 Quantification of myocellular bioenergetics: glucose lowers the oxygen cost of total ATP supply

3.1 Introduction

Accounting for 40%–45% of total body mass (Kim *et al.*, 2016), skeletal muscle is the primary site of insulin-sensitive glucose disposal in the human body (DeFronzo *et al.*, 1981; Baron *et al.*, 1988). Besides its role in glucose homeostasis, skeletal muscle is responsible for the maintenance of posture, movement and contraction (Barclay, 2017). Muscle mass and function correlate positively with good health (Minetto *et al.*, 2019). Indeed, muscle dysfunction is associated with many diseased states, such as chronic obstructive pulmonary disease (Mador *et al.*, 2001), cancer cachexia (Penna *et al.*, 2019), diabetes (Perry *et al.*, 2016), heart failure (Keller-Ross *et al.*, 2019), and ageing (Nair, 2005).

Much research has been performed to clarify the molecular and cellular mechanisms that underpin the important roles of skeletal muscle in health and disease, and skeletal muscle cell lines (e.g. L6 and C2C12) have been used to study many myocellular processes. Specifically, L6 cells have been used to explore proliferation (Pinset *et al.*, 1982), cell differentiation (Cui *et al.*, 2009), muscle contraction (Arias-Calderón *et al.*, 2016), insulin signalling and resistance (Nisr *et al.*, 2016), glucose uptake (Li *et al.*, 2014; Nisr *et al.*, 2014), muscle mitochondrial function (Nisr *et al.*, 2014; Genders *et al.*, 2019; Ahmed *et al.*, 2020), and involvement of muscle in immunity (Pillon *et al.*, 2014). Therefore, I decided to use L6 cells as our experimental muscle model to explore the acute effects of nitrite and insulin on cellular bioenergetics.

In this chapter, the energy metabolism of L6 myoblasts and myotubes is characterised in detail. Extracellular flux analysis is applied to monitor real-time oxygen consumption and medium acidification by these muscle cells in various bioenergetic states, and against different nutritional backgrounds. I demonstrate how these extracellular fluxes can be used to calculate intracellular ATP synthesis rates, and thus reveal that glucose lowers the apparent oxygen cost of myocellular ATP supply. This novel observation sets the scene for subsequent bioenergetic experiments involving nitrite and insulin.

3.2 Results

Respiration and medium acidification by L6 myoblasts and myotubes

In the first set of experiments, respiration and extracellular acidification by L6 myoblasts and fully differentiated L6 myotubes were measured under conditions where 5mM glucose was present throughout the experiment. Figure 3.1A shows typical XF traces that reflect the oxygen consumption rate (OCR) for L6 myoblasts and myotubes, respectively, in various bioenergetic states. In both myoblasts and myotubes, the OCR decreases when mitochondrial ATP synthesis is inhibited with oligomycin. Uncoupling of oxidative phosphorylation by BAM15 stimulates oxygen consumption, and inhibition of the ETC by a mixture of rotenone and antimycin A diminishes mitochondrial OCR, leaving non-mitochondrial respiration (Figure 3.1, A). This non-mitochondrial respiration is subtracted from other OCRs to reveal the mitochondrial respiratory rates shown in Figure 3.1C. Generally, cells increase glycolysis to meet their energetic demands when oxidative phosphorylation is prevented (Brand *et al.*, 2011), e.g., by oligomycin and BAM15. Such compensation is apparent in our experiments by the increase in ECAR in response to the applied mitochondrial effectors (Figure 3.1, B).

Analysis of multiple XF traces reveals that basal mitochondrial OCR (Figure 3.1, C) and basal ECAR (Figure 3.1, D) are significantly lower in myotubes compared to myoblasts. The decreased basal respiration arises from a significant decrease in ATP-synthesis-linked (oligomycin-sensitive) respiration in myotubes, as proton-leak-linked (oligomycin-insensitive) respiration remains the same when comparing the two differentiation states (Figure 3.1, C). The BAM15-uncoupled rate and spare respiratory capacity (uncoupled minus basal OCR) are significantly higher in myotubes compared to myoblasts, while non-mitochondrial respiration remains unaffected by differentiation state (Figure 3.1, C). The proportion of respiration that is used to produce ATP is significantly lower in myotubes than in myoblasts (71.6% versus 83%) (Figure 3.1, E), owing to the lower basal and ATP-linked respiration upon differentiation. Finally, the cell respiratory control ratio (ratio between the BAM15-uncoupled and oligomycin-insensitive OCRs) is significantly higher in myotubes than myoblasts (Figure 3.1, F). This increase in the respiratory control ratio is due to the increased uncoupled rate in myotubes, as proton leak-linked respiration is the same in both differentiation states.

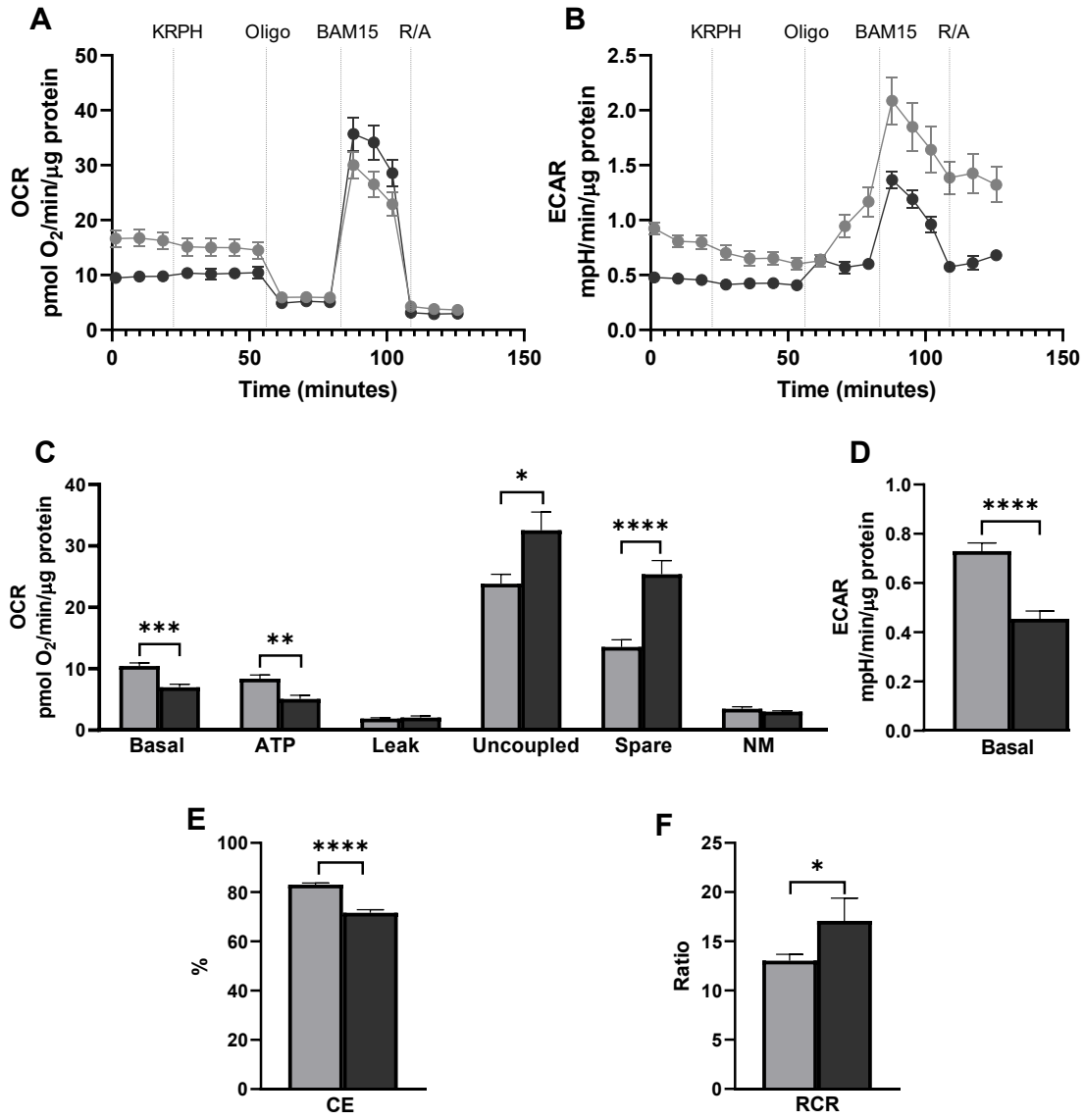

Figure 3.1 - Oxygen uptake and extracellular acidification by L6 myoblasts and differentiated myotubes.

*Myoblasts (light-grey symbols) and myotubes (dark-grey symbols) were grown in supplemented medium containing 5mM glucose. Rates by which the cells consume oxygen (OCR) and acidify their medium (ECAR) were measured simultaneously in KRPH that contained 5mM glucose from the point cells were washed into it, i.e., 90 minutes before the XF assay. OCR and ECAR measurements were made in the absence and in the cumulative presence of 5 µg/mL oligomycin (Oligo), 0.7µM BAM15, and a mix of 1µM rotenone and 1µM antimycin A (R/A) as shown by the XF traces in panels A and B, respectively. Mitochondrial respiratory activities (panel C); Basal: mitochondrial OCR in the absence of effectors; ATP: OCR coupled to ATP synthesis; Leak: OCR linked to mitochondrial proton leak; Uncoupled: mitochondrial OCR stimulated by BAM15; Spare: the difference between Uncoupled and Basal. Basal ECAR (panel D), the coupling efficiency of oxidative phosphorylation (CE, panel E) and the cell respiratory control ratio (RCR, panel F). Rates represent the means and standard error of the mean of 2-5 biological repeats, each containing 3-5 technical repeats. Significance was tested using an unpaired T-test. * = p <0.05, ** = p <0.01, *** = p <0.001, **** = p <0.0001.*

Myocellular ATP supply rates

Glycolytic and mitochondrial ATP supply fluxes, calculated from OCR and ECAR ((Mookerjee *et al.*, 2017); see Chapter 2), are shown in Figure 3.2, A. As predicted by the lower ATP-synthesis-linked OCR and basal ECAR, the rate at which ATP is supplied by glycolytic and mitochondrial means is significantly lower in myotubes than in myoblasts (Figure 3.2, A). As such, total supply flux is significantly lower in myotubes than in myoblasts (Figure 3.2, A). However, the difference in the amount of ATP supplied through glycolysis between the two differentiation states disappears when glycolytic ATP supply is expressed as a percentage of overall ATP supply (Glycolytic Index) (Figure 3.2, B), which indicates that glycolysis and mitochondria contribute proportionally the same to total ATP synthesis in both differentiation states. Normalising total ATP supply to total *cellular* respiration yields a significantly lower ATP/O_2 ratio for myotubes compared to myoblasts (Figure 3.2, C). This difference reflects the relatively low coupling efficiency of myotubes (Figure 3.1, E), rather than changes in the contribution of glycolytic and mitochondrial ATP supply, as the glycolytic index remains the same in both differentiation states. This result suggests that the apparent oxygen cost of ATP synthesis is higher for myotubes than myoblasts.

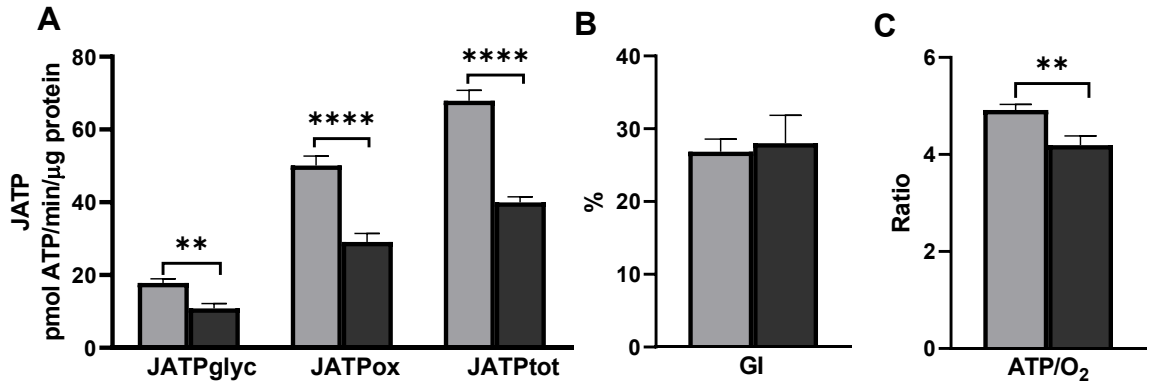

Figure 3.2 – ATP supply fluxes for L6 myoblasts and myotubes in the presence of 5mM glucose.

*Myoblasts (light-grey) and myotubes (dark-grey) were grown in supplemented medium containing 5mM glucose. Rates of glycolytic (JATPglyc), mitochondrial (JATPox) and total (JATPtot) ATP synthesis (panel A), the glycolytic index (GI, panel B) and the cellular ATP/O_2 ratio (panel C) were calculated from the XF traces as explained in chapter 2. Rates represent the means and standard error of the mean of 2-5 biological repeats, each containing 3-5 technical repeats. Significance was tested using an unpaired T-test. * = p <0.05, ** = p <0.01, *** = p <0.001, **** = p <0.0001.*

The effects of nutrient deprivation on L6 myocyte energy metabolism

In previous studies (Ching *et al.*, 2010; Nisr *et al.*, 2014), myocytes were sensitised to insulin by glucose starvation and, in the case of myoblasts, also by depletion of the serum concentration. Since the following chapters of this thesis seek to establish the effects of nitrite and insulin on the bioenergetics of L6 cells, it was deemed important to establish how myocyte energy metabolism responds to this nutrient withdrawal and to acute addition of glucose in the XF assay. Nutrient withdrawal included a 90-minute deprivation of glucose in both myoblasts and myotubes and a reduction in FBS from 10% to 2% overnight for myoblasts.

Depriving myocytes of glucose lowers maximum and spare respiratory capacity

Basal mitochondrial respiration and respiration coupled to ATP synthesis are not significantly affected by nutrient withdrawal in myoblasts (Figure 3.3, A) and myotubes (Figure 3.4, A). In myoblasts, these rates remain unaffected by glucose reintroduction during the XF assay following such deprivation (Figure 3.3, A). In myotubes, glucose reintroduction following deprivation causes significant increases in basal mitochondrial respiration compared to when glucose is present throughout the assay and significantly increases ATP-synthesis-linked respiration compared to glucose-deprived cells (Figure 3.4, A). In both differentiation states, maximum respiratory capacity is significantly decreased following glucose deprivation, compared to when glucose is available throughout the assay (Figures 3.3 & 3.4, A). Consequently, cells lose their spare respiratory capacity when deprived of glucose, falling from 14 to -5 pmol O_2/min/µg protein in myoblasts (Figure 3.3, A), and from 25 to 1 pmol O_2/min/µg protein in myotubes (Figure 3.4, A).

Myoblasts

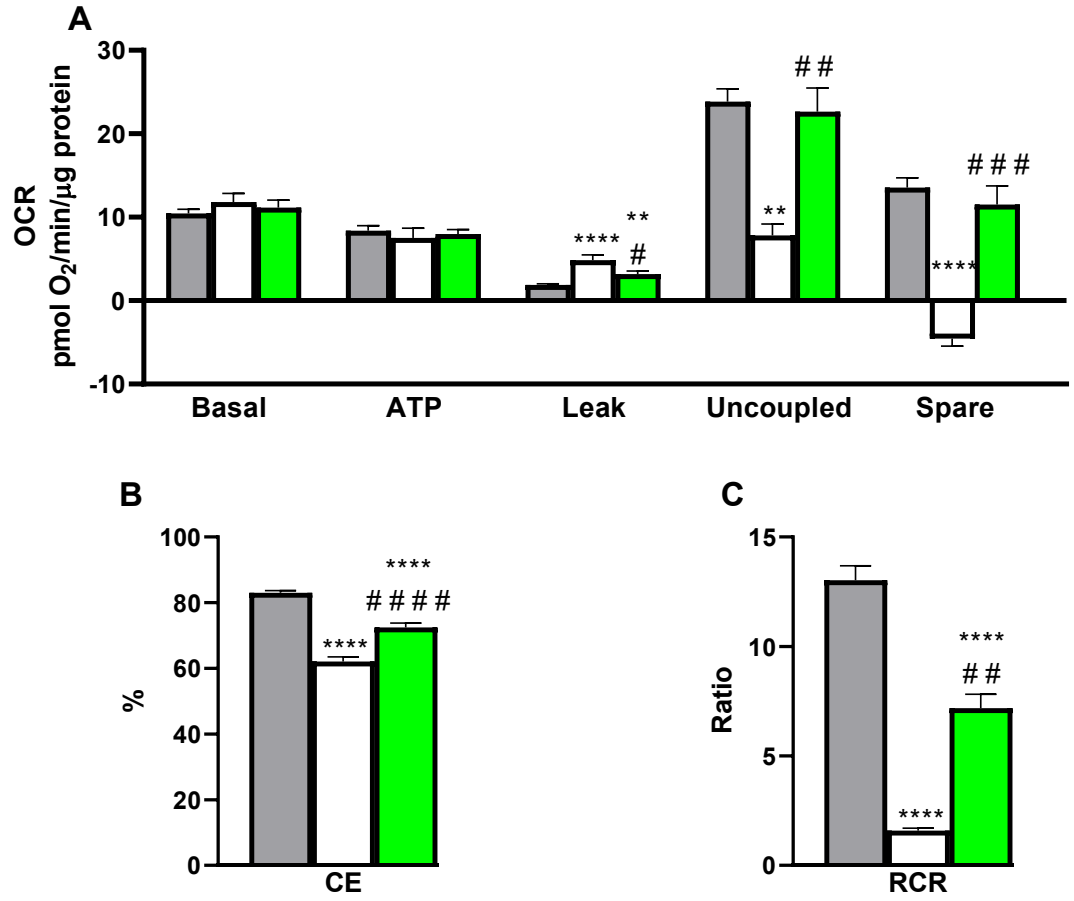

Figure 3.3 – The effects of changes in nutritional background on bioenergetics in L6 myoblasts, as measured by Extracellular Flux Analysis.

L6 myoblasts were grown and assayed as described in the Methods section (light-grey), or were deprived of glucose during a 90-minute incubation in glucose-free KRPH before the XF assay (white and light-green bars). Nutrient-deprived cells were assayed without glucose (white bars) or were subjected to 5mM glucose in the assay before other effectors were added (light-green bars). The serum concentration of the growth medium was lowered to 2% (v/v) 16 hours before cells were washed into KRPH. Rates represent the means and standard error of the mean of 3-5 biological repeats, each containing 3-5 technical repeats. Differences between groups were evaluated for statistical significance by one-way ANOVA with Tukey's post-hoc analysis. Asterisks and hashtags indicate significant differences from the fed (grey bars) and glucose-free (white bars) values, respectively (,# $P < 0.05$, **,## $P < 0.01$, ***,### $P < 0.001$, ****,#### $P < 0.0001$). Abbreviations are the same as in Figure 3.1.*

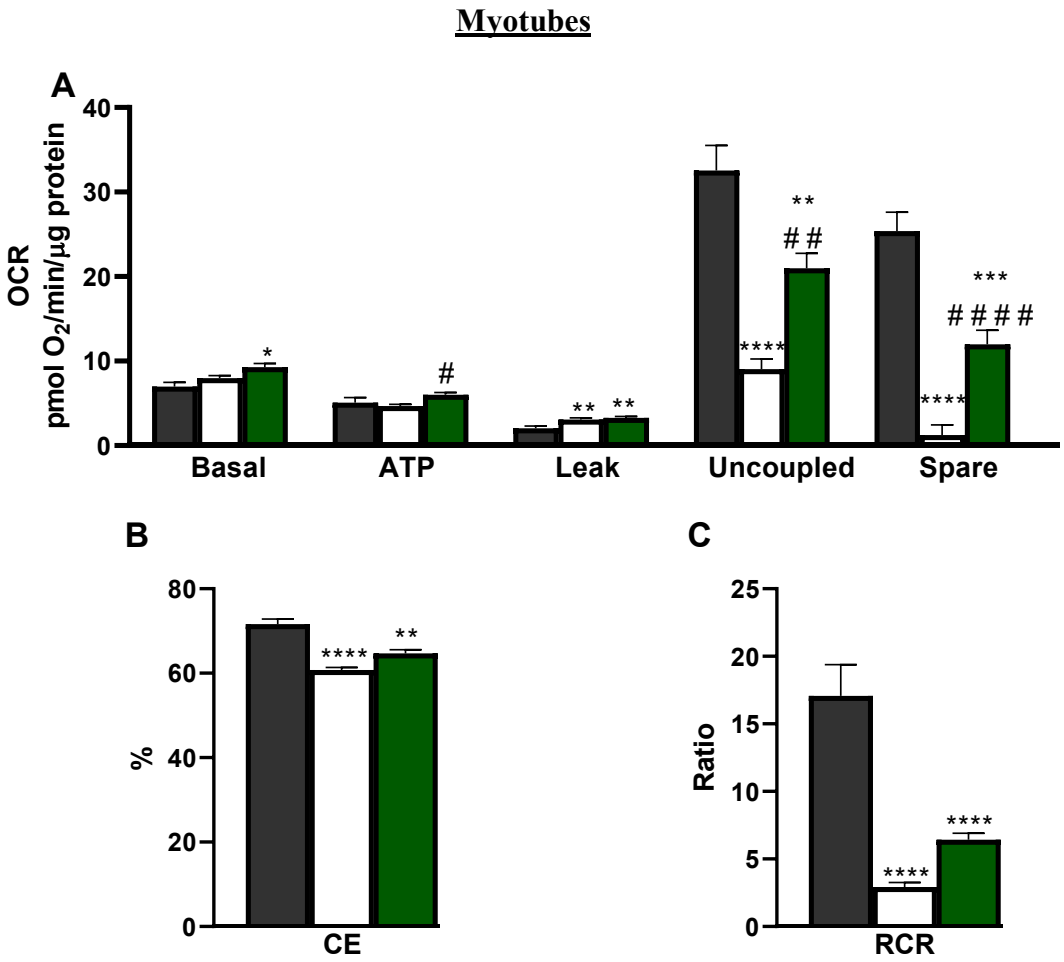

Figure 3.4 – The effects of changes in nutritional background on bioenergetics in L6 myotubes, as measured by Extracellular Flux Analysis.
L6 myotubes were grown and assayed as described in the Methods section (dark-grey), or were deprived of glucose during a 90-minute incubation in glucose-free KRPH before the XF assay (white and dark-green bars). Nutrient-deprived cells were assayed without glucose (white bars) or were subjected to 5mM glucose in the assay before other effectors were added (dark-green bars). Rates represent the means and standard error of the mean of 1-4 biological repeats, each containing 3-5 technical repeats. Differences between groups were evaluated for statistical significance by one-way ANOVA with Tukey's post-hoc analysis. Asterisks and hashtags indicate significant differences from the fed (grey bars) and glucose-free (white bars) values, respectively (,# $P < 0.05$, **,## $P < 0.01$, ***,### $P < 0.001$, ****,#### $P < 0.0001$). Abbreviations are the same as in Figure 3.1.*

Glucose deprivation increases proton leak and thus lowers the coupling efficiency of oxidative phosphorylation

Glucose deprivation causes significant increases in proton-leak-linked respiration in myoblasts and myotubes (Figures 3.3 & 3.4, A). Consequently, the coupling efficiency of oxidative phosphorylation is significantly decreased when cells are deprived of glucose (Figures 3.3 & 3.4, B). Furthermore, the cell respiratory control ratio is also significantly decreased when glucose is withdrawn (Figures 3.3 & 3.4, C), owing to increased proton leak and decreased respiratory capacity (Figures 3.3 & 3.4, A).

Glucose addition partially recovers respiratory effects of glucose deprivation

The reintroduction of glucose during the XF assay following nutrient deprivation recovers the loss of maximum and spare respiratory capacity in glucose-deprived cells, fully in myoblasts (Figure 3.3, A) and partially in myotubes (Figure 3.4, A). Furthermore, glucose addition significantly lowers proton-leak-linked respiration compared to the glucose-deprived state in myoblasts. However, although decreased significantly, the proton leak rate is still significantly higher than that seen in cells that had not been deprived of glucose (Figure 3.3, A). Consequently, the coupling efficiency is significantly increased compared to the glucose-deprived state when glucose is reintroduced to the XF assay in myoblasts (Figure 3.3, B). However, mitochondrial efficiency is not fully restored, as it fails to reach the high coupling efficiency seen in cells that had not been deprived of glucose (Figure 3.3, B). Myotubes differ from myoblasts, as injection of glucose does not attenuate the significant increase in proton-leak-linked respiration seen when cells are deprived of glucose. There is, in fact, a slight increase in proton leak compared to the glucose-deprived state when glucose is

reintroduced to the cells (Figure 3.4, A). However, glucose addition increases the ATP-synthesis-linked OCR (Figure 3.4, A), and thus recovers the decrease in coupling efficiency, albeit only marginally (Figure 3.4, B). Finally, re-applying 5mM glucose following glucose deprivation increases the cell respiratory control ratio compared to the glucose-deprived state significantly in myoblasts (Figure 3.3, C) and marginally in myotubes (Figure 3.4, C). However, the reintroduction of glucose does not restore the respiratory control ratio to its original state, as there is still a significant difference between the respiratory control ratio when glucose is freely available and when glucose is reintroduced into the assay following deprivation (Figures 3.3 & 3.4, C).

Glucose stimulates glycolytic ATP supply

In myoblasts, glucose deprivation significantly lowers basal ECAR, resulting in a significant decrease of the glycolytic ATP supply rate (Figure 3.5, A & B). Since the mitochondrial ATP supply rate is unaffected by nutrient deprivation (Figures 3.5, B), total ATP supply and the glycolytic index are significantly decreased in myoblasts (Figure 3.5, B & C). In myotubes, glucose deprivation does not affect basal ECAR (Figure 3.6, A), glycolytic, mitochondrial or total ATP supply (Figure 3.6, B), nor the glycolytic index (Figure 3.6, C). Notably, the ATP/O_2 ratio is significantly decreased following glucose deprivation in both myoblasts and myotubes (Figures 3.5 & 3.6, D), which reflects the starvation-induced decrease in coupling efficiency (Figures 3.3 & 3.4, B) and decreases in glycolytic ATP supply in myoblasts (Figure 3.5, B).

Glucose addition not only reverses the negative effect of glucose deprivation on glycolytic ATP supply in myoblasts but stimulates the rate to a higher level than that seen in cells that had not been deprived of glucose (Figure 3.5, B). This glucose-induced

stimulation of glycolytic ATP supply is also seen in myotubes (Figure 3.6, B). Accordingly, glucose addition following deprivation significantly increases the glycolytic index in both myoblasts (Figure 3.5, C) and myotubes (Figure 3.6, C). Glucose addition also stimulates the ATP/O_2 ratio in both differentiation states (Figures 3.5 & 3.6, D).

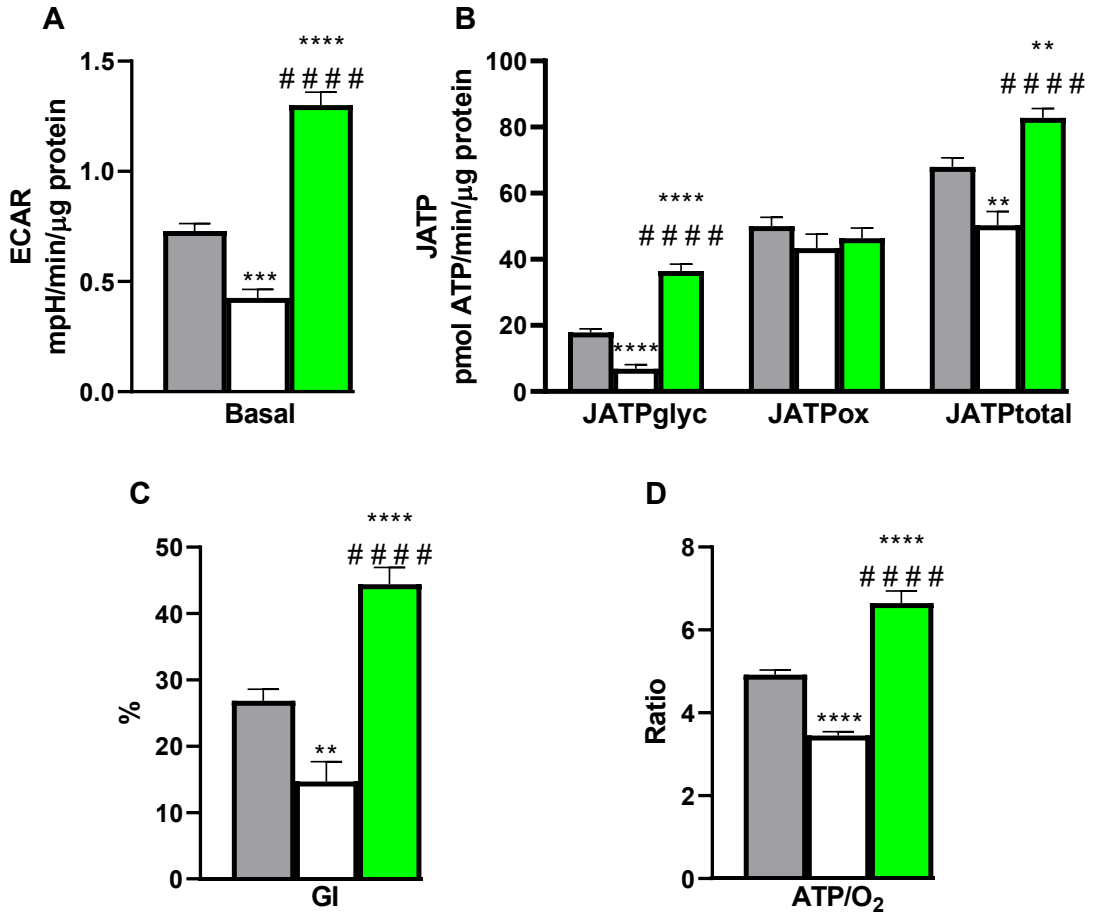

Figure 3.5 – The effects of changes in nutritional background on ECAR and ATP supply in L6 myoblasts, as measured by Extracellular Flux Analysis.
L6 myoblasts were grown and assayed as described in the Methods section (light-grey), or were deprived of glucose during a 90-minute incubation in glucose-free KRPH before the XF assay (white and light-green bars). Nutrient-deprived cells were assayed without glucose (white bars) or were subjected to 5mM glucose in the assay before other effectors were added (light-green bars). The serum concentration of the growth medium was lowered to 2% (v/v) 16 hours before cells were washed into KRPH. Rates represent the means and standard error of the mean of 3-5 biological repeats, each containing 3-5 technical repeats. Differences between groups were evaluated for statistical significance by one-way ANOVA with Tukey's post-hoc analysis. Asterisks and hashtags indicate significant differences from the fed (grey bars) and glucose-free (white bars) values, respectively (,# $P < 0.05$, **,## $P < 0.01$, ***,### $P < 0.001$, ****,#### $P < 0.0001$). Abbreviations are the same as in Figure 3.2.*

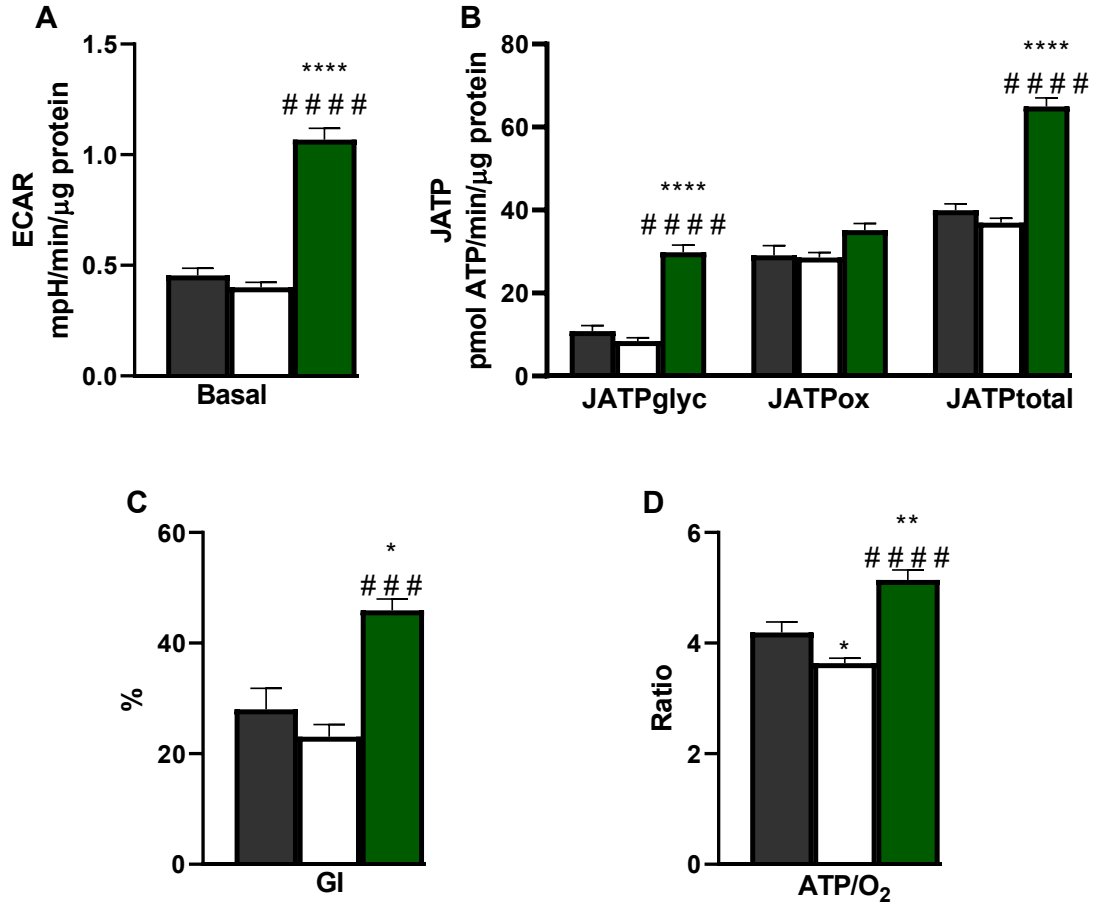

Figure 3.6 – The effects of changes in nutritional background on ECAR and ATP supply in L6 myotubes, as measured by Extracellular Flux Analysis.
L6 myotubes were grown and assayed as described in the Methods section (dark-grey), or were deprived of glucose during a 90-minute incubation in glucose-free KRPH before the XF assay (white and dark-green bars). Nutrient-deprived cells were assayed without glucose (white bars) or were subjected to 5mM glucose in the assay before other effectors were added (dark-green bars). Rates represent the means and standard error of the mean of 1-4 biological repeats, each containing 3-5 technical repeats. Differences between groups were evaluated for statistical significance by one-way ANOVA with Tukey's post-hoc analysis. Asterisks and hashtags indicate significant differences from the fed (grey bars) and glucose-free (white bars) values, respectively (,# $P < 0.05$, **,## $P < 0.01$, ***,### $P < 0.001$, ****,#### $P < 0.0001$). Abbreviations are the same as in Figure 3.2.*

3.3 Discussion

The extracellular flux data shown in this chapter provides a detailed characterisation of the bioenergetic behaviour of static and differentiated L6 myocytes when different nutritional states are applied. These data reveal clear bioenergetic differences between myoblasts and myotubes. These data also reveal that total and spare respiratory capacity diminishes upon glucose deprivation, leading to decreases in the cell respiratory control ratio. Proton-leak-linked respiration increases upon glucose deprivation, leading to significant decreases in the efficiency of mitochondrial ATP production. The detrimental effects of deprivation on these parameters can be partially rescued through the reintroduction of glucose during the XF assay. Basal cellular respiration and mitochondrial ATP supply remain largely unaffected by the nutritional state. However, glucose addition following deprivation stimulates ECAR and glycolytic ATP supply to rates that exceed those that were seen when cells were maintained in glucose throughout the assay. Thus, glucose increases the glycolytic index and lowers the apparent oxygen cost of total ATP supply.

Bioenergetic differences between myoblasts and myotubes

Myotubes have a significantly higher maximum and spare respiratory capacity compared to myoblasts (Figure 3.1, C) when grown and assayed without glucose restriction, which is reflected by a significantly higher cell respiratory control ratio (Figure 3.1, F). These results demonstrate that following differentiation, myotubes have a higher upper limit of ETC activity, a greater ability to oxidise substrates, and that they have a larger capacity to respond to increases in ATP demand compared to myoblasts (Brand *et al.*, 2011). Expression of proteins involved in glucose metabolism, oxidative

phosphorylation, and electron transport are increased by at least 1.5 fold following differentiation of L6 cells (Cui *et al.*, 2009), which is consistent with the increased maximum and spare respiratory capacities observed here.

Although myotubes have a higher (spare) respiratory capacity than myoblasts, their coupling efficiency of oxidative phosphorylation is comparably low (Figure 3.1, E), which is due to a relatively low ATP-synthesis-linked OCR (Figure 3.1, C). Low ATP-synthesis-linked respiration is reflected by a mitochondrial ATP supply rate that is lower in myotubes than in myoblasts (Figure 3.2, A). Notably, glycolytic ATP supply is lower in myotubes than in myoblasts as well (Figure 3.2, A), as is reflected by an ECAR difference (Figure 3.1, D). Consequently, the rate of total ATP supply is lower in myotubes than in myoblasts, which could reflect a relatively low ATP demand (Brand *et al.*, 2011) upon differentiation, as the myotubes are no longer dividing. Notably, the percentage of total ATP supply accounted for by glycolysis is the same in myoblasts and myotubes (Figure 3.2, B), but the oxygen cost of total ATP supply is relatively high in myotubes (Figure 3.2, C).

Glucose control over L6 respiration

Glucose deprivation lowers the maximum (uncoupled) respiratory activity of both myoblasts and myotubes, such that the respiratory capacity of these systems appears the same (Figures 3.3 & 3.4, C). This observation demonstrates that the uncoupled OCR is controlled by glucose availability. In other words, uncouplers increase ATP demand artificially (Brand *et al.*, 2011) and shift control to glucose oxidation. Diminished maximum capacity occurred after only ~2 hours following glucose deprivation and resulted in a negative spare capacity in myoblasts (Figure 3.3). Clearly, it is not possible

to have a spare capacity that is lower than 0. This may have arisen due to the time difference in measurements between basal and maximum respiration (ie when available nutrients may have been lacking). The notion that uncouplers shift control of ATP turnover to glucose oxidation is indeed corroborated by the effect of glucose addition during the XF assay, which rescues (spare) respiratory capacity in glucose-deprived myocytes, fully in myoblasts (Figure 3.3, A) and partially in myotubes (Figure 3.4, A). In other words, such capacity is there but remains unnoticed without fuel. Uncoupled OCRs should thus only be used to estimate (spare) respiratory capacities when substrate supply is not a limiting factor.

Glucose deprivation increases proton leak in myoblasts and myotubes (Figures 3.3 & 3.4, A), which lowers coupling efficiency (Figures 3.3 & 3.4, B). This observation may explain why L6 myotube coupling efficiencies reported by others are somewhat higher than the value presented here (71.6%) (Figure 3.4, B). For example, coupling efficiencies of 77% and 87% were measured by Ahmed *et al.* (2020) and Genders *et al.* (2019), respectively, in respiratory assays fuelled by 5mM glucose + 4mM glutamine and 25mM glucose, i.e., substrate levels higher than the 5mM glucose alone applied here. The mechanism of this starvation-induced increase in proton leak is presently unclear but may be speculated to involve reactive oxygen species (Brand, 2000). In support of such speculation, starvation increases reactive oxygen species generation in CHO and HeLa cells in as little as 15 minutes (Scherz-Shouval *et al.*, 2007), and mRNA levels of uncoupling protein 2 and uncoupling protein 3, which likely play a part in proton leak (Divakaruni *et al.*, 2011), are increased by starvation in rat skeletal muscle (Cadenasa *et al.*, 1999). Moreover, mice under-expressing uncoupling protein 3, which has been shown to decrease reactive oxygen species production in skeletal muscle mitochondria (Toime *et al.*, 2010), have increased ROS-induced

damage (Brand *et al.*, 2002). Thus, increased reactive oxygen species production, due to starvation, may initiate the upregulation and activation of uncoupling proteins, leading to increased proton leak to protect the cells from the detrimental effects of oxidative stress. The apparent irreversibility of the glucose-deprivation-induced proton leak increase in myotubes (Figure 3.4, A) is consistent with such a mechanism, but the suggestion is weakened by the observation that glucose addition during the XF assay *acutely* lowers proton leak of glucose-deprived myoblasts (Figure 3.3, A). To test whether starvation-induced ROS production and UCP activation plays a role in increased proton leak, UCP knock-down cells could be cultured and subjected to starvation, with measurements of ROS production by fluorescent probes, such as dihydroethidum (Scherz-Shouval *et al.*, 2007) and proton leak via XF analysis.

Glucose lowers the apparent oxygen cost of ATP synthesis

In addition to the respiratory effects discussed above, arguably the most striking observation reported in this chapter is the acute significant glucose stimulation of glycolytic ATP supply (Figures 3.5 & 3.6, B). This stimulation is consistent with glucose-induced ECAR increases reported before (Nisr *et al.*, 2014). The glucose-induced increase in glycolytic ATP supply raises the glycolytic index of both myoblasts and myotubes, and, consequently, lowers the apparent oxygen cost of total ATP supply (Figures 3.5 & 3.6, C & D). This observation suggests that any agent that modulates glucose availability may regulate the oxygen cost of ATP supply. Insulin is known to increase glucose uptake in skeletal muscle cells (Nisr *et al.*, 2014, 2016), and nitrogen species increase the expression (Vaughan *et al.*, 2016) and translocation (Jiang *et al.*, 2014) of GLUT4, which could indicate an increase in glucose uptake. It is thus conceivable that nitrite and insulin lower the oxygen cost of myocellular ATP synthesis. This possibility is tested in the next chapter.

4 Nitrite and insulin decrease the oxygen cost of ATP synthesis in skeletal muscle cells by increasing the rate of glycolytic ATP supply

4.1 Introduction

Dietary nitrate supplementation lowers the oxygen cost of submaximal exercise by decreasing the respiratory activity required to drive skeletal muscle work at a set rate (Larsen *et al.*, 2007; Lansley, Winyard, Fulford, *et al.*, 2011). Nitrate supplementation also benefits exercise by increasing exercise tolerance by ~22% (Breese *et al.*, 2013; Bailey *et al.*, 2015) and improving power output and performance (Lansley, Winyard, Bailey, *et al.*, 2011; Murphy *et al.*, 2012). Mechanistic understanding of how nitrate improves human skeletal muscle function is incomplete, but most models predict changes in skeletal muscle bioenergetics. The lowered oxygen cost of exercise following nitrate supplementation (Larsen *et al.*, 2007) has been attributed to improved efficiency of oxidative phosphorylation through lowered proton leak (Larsen *et al.*, 2011). These effects on myocyte energy metabolism have also been found in response to insulin, which lowers proton leak, resulting in increased coupling efficiency (Nisr *et al.*, 2014). Furthermore, nitrogen species improve the diabetic phenotype in mice (Jiang *et al.*, 2014; Singamsetty *et al.*, 2015) and may increase glucose uptake by cells (Vaughan *et al.*, 2016), possibly by improving insulin sensitivity. It is thus conceivable that dietary nitrate and insulin affect myocellular bioenergetics through similar mechanisms.

The idea that dietary nitrate lowers the oxygen cost of exercise by increasing the coupling efficiency of oxidative phosphorylation (Larsen *et al.*, 2011) remains controversial (Whitfield *et al.*, 2016; see Chapter 1). The data presented in Chapter 3

demonstrate that the oxygen cost of myocellular ATP synthesis is acutely lowered by glucose. This finding suggests the possibility that dietary nitrate lowers the oxygen cost of exercise by increasing glucose availability. It is generally thought (Larsen *et al.*, 2007; Shannon *et al.*, 2017) that the exercise benefit of nitrate is mediated by nitric oxide. However, nitrate is unlikely fully reduced to nitric oxide during submaximal exercise (Affourtit *et al.*, 2015; see Introduction), which is why I decided to determine how nitrite (the reduction intermediate between nitrate and nitric oxide) affects the bioenergetic behaviour of L6 myocytes. Because of possible mechanistic overlap, I explored the effect of insulin in the same set of experiments. The data reported in this chapter show that both nitrite and insulin acutely lower the oxygen cost of total ATP synthesis by increasing the rate of glycolytic ATP supply.

4.2 Results

Nitrite and insulin effects on mitochondrial respiration

L6 myocytes grown in 5mM glucose were exposed for 30 minutes to 1μM $NaNO_2$ or 100nM insulin before XF analysis. Acute effects of nitrite and insulin on myoblast and myotube respiration are summarised in Figures 4.1 and 4.2, respectively. In myoblasts, nitrite lowers basal mitochondrial respiration, respiration associated with proton leak, respiration coupled to ATP synthesis and uncoupled respiration, as well as the spare respiratory capacity, and marginally increases the cell respiratory control ratio (Figure 4.1, A and B), but only the effect on basal respiration is statistically significant (Figure 4.1, G). Notably, nitrite does *not* affect the coupling efficiency of oxidative phosphorylation (Figure 4.1, G). In myotubes, none of the respiratory parameters, including coupling efficiency, are affected significantly by nitrite exposure (Figure 4.2, A, B, D, E and G).

Insulin has little effect on oxygen consumption in myoblasts, (Figure 4.1, A, C, D, F & H). A statistically non-significant decrease in proton-leak-linked respiration, without a change in maximum respiration, tends to marginally increase the cell respiratory control ratio (Figure 4.1, H). Because there is no change in basal or ATP-synthesis-linked respiration, there is no effect of insulin on coupling efficiency in myoblasts (Figure 4.1, H). In myotubes on the other hand (Figure 4.2), insulin significantly lowers respiration linked to mitochondrial proton leak (Figure 4.2, A, C & H). The insulin-induced decrease in proton leak leads to significant increases in coupling efficiency and the cell respiratory control ratio (Figure 4.2, D, F & H). Other mitochondrial respiratory rates remain unaffected by insulin in myotubes (Figure 4.2, A, C and H).

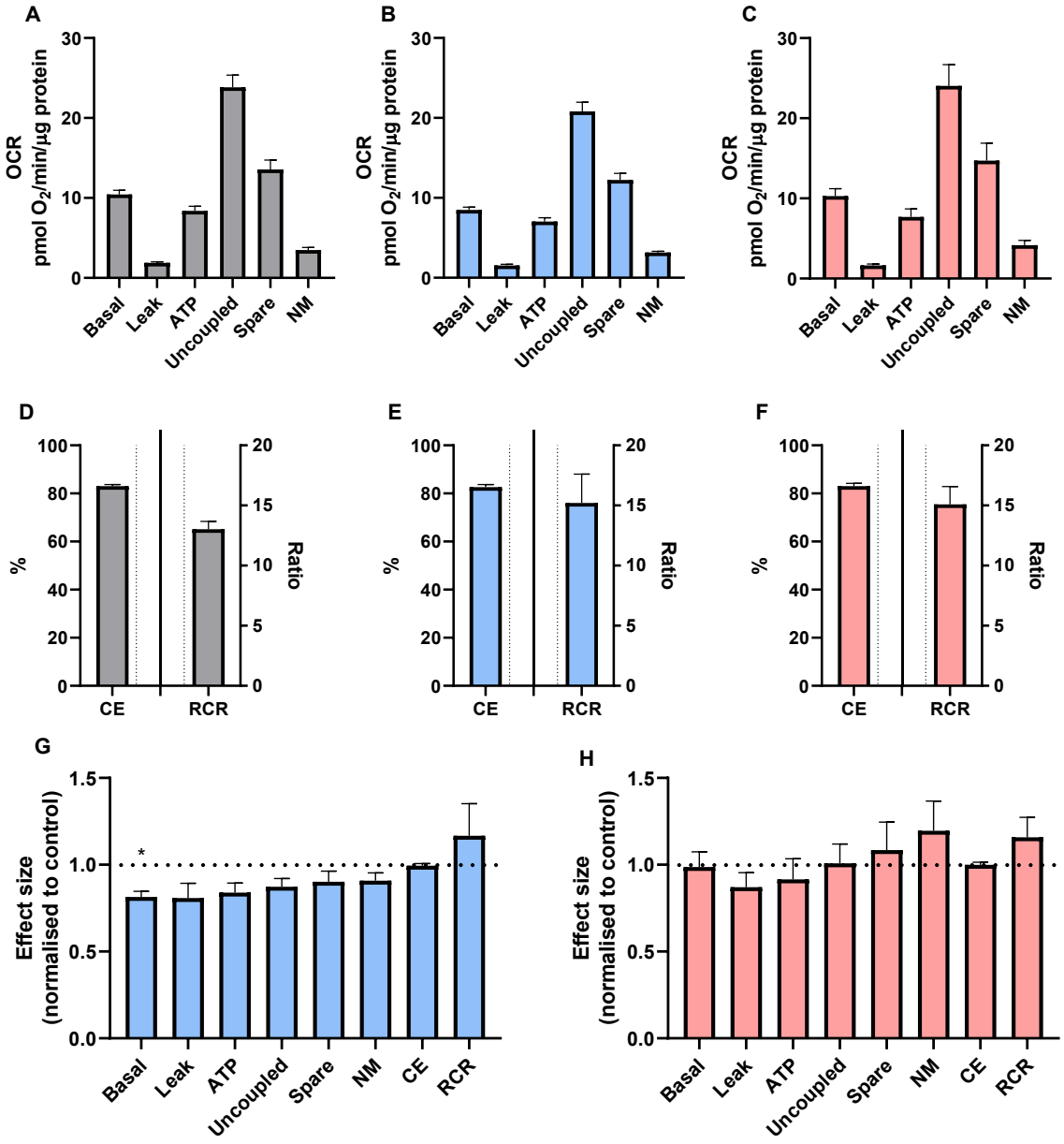

Figure 4.1 – nitrite and insulin effects on the respiratory activity of L6 myoblasts
*The protein-normalised respiratory activity (A, B & C), coupling efficiency (CE) and respiratory control ratio (RCR) (D, E & F) by L6 myoblasts as measured by Extracellular Flux Analysis. Cells cultured in fully supplemented medium were incubated for 90 minutes in KRPH containing 5mM glucose before XF analysis, and then assayed without (grey bars: control data also shown in. Chapter 3) or with 100nM human insulin (red bars). Another group of cells was subjected to 1µM $NaNO_2$ for the last 30 min of the pre-incubation and assayed without insulin (blue bars). The control-normalised rates obtained in the presence of 1µM $NaNO_2$ (G) and 100nM insulin (H) are also shown. All rates were obtained in the same manner as described by the oxygen consumption traces reported in Chapter 3 and were calculated as described in the Methods. Rates represent the mean and standard error of the mean of 2-3 biological repeats, each containing 3-5 technical repeats. Significance was tested using an unpaired T-test in G & H. * = p <0.05, ** = p <0.01, *** = p <0.001, **** = p <0.0001.*

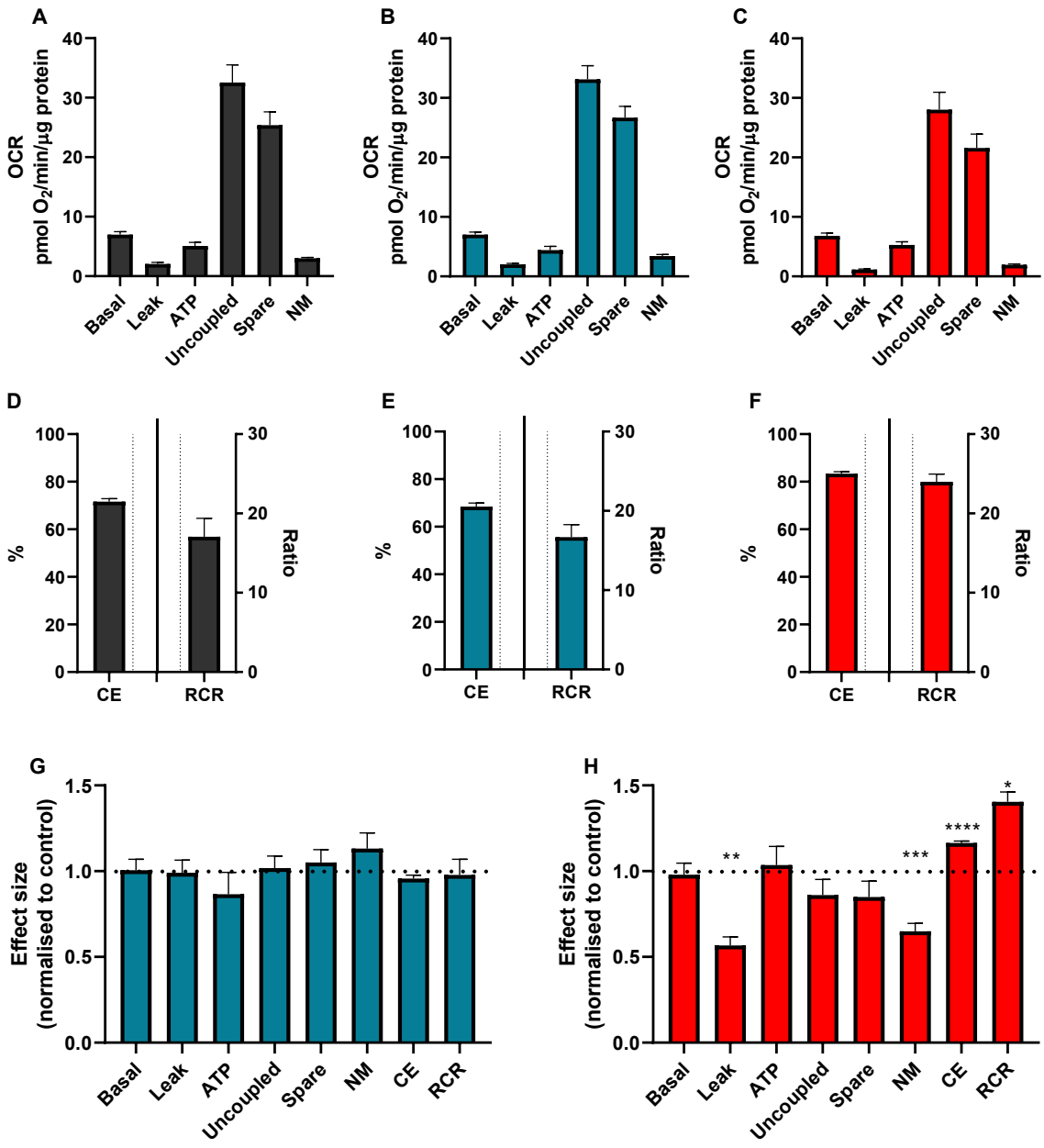

Figure 4.2 – The respiratory activity of L6 myotubes in response to nitrite and insulin.
*The protein-normalised respiratory activity (A, B & C), coupling efficiency (CE) and respiratory control ratio (RCR) (D, E & F) by L6 myotubes as measured by Extracellular Flux Analysis. Cells cultured in fully supplemented medium were incubated for 90 minutes in KRPH containing 5mM glucose before XF analysis, and then assayed without (grey bars: control data also shown in. Chapter 3) or with 100nM human insulin (red bars). Another group of cells was subjected to 1µM $NaNO_2$ for the last 30 min of the pre-incubation and assayed without insulin (blue bars). The control-normalised rates obtained in the presence of 1µM $NaNO_2$ (G) and 100nM insulin (H) are also shown. All rates were obtained in the same manner as described by the oxygen consumption traces reported in Chapter 3 and were calculated as described in the Methods. Rates represent the mean and standard error of the mean of 2 biological repeats, each containing 3-5 technical repeats. Significance was tested using an unpaired T-test in G & H. * = p <0.05, ** = p <0.01, *** = p <0.001, **** = p <0.0001.*

Nitrite and insulin effects on ATP synthesis

In addition to effects on respiration, acute effects of nitrite and insulin on medium acidification by L6 myoblasts (Figure 4.3) and myotubes (Figure 4.4) were measured. Acidification and respiratory data were combined to calculate the effects of nitrite and insulin on ATP supply rates, the glycolytic index, and the ATP/O_2 ratio. Nitrite significantly increases basal ECAR in both myoblasts (Figure 4.3, G) and myotubes (Figure 4.4, G) by about 40%. The nitrite-induced increase in basal ECAR is reflected by rises in the rate of glycolytic ATP supply in both differentiation states by 60%. Nitrite does not significantly affect the rate of mitochondrial ATP synthesis in myotubes (Figure 4.4, G), but lowers this rate significantly in myoblasts (Figure 4.3, G) from 50 pmol ATP/min/µg protein in the control (Figure 4.3, A) to 40 pmol ATP/min/µg protein after nitrite exposure (Figure 4.3, B). As glycolytic ATP supply is significantly increased, but mitochondrial ATP supply is significantly decreased in myoblasts exposed to 1µM $NaNO_2$, total ATP supply remains unaffected when compared to the control (Figure 4.3, G). Total ATP supply is significantly increased by nitrite in myotubes (Figure 4.4, G), rising from approximately 40 pmol ATP/min/µg protein in the control (Figure 4.4, A) to 46 pmol ATP/min/µg protein after nitrite exposure (Figure 4.4, B).

Because nitrite has a significant impact on glycolytic ATP supply, the glycolytic index is also increased (Figures 4.3 & 4.4, D, E & G): it rises from 27% to 41% in myoblasts and from 28% to 37% in myotubes. In myoblasts, this increase is highly statistically significant when normalised to the control (Figure 4.3, G). Thus, nitrite pushes both systems acutely toward a more glycolytic phenotype. Furthermore, nitrite lowers the apparent oxygen cost of total ATP synthesis. Nitrite significantly increases the ATP/O_2 ratio (ATP supply normalised to total cellular respiration) from 4.9 to 6.3 in

myoblasts (Figure 4.3, E & G), and tends to increase it in myotubes (Figure 4.4, E & G), raising the ratio from 4.2 to 4.6.

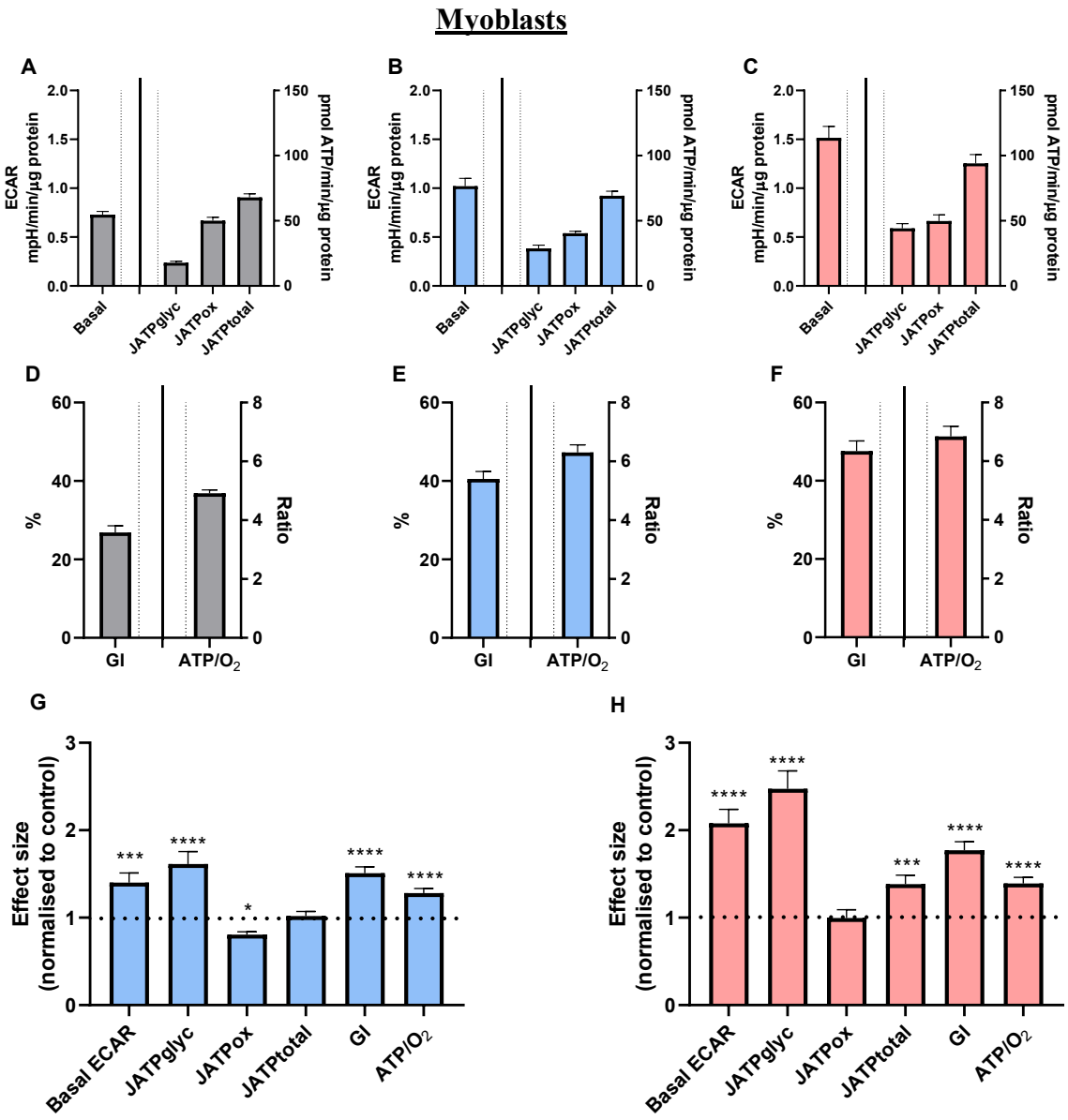

Figure 4.3 – The ATP supply rates of L6 myoblasts in response to nitrite and insulin.
*Cells cultured in fully supplemented medium were incubated for 90 minutes in KRPH containing 5mM glucose before XF analysis, and then assayed without (grey bars: control data also shown in. Chapter 3) or with 100nM human insulin (red bars). Another group of cells was subjected to 1µM $NaNO_2$ for the last 30 min of the pre-incubation and assayed without insulin (blue bars). Basal ECAR, ATP supply rates (J_{ATP}), the glycolytic index (GI) and the ATP/O_2 ratio are given as absolute (panels A-F) and control-normalised (panel G-H) values, and are means ± SEM of 2-3 independent XF runs, each containing 3-5 technical repeats. Significance was tested using an unpaired T-test in G & H. * = p <0.05, ** = p <0.01, *** = p <0.001, **** = p <0.0001.*

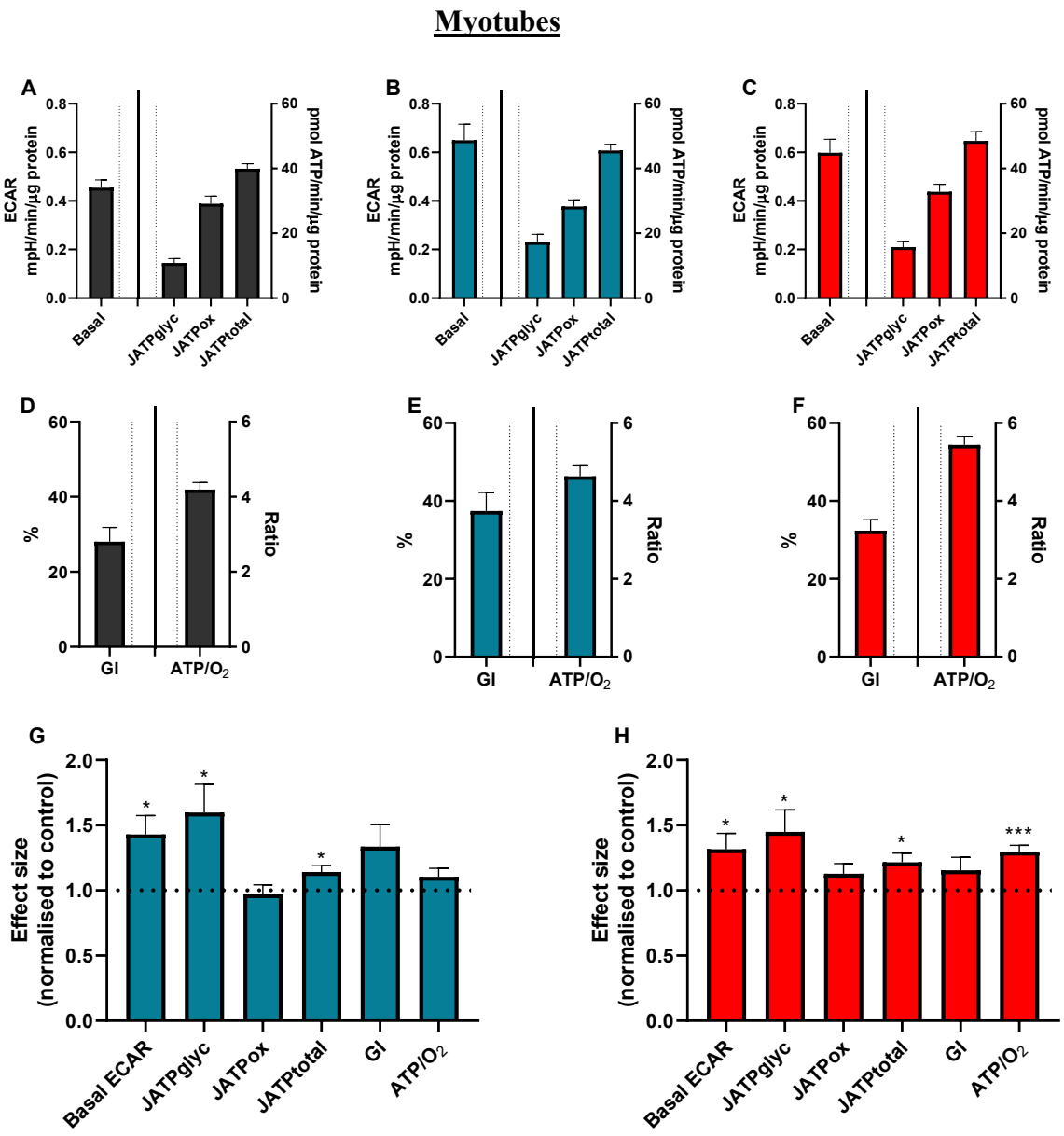

Figure 4.4 - The ATP supply rates of L6 myotubes in response to nitrite and insulin.
*Cells cultured in fully supplemented medium were incubated for 90 minutes in KRPH containing 5mM glucose before XF analysis, and then assayed without (grey bars: controls; cf. Chapter 3) or with 100nM human insulin (red bars). Another group of cells was subjected to 1µM $NaNO_2$ for the last 30 min of the pre-incubation and assayed without insulin (blue bars). Basal ECAR, ATP supply rates (J_{ATP}), the glycolytic index (GI) and the ATP/O_2 ratio are given as absolute (panels A-F) and control-normalised (panel G-H) values, and are means ± SEM of 2 independent XF runs, each containing 3-5 technical repeats. Significance was tested using an unpaired T-test in G & H. * = p <0.05, ** = p <0.01, *** = p <0.001, **** = p <0.0001.*

Insulin significantly increases basal ECAR in both myoblasts (Figure 4.3, C & H) and myotubes (Figure 4.4, C & H). This increase is reflected by a statistically significant rise in glycolytic ATP supply (Figures 4.3 & 4.4, H). The rise in glycolytic ATP supply is from 18 to 44 pmol ATP/min/µg protein in myoblasts (Figure 4.3, A & C), and from 11 to 16 pmol ATP/min/µg protein in myotubes (Figure 4.4, A & C). Insulin does not significantly affect the rate of mitochondrial ATP synthesis and therefore the increased glycolytic ATP supply raises total ATP supply in both myoblasts and myotubes (Figures 4.3 & 4.4, H). The difference in total ATP supply between the control and when insulin is applied is 26 pmol ATP/min/µg protein for myoblasts (Figure 4.3, A & C) and 9 pmol ATP/min/µg protein for myotubes (Figure 4.4, A & C).

The stimulation of glycolytic ATP synthesis by insulin pushes myoblasts into a more glycolytic phenotype, as seen by the significant increase in the glycolytic index (Figure 4.3, F & H). Insulin only slightly increases the glycolytic index in myotubes (Figure 4.4, F & H). The effect of insulin on the glycolytic index in myotubes is not statistically significant, likely because the magnitude of glycolytic ATP supply stimulation is not as substantial in myotubes compared to myoblasts. Insulin also lowers the apparent oxygen cost of total ATP synthesis. Insulin causes significant increases in the ATP/O_2 ratio in myoblasts (Figure 4.3, F & H), rising from 4.9 to 6.8, and in myotubes (Figure 4.4, F & H), rising from 4.2 to 5.4.

The XF analysis presented in Figures 4.3 and 4.4 demonstrates that both nitrite and insulin lower the oxygen cost of ATP supply by increasing the rate of glycolysis. A comparably high glycolytic activity is reflected by nitrite- and insulin-induced stimulation of ECAR. Seeking independent support for increased medium acidification, lactate release from L6 myocytes was measured directly. Lactate is released at a rate of 3.8 ± 0.39 pmol/min/µg protein in myoblasts (Figure 4.5, A). This rate is increased by

nitrite and insulin, respectively, to 4.2 ± 0.27 and 5.1 ± 0.24 pmol/min/µg (Figure 4.5, A). Nitrite and insulin thus stimulate lactate release 1.1-fold and 1.3-fold, respectively. The 95% confidence intervals given in the legend to Figure 4.5 suggest that the stimulatory effect of insulin is statistically significant. Although comparably modest, the nitrite and insulin effects are both consistent with the observed changes in basal ECAR and glycolytic ATP supply (Figure 4.3, G & H). Nitrite tends to increase the rate of lactate release from myotubes (from 4.1 ± 0.28 to 4.4 ± 0.28 pmol lactate/min/ µg protein), but this effect is not statistically significant (Figure 4.5, B). Insulin does not increase lactate release from myotubes (Figure 4.5, B).

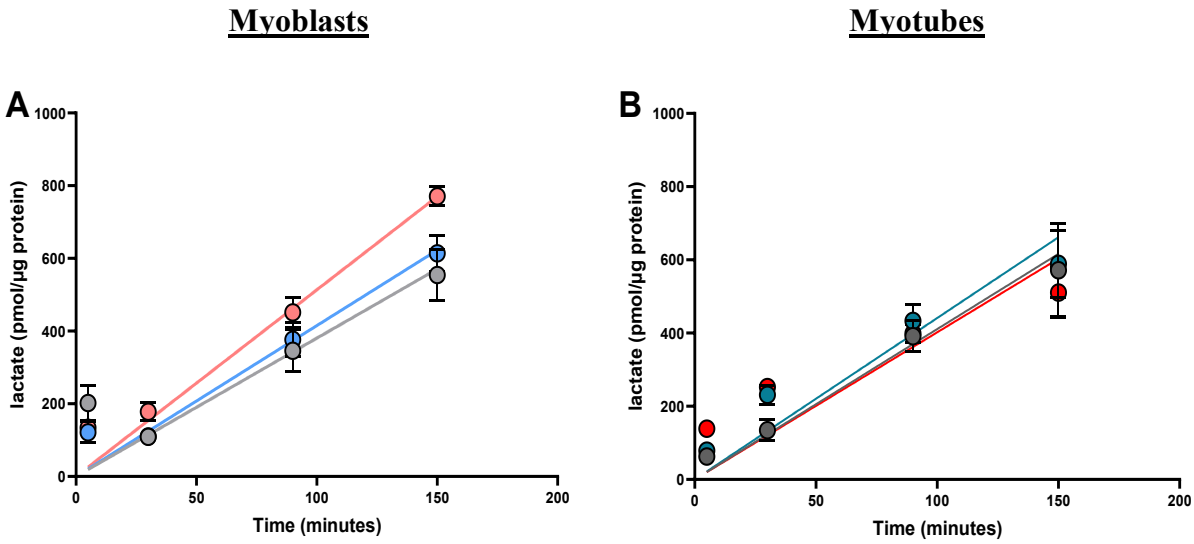

Figure 4.5 – Lactate release by L6 myoblasts and myotubes in response to nitrite and insulin.

Lactate release was measured after 5, 30, 90 and 150 minutes in L6 myoblasts (panel A) and myotubes (panel B) grown in the presence of 5mM glucose. Culture medium was removed from the cells and they were immediately incubated in KRPH under air at 37 ºC without (grey symbols) or with either 1µM $NaNO_2$ (blue symbols) or 100nM insulin (red symbols). Data are means ± SEM of 8-21 separate measurements from 2-5 independent assays, and were fitted to linear expressions 'forced' through the origin. The mean (SEM) fit slopes for myoblasts are 3.8 (0.39), 4.2 (0.27) and 5.1 (0.24) pmol lactate released per min per µg protein for control, nitrite-exposed and insulin-exposed cells, respectively, with 95% confidence intervals of 3.0-4.6, 3.6-4.7 and 4.7-5.6 pmol/min/µg. The mean (SEM) fit slopes for myotubes are 4.1 (0.24), 4.4 (0.23) and 4.0 (0.25) pmol lactate released per min per µg protein for control, nitrite-exposed and insulin-exposed cells, respectively, with 95% confidence intervals of 3.5-4.7, 3.9-5.0 and 3.4-4.5 pmol/min/µg.

4.3 Discussion

This chapter aimed to explore and compare the effects of nitrite and insulin on the bioenergetics of L6 myocytes. These experiments aimed to explore the hypothesis that nitrite may lower the oxygen cost of ATP synthesis and that, due to their previously reported similarities, nitrite and insulin may impact skeletal muscle bioenergetics in the same way. The data reported in this chapter reveal that both nitrite and insulin indeed lower the oxygen cost of total ATP supply in myoblasts and myotubes. In both cases, the effect is owing to an increased glycolytic index that follows from stimulation of glycolytic ATP supply. This novel observation demonstrates the depth of insight that may be obtained from analysing XF data in detail, as the bioenergetic shift towards a more glycolytic phenotype is not immediately obvious from the oxygen consumption and medium acidification data *per se*. Notably, nitrite does not increase the efficiency of oxidative phosphorylation. These findings inform the ongoing debate as to how dietary nitrate lowers the oxygen cost of exercise.

Nitrite does not increase mitochondrial efficiency

Dietary nitrate supplementation increases circulating nitrite (Govoni *et al.*, 2008). Therefore, the effect of nitrite on muscle bioenergetics was tested. Nitrite does *not* increase coupling efficiency acutely, neither in myoblasts nor myotubes (Figures 4.1 & 4.2, E & G). These results are at odds with the reported stimulatory effect of sodium nitrate on mitochondrial efficiency (Larsen *et al.*, 2011), but consistent with the reported lack of beneficial effect of dietary nitrate on oxidative metabolism (Whitfield *et al.*, 2016; Ivarsson *et al.*, 2017). One reason my results are at odds could be that the exposure time to nitrite used here is insufficient to elicit such a response. Larsen and

colleagues (2011) implemented a supplementation protocol that included 3 days exposure to sodium nitrate, and cellular studies that show improvement in coupling efficiency, albeit due to increased basal respiration rather than decreased proton leak, exposed cells to beetroot juice for 24 hours (Vaughan *et al.*, 2016). However, 7 days supplementation of beetroot juice in humans had an exercise benefit without a change in coupling efficiency (Whitfield *et al.*, 2016), and 3 weeks of sodium nitrate supplementation in mice decreased the P/O ratio compared to a control (Ivarsson *et al.*, 2017). Furthermore, no difference was observed in oxidative phosphorylation, proton leak and the P/O ratio in mitochondria isolated from zebrafish given sodium nitrate or sodium nitrite in their water for 21 days and control mitochondria (Axton *et al.*, 2019). It was hypothesised that nitrite effects on myocyte bioenergetics might occur similarly to insulin, as both insulin (Nisr *et al.*, 2014) and nitrogen species (Larsen *et al.*, 2011) have been found to decrease proton leak, leading to increased coupling efficiency. Here, nitrite does not improve coupling efficiency in either myoblasts or myotubes. Importantly, the lack of acute nitrite effect on coupling efficiency is not due to assay limitations, as the data demonstrate insulin acutely increases coupling efficiency in myotubes (Figure 4.2, H).

Insulin lowers proton-leak-linked respiration, leading to increases in the coupling efficiency and cell respiratory control ratio in myotubes (Figure 4.2, F & H). The insulin effect on respiration rates in myotubes is consistent with those reported previously (Nisr *et al.*, 2014). However, the lack of effect of insulin on respiration rates in myoblasts (Figure 4.1, C, F & H) is not. It has previously been reported that myocytes need to be deprived from FBS and glucose to induce a cellular response to insulin (Ching *et al.*, 2010; Nisr *et al.*, 2014). Here, myoblasts were not cultured in decreased FBS and did not undergo glucose restriction during the assay. The differences

in results could also be explained by differences in cell culture, as previously myoblasts were seeded at a higher density, grown for a further 48 hours in DMEM with 25mM glucose, and underwent reductions in FBS and glucose (5mM) overnight (Nisr *et al.*, 2014). The relatively high confluence expected from the previous cell culture regime may have provoked some myoblast differentiation, as L6 cells differentiate on confluence (Pinset *et al.*, 1982). Therefore, insulin's effect on coupling efficiency and respiratory control is much stronger in, and may be exclusive to, myotubes. However, insulin does indeed increase coupling efficiency in myoblasts that are deprived of nutrients (Chapter 5, Figure 5.4). Notably, nitrite and insulin affect the oxidative metabolism of L6 myocytes in different ways.

Insulin effects on mitochondrial ATP synthesis

Insulin effects on mitochondrial function have been reported by others before. Insulin was found to stimulate mitochondrial ATP synthesis, which was attributed to the increased oxidative capacity of mitochondria, through increased mitochondrial protein synthesis, and increases in the activity of citrate synthase and cytochrome *c* oxidase (Stump *et al.*, 2003). The insulin effect on coupling efficiency and cell respiratory control reported in this chapter (Figure 4.2, F & H) are exclusively owing to decreased proton leak, as other respiratory rates are unaffected. These data agree with previously reported findings (Nisr *et al.*, 2014) but disagree with insulin's ability to increase respiratory capacity in both human (Stump *et al.*, 2003) and C2C12 myotubes (Yang *et al.*, 2012). This discrepancy may be related to the different insulin exposure times.

The mechanism by which insulin decreases proton leak is unknown at present. Mitochondrial efficiency may be increased by insulin's stimulatory effect on

mitochondrial protein synthesis (Boirie *et al.*, 2001; Stump *et al.*, 2003; Robinson *et al.*, 2014) and the increased expression and activity of enzymes involved in oxidative phosphorylation (Stump *et al.*, 2003; Robinson *et al.*, 2014). However, exposure to insulin in the studies mentioned occurred over a much longer time, compared to the 30-minute exposure herein. Because the insulin effect on proton leak reported here emerges on a relatively short timescale, the changes are unlikely related to protein expression effects. Thus, insulin's effect on coupling efficiency and respiratory control here is likely due to a 'direct' attenuation of proton leak. Again, however, the underlying mechanism is unclear. One possibility that cannot be excluded at this stage is that insulin lowers proton leak indirectly by increasing energy demand. As discussed in detail in the Introduction, insulin likely increases ATP demand substantially. Insulin-induced energy demand will lower the ATP/ADP ratio and consequently the proton-motive force. It is conceivable that the contribution of proton leak to overall respiration is relatively low at the decreased proton-motive force, which would be reflected by a relatively high coupling efficiency (Affourtit *et al.*, 2006).

Nitrite and insulin effects on glycolytic ATP supply

Although the respiratory effects of nitrite and insulin appear different, both compounds were found to increase extracellular acidification and glycolytic ATP supply, regardless of L6 differentiation state, thus pushing the cells into a more glycolytic phenotype (Figures 4.3 & 4.4, G & H). The effect of insulin on ECAR is consistent with insulin's significant effect on ECAR in C2C12 myotubes (Yang *et al.*, 2012) and the insulin-induced increases in ECAR in human and L6 myocytes (Nisr *et al.*, 2014). The rise in glycolytic ATP supply was sufficient to raise overall ATP supply leading to increases in the ATP/O_2 ratio (Figures 4.3 & 4.4, G & H). Stimulation of glycolytic ATP supply and

the ATP/O_2 ratio in response to nitrite and insulin lowers the apparent oxygen cost of ATP synthesis, which is not clear from the 'raw' oxygen uptake and medium acidification data.

The finding that nitrite lowers the apparent oxygen cost of ATP synthesis, by increasing glycolytic ATP production, offers a possible explanation for the lowering effect of dietary nitrate on the oxygen cost of exercise (Larsen *et al.*, 2007; Bailey *et al.*, 2009; Lansley, Winyard, Fulford, *et al.*, 2011). The data presented here show that glycolytic ATP synthesis is significantly increased following a 30-minute exposure to nitrite (Figure 4.3 & 4.4, G). The stimulatory effect of nitrite on glycolytic ATP supply is present regardless of L6 differentiation state, although it is more pronounced in undifferentiated myoblasts than in myotubes. These XF data disagree with the reported lack of change in blood lactate levels following nitrate supplementation (Larsen *et al.*, 2007) and the significantly decreased basal and peak ECAR in C2C12 myocytes treated with beetroot juice (Vaughan *et al.*, 2016). The data also disagree with a study that reported a lack of nitrate effect of glycolytic ATP supply, which was assessed using ^{31}P-MRS, following 6 days supplementation with beetroot juice (Bailey *et al.*, 2010). However, human studies utilising different exercise and supplementation protocols observe increases in blood lactate levels in response to nitrogen species (Wylie *et al.*, 2016; Domínguez, Garnacho-Castaño, *et al.*, 2017; Shannon *et al.*, 2017), indicating that ATP synthesis through anaerobic glycolysis may be increased. Furthermore, sodium nitrate and sodium nitrite treatment in zebrafish significantly increase the abundance of several glycolytic intermediates and lactate at rest (Axton *et al.*, 2019). These findings support the assertion that nitrogen species may decrease oxygen uptake during submaximal workloads (Larsen *et al.*, 2007; Bailey *et al.*, 2009; Lansley,

Winyard, Fulford, *et al.*, 2011) by increasing the activity of non-oxidative ways of ATP production, thus lowering the apparent oxygen cost of total ATP synthesis.

The lactate measurements obtained here (Figure 4.5) only partially support the findings obtained by XF Analysis. The cause for the difference in results could be due to the difference in experimental design. During XF analysis, several wash and incubation steps occur prior to placement into the analyser, which was not possible during the lactate assay as the medium contains the lactate. Furthermore, during XF analysis, DMEM, which contains other energy sources such as sodium pyruvate and glutamine, was removed and cells were incubated in KRPH with glucose as the only fuel for 1 hour, before removal and exposure to nitrite for 30 minutes, which was then removed and followed by exposure to insulin for 20 minutes. During the lactate assay, DMEM was removed and KRPH +/- nitrite and +/- insulin was added immediately, followed by medium removals at the stated time points. It could be that the cells require an initial period without the other nutrients available in DMEM to obtain the results seen during XF analysis. Finally, there is also a potential that the experiment did not work. High lactate measurements were obtained at the 5 minute point and this results in no change in lactate release in some of the conditions between 5 minutes and 30 minutes, which could indicate an issue with the experiment itself. However, increased lactate release in L6 myocytes exposed to nitrite and insulin have been observed previously in our hands (Wynne and Affourtit, unpublished data).

Insulin stimulates glycolytic ATP supply more strongly in myoblasts than in myotubes (Figures 4.3 & 4.4, H). This difference in magnitude to which insulin stimulates glycolytic ATP supply indicates that this effect is mechanistically distinct from the insulin effect on coupling efficiency and the respiratory control ratio, which appears to be exclusive to myotubes. This mechanistic distinction is also suggested by

the similarity between the nitrite and insulin effects on glycolytic ATP supply and the observation that nitrite does not affect proton leak or indeed coupling efficiency. Thus, while their effects on oxygen consumption are not the same, at face value nitrite and insulin effects on glycolytic ATP supply are comparable.

4.4 Conclusion

Nitrite does not impact oxygen consumption by L6 myocytes, which strengthens the hypothesis that nitrogen species do not improve mitochondrial efficiency. Insulin, on the other hand, improves coupling efficiency and the cell respiratory control ratio in myotubes, likely because of direct attenuation of proton leak. The rate of glycolytic ATP synthesis in skeletal muscle cells is increased by exposure to nitrite and insulin, which decreases the apparent oxygen cost of ATP supply. The nitrite and insulin effects on glycolytic ATP supply are similar to those achieved by glucose addition (Chapter 3, Figures 3.5 & 3.6) and may be owing to the stimulation of glucose uptake. This possibility is explored in the following chapter.

5 Nitrite and insulin stimulate glycolytic ATP supply irrespective of glucose availability

5.1 Introduction

Nitrite and insulin were found to stimulate glycolytic ATP supply in L6 myoblasts and myotubes, which was sufficient to cause rises in total ATP supply (Chapter 4, Figures 4.3 & 4.4). Similar bioenergetic effects have been observed in response to direct glucose addition (Chapter 3, Figures 3.5 & 3.6). Insulin drives glucose uptake in skeletal muscle cells (Richter *et al.*, 2013) and injection of 2mM glucose instantly stimulates acidification of the extracellular medium but leaves oxygen consumption unaffected in L6 cells exposed to insulin (Nisr *et al.*, 2014). Furthermore, beetroot juice was shown to increase GLUT4 gene and protein expression in C2C12 myocytes (Vaughan *et al.*, 2016). Thus, nitrite and insulin-induced increases in glycolytic ATP synthesis could be secondary to increased glucose availability, which was shown to render L6 myocytes more glycolytic, thus lowering the oxygen cost of ATP synthesis (Chapter 3, Figures 3.5 & 3.6). This chapter aimed to assess whether increases in glycolytic ATP supply in response to nitrite and insulin are secondary to increased glucose availability. Glucose uptake assays and XF analysis with nutrient-deprived L6 myocytes reveal that this is not the case, as the data reported in this chapter demonstrate that glycolytic stimulation occurs irrespective of glucose availability.

5.2 Results

Nitrite and insulin stimulation of glycolytic ATP supply does not result from increased glucose uptake

Glucose (2DG) uptake was measured in L6 myoblasts and myotubes (Figure 5.1, A) to explore the possibility that the bioenergetic effects of nitrite and insulin are due to increased intracellular glucose availability. Following published protocols (Ching *et al.*, 2010; Nisr *et al.*, 2014), the 2DG uptake experiments were performed in glucose-restricted (myoblasts and myotubes) and serum-restricted (myoblasts) cells. Bioenergetic experiments with nutrient-deprived myoblasts were conducted in parallel to allow exact comparison with the 2DG uptake experiments. The day before XF analysis, the concentration of FBS was thus lowered from 10% to 2% overnight in the myoblast growth medium and cells were incubated in glucose-free KRPH for ~2 hours before the assay. Mimicking the 2DG uptake assay, 5mM glucose was injected during the XF run. Glycolytic ATP supply rates are thus calculated for glucose-starved cells and for cells acutely exposed to 5mM glucose (Figure 5.1, B). The latter ATP supply rates may be compared directly with the 2DG uptake rates (Figure 5.1, A).

The rate of glucose uptake is not stimulated by exposure to nitrite alone and insulin alone and is lower in myotubes exposed to nitrite alone (Figure 5.1, A). Strikingly, however, the 2DG uptake rate is significantly increased in cells exposed to both nitrite and insulin (Figure 5.1, A). Thus, the 2DG assay reveals a synergistic stimulation of glucose uptake when nitrite and insulin are applied together to L6 myocytes. Figure 5.1 (B) demonstrates again that both nitrite and insulin significantly increase glycolytic ATP supply when administered alone in myoblasts. Following acute exposure to glucose, these effects are less pronounced than reported in Chapter 4

(Figure 4.3, G & H), which is likely owing to the difference in nutritional background. The synergistic effect of nitrite and insulin on glucose uptake (Figure 5.1, A) is not reflected by the rate of glycolytic ATP supply, as the stimulation of glycolytic ATP supply is not amplified to the same extent when cells are exposed to nitrite and insulin together (Figure 5.1, B & C). The lack of increased 2DG uptake in response to nitrite and insulin alone as well as the 'synergy discrepancy', disconnect glycolytic ATP supply stimulation from glucose uptake (Figure 5.1, C). The mechanistic disconnection revealed by these experiments shows that changes in bioenergetics in response to nitrite and insulin cannot be caused by increased glucose availability alone.

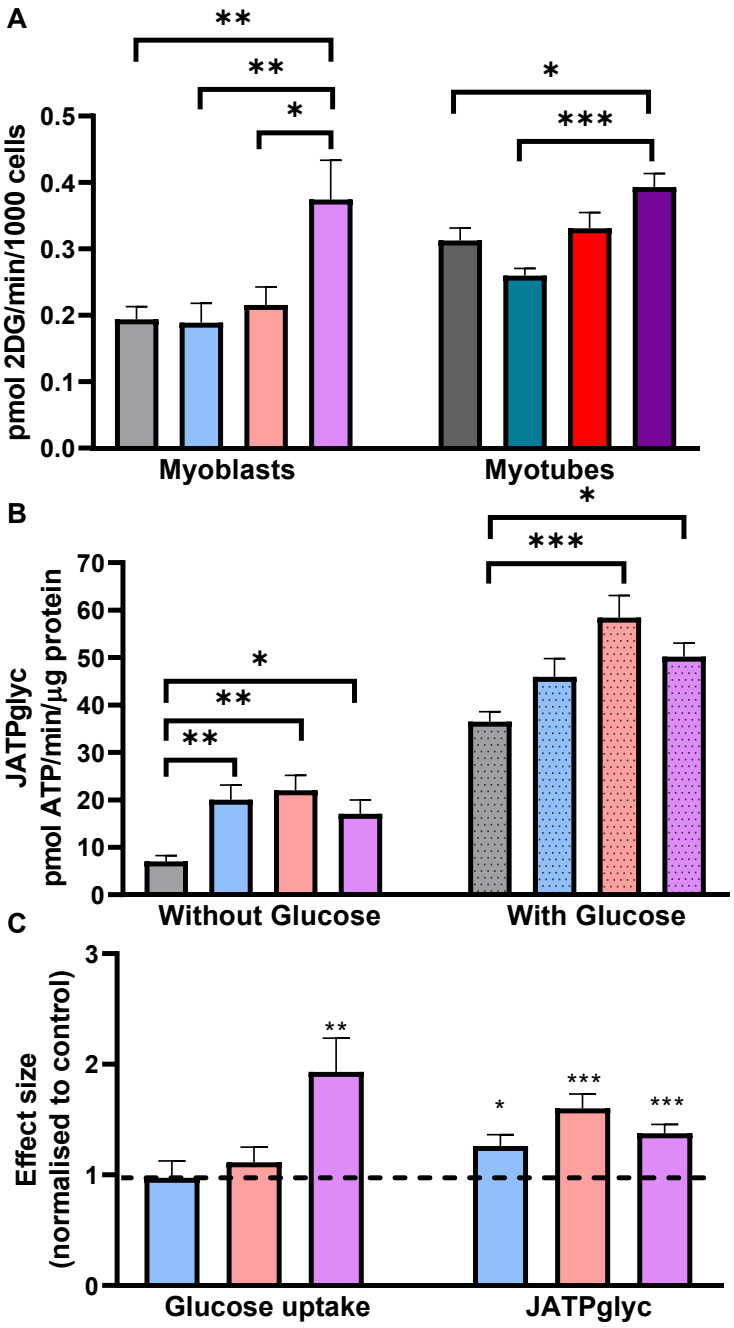

Figure 5.1 – Glucose (2DG) uptake in L6 myoblasts and myotubes.
Glucose uptake (A) was measured as the accumulation of 2DG in L6 myoblasts and myotubes exposed to nitrite (blue bars), insulin (red bars), both nitrite and insulin (purple bars) or to neither (grey bars). Data are means ± SEM of 12 and 9 separate measurements from 4 and 3 independent assays for myoblasts and myotubes, respectively. Glycolytic ATP supply (JATPglyc) (B) was measured in myoblasts deprived of serum and glucose (without glucose) as in the 2DG assay, and subjected to 5mM glucose in the XF assay before other effectors were added (with glucose). Data are means ± SEM of 12-15 separate measurements from 3 independent XF runs. The control-normalised rates for comparison of glucose uptake versus glycolytic ATP supply following glucose injection are shown in C. Differences between absolute values were evaluated for statistical significance by one-way ANOVA with Tukey's post-hoc analysis. Significance of normalised effects was assessed by an unpaired t-test ($P < 0.05$, ** $P < 0.01$, *** $P < 0.001$).*

Nitrite and insulin increase glycolytic ATP supply even when glucose is not available

Interestingly, nitrite and insulin increase glycolytic ATP supply in myoblasts both in the absence and presence of glucose. Bioenergetic stimulation in response to nitrite and insulin thus occurs irrespective of nutrient deprivation, and even appears somewhat stronger without glucose addition during the XF assay (Figure 5.1, B). This observation strengthens the assertion that increases in glycolytic ATP supply in response to nitrite and insulin are not the result of increased glucose availability in myoblasts. Wishing to explore the interesting observations made above further, the effect of nitrite and insulin on bioenergetics of nutrient-deprived myocytes was assessed. Experiments were performed in glucose-restricted (myoblasts and myotubes) and serum-restricted (myoblasts) cells. XF Analysis was then carried out in a buffer lacking glucose, with no addition of glucose made throughout the experiment.

Figures 5.2 and 5.3 summarise the protein-normalised basal ECAR, ATP supply rates, the glycolytic index, and the ATP/O_2 ratio of L6 myoblasts and myotubes, for the control (A & D), when 1μM $NaNO_2$ was applied (B & E), and when 100nM insulin was applied (C & F). The control data is given for reference purposes and are the same as shown in Chapter 3. Similar to the observation made above (Figure 5.1, B), stimulation of glycolytic ATP supply by nitrite and insulin occurs irrespective of glucose availability. Both nitrite and insulin provoke increases basal ECAR compared to the control, translating to significant increases in glycolytic ATP supply in nutrient-deprived myoblasts (Figure 5.2, G & H) and myotubes (Figure 5.3, G & H). Glycolytic ATP supply is increased by 94% and 192% in myoblasts exposed to nitrite and insulin, respectively (Figure 5.2, G & H). Thus, nutrient deprivation increases the effect size compared to when glucose is available (which were 60% and 147% in response to

nitrite and insulin, respectively; see Chapter 4, Figure 4.3, G & H). In contrast, nitrite and insulin both increase glycolytic ATP supply by approximately 35% in nutrient-deprived myotubes (Figure 5.3, G & H). Thus, glucose deprivation lowers the effect size in myotubes compared to when glucose is available throughout the assay (which were 60% and 45% in response to nitrite and insulin, respectively; Chapter 4, Figure 4.4, G & H).

Mitochondrial ATP supply is slightly lowered by nitrite and insulin in myoblasts (Figure 5.2, G & H). Therefore, total ATP supply is unaffected by nitrite and insulin in myoblasts (Figure 5.2, G & H). Because glycolytic ATP supply is significantly increased but mitochondrial ATP supply is slightly lowered, nitrite and insulin significantly increase the glycolytic index in nutrient-deprived myoblasts (Figure 5.2, G & H). In myotubes, mitochondrial ATP supply is unaffected by nitrite (Figure 5.3, G) but is significantly increased in response to insulin (Figure 5.3, H). The stimulatory effect of nitrite and insulin on glycolytic and mitochondrial (insulin only) ATP supply is sufficient to significantly increase total ATP supply in both conditions (Figure 5.3, G & H). Both conditions push myotubes deprived of glucose into a more glycolytic phenotype, but this push is non-significant (Figure 5.3, G & H). Insulin provokes a smaller increase in the glycolytic index compared to nitrite because it also provokes a significant increase in mitochondrial ATP supply. Finally, insulin causes a significant increase in the ATP/O_2 ratio compared to the control, thus lowering the apparent oxygen cost of total ATP synthesis in myoblasts (Figure 5.2, H) and myotubes (Figure 5.3, H). However, nitrite has no effect on the ATP/O_2 ratio in either myoblasts (Figure 5.2, H) or myotubes (Figure 5.3, H).

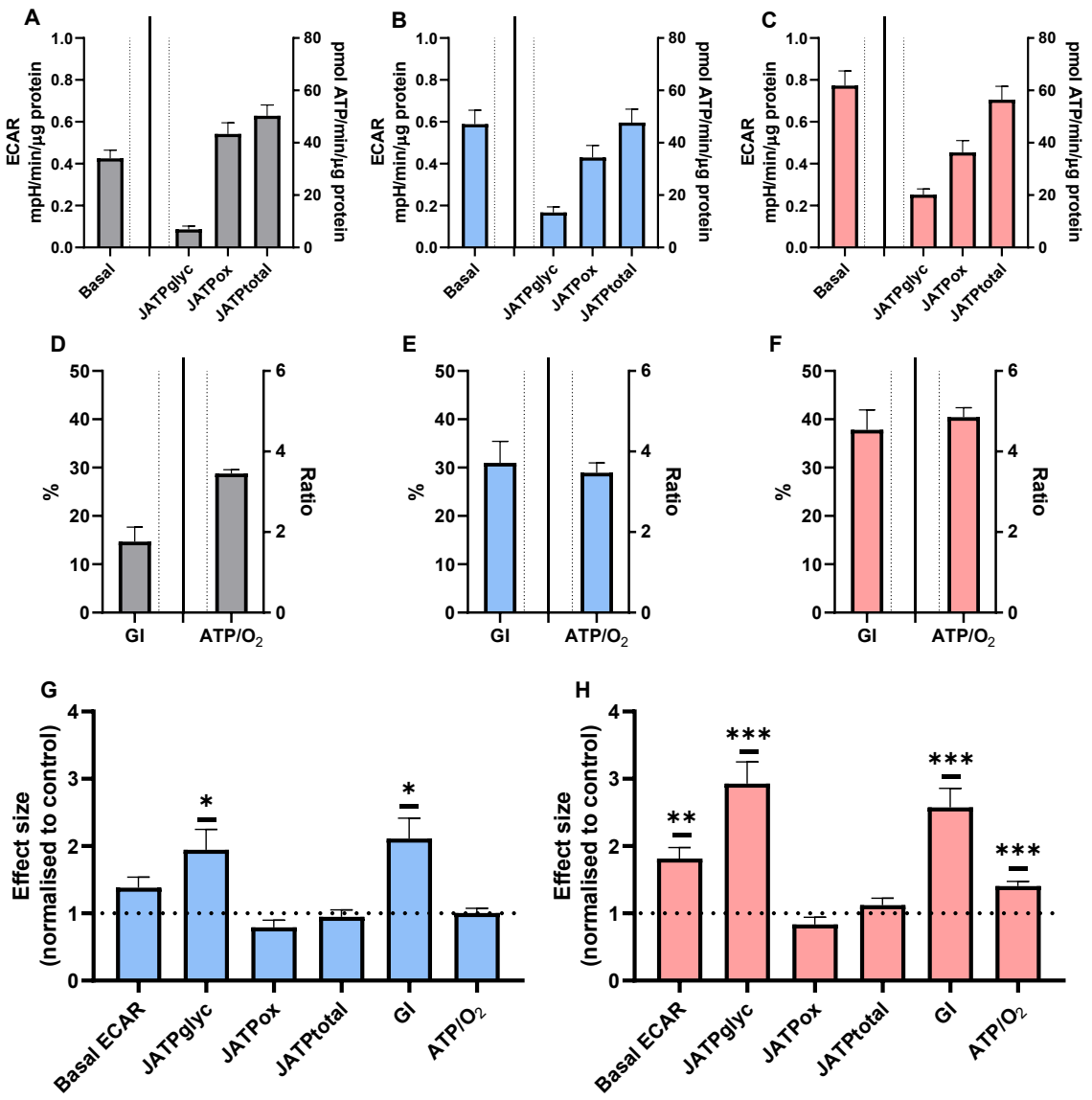

Figure 5.2 – The ATP supply fluxes of glucose-deprived L6 myoblasts.
*Myoblasts were cultured in fully supplemented medium but underwent a reduction in FBS from 10% to 2% overnight. Cells were incubated in KRPH without glucose for 90 minutes before XF analysis and glucose was not injected during the assay. Cells were assayed without (grey bars: controls) or with 100nM human insulin (red bars). Another group of cells was subjected to 1µM $NaNO_2$ for the last 30 min of the pre-incubation and assayed without insulin (blue bars). Basal ECAR, ATP supply rates (JATP), the glycolytic index (GI) and the ATP/O_2 ratio are given as absolute (panels A-F) and control-normalised (panel G-H) values, and are means ± SEM of 3 independent XF runs, each containing 3-5 technical repeats. Significance was tested using an unpaired T-test. * = p <0.05, ** = p <0.01, *** = p <0.001, **** = p <0.0001.*

Myotubes

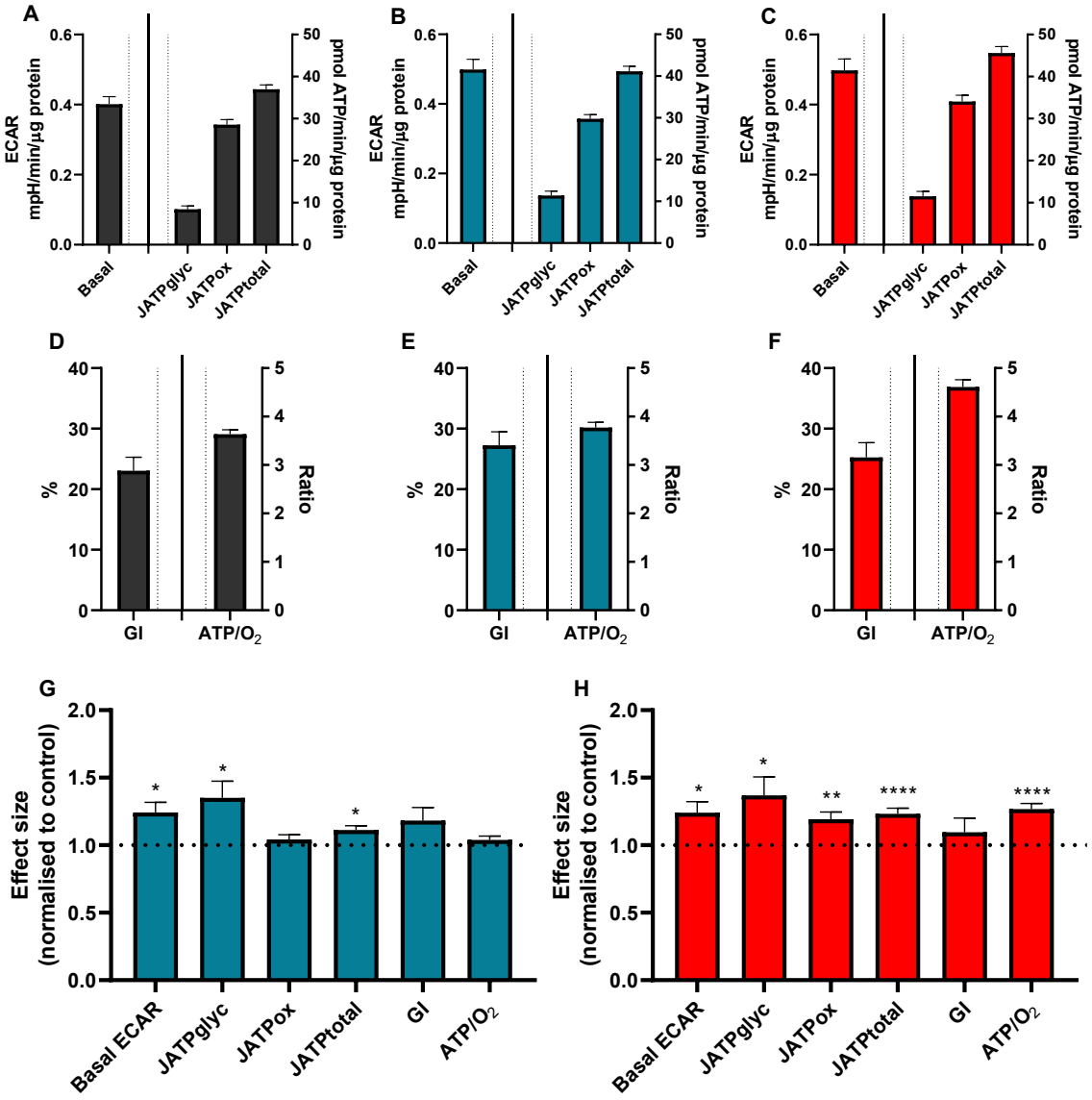

Figure 5.3 – The ATP supply fluxes of glucose-deprived L6 myotubes.
*Myotubes were cultured in fully supplemented medium and were incubated in KRPH without glucose for 90 minutes before XF analysis. Glucose was not injected during the assay. Cells were assayed without (grey bars: controls) or with 100nM human insulin (red bars). Another group of cells was subjected to 1µM $NaNO_2$ for the last 30 min of the pre-incubation and assayed without insulin (blue bars). Basal ECAR, ATP supply rates (JATP), the glycolytic index (GI) and the ATP/O_2 ratio are given as absolute (panels A-F) and control-normalised (panel G-H) values, and are means ± SEM of 4 independent XF runs, each containing 3-5 technical repeats. Significance was tested using an unpaired T-test. * = p <0.05, ** = p <0.01, *** = p <0.001, **** = p <0.0001.*

Insulin decreases proton leak in myoblasts when nutrients are deprived

Figures 5.4 and 5.5 summarise the respiratory analysis of nutrient-deprived L6 myoblasts and myotubes, respectively. Similar to when glucose is available throughout the assay (Chapter 4, Figure 4.1, G), in myoblasts nitrite lowers all respiratory parameters (Figure 5.4, A and B), with the effect on spare respiration nearing significance (Figure 5.4, G). Notably, nitrite significantly *lowers* the coupling efficiency of oxidative phosphorylation when glucose is deprived (Figure 5.4, D, E & G). Furthermore, there was no effect of nitrite on parameters related to oxygen consumption during nutrient deprivation in myotubes (Figure 5.5, A, B & G). Although variable, there is a decrease in spare respiration compared to the control and slight decreases in cell respiratory control, while non-mitochondrial respiration slightly increases in response to nitrite in myotubes (Figure 5.5, G).

In contrast to when glucose is available throughout the assay (Chapter 4, Figure 4.1, H), in myoblasts insulin lowers basal mitochondrial respiration, respiration associated with proton leak, respiration coupled to ATP synthesis and uncoupled respiration (Figure 5.4, A, C & H). However, only the effects on proton leak and uncoupled respiration are statistically significant (Figure 5.4, H). The insulin-induced decrease in proton leak leads to significant increases in coupling efficiency in glucose-deprived myoblasts (Figure 5.4, F & H). Consistent with earlier observations (Chapter 4, Figure 4.2, H), insulin lowers respiration linked with mitochondrial proton leak (Figure 5.5, C & H), leading to increases in coupling efficiency in myotubes (Figure 5.5, F & H). Cell respiratory control is also increased in response to insulin, but this fails to reach significance when glucose is withdrawn (Figure 5.5, H). There is a rise in ATP-synthesis-linked respiration, which approaches significance, while non-mitochondrial respiration is decreased by insulin (Figure 5.5, H). Thus, nutrient

deprivation does not notably change how nitrite and insulin affect the respiratory activity of L6 myotubes. As reported before (Nisr *et al.*, 2014), insulin increases the coupling efficiency of nutrient-deprived myoblasts, an effect that was not apparent in 'fed' cells (Chapter 4, Figure 4.1).

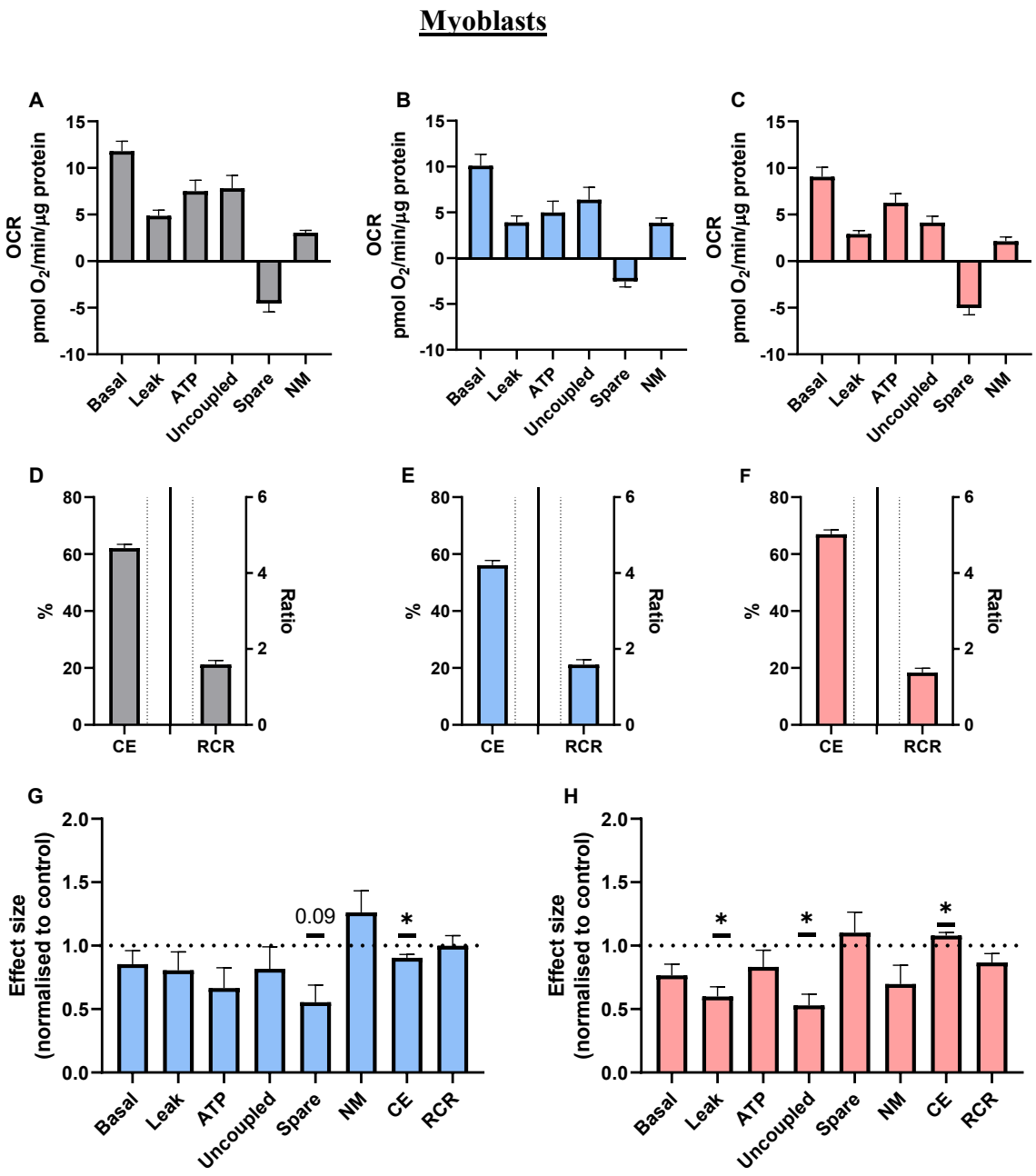

Figure 5.4 – The respiratory activity of glucose-deprived L6 myoblasts in response to nitrite and insulin.

*The protein-normalised respiratory activity (A, B & C), coupling efficiency (CE) and respiratory control ratio (RCR) (D, E & F) by L6 myoblasts as measured by Extracellular Flux Analysis. Cells were cultured in fully supplemented medium but underwent a reduction in FBS from 10% to 2% overnight. Cells were incubated in KRPH without glucose for 90 minutes before XF analysis and glucose was not injected during the assay. Cells were assayed without (grey bars: controls) or with exposure to either 1µM $NaNO_2$ (blue bars) or 100nM human insulin (red bars). The control-normalised rates obtained in the presence of 1µM $NaNO_2$ (G) and 100nM insulin (H) are also shown. All rates were obtained in the same manner as described by the oxygen consumption traces reported in Chapter 3 and were calculated as described in the Methods. Rates represent the mean and standard error of the mean of 3 biological repeats, each containing 3-5 technical repeats. Significance was tested using an unpaired T-test. * = p <0.05, ** = p <0.01, *** = p <0.001, **** = p <0.0001.*

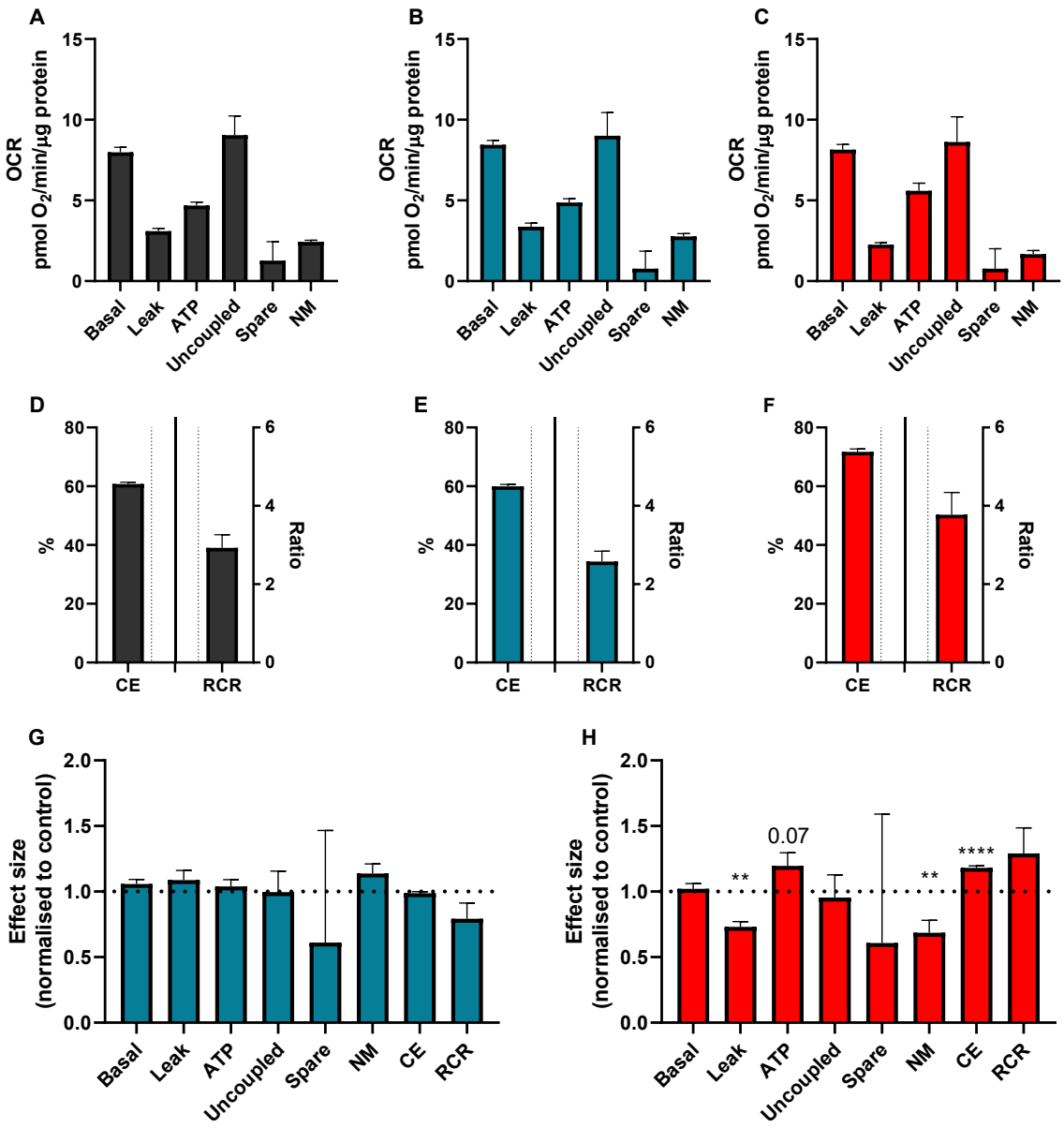

Figure 5.5 – The respiratory activity of glucose-deprived L6 myotubes in response to nitrite and insulin.

*The protein-normalised respiratory activity (A, B & C), coupling efficiency (CE) and respiratory control ratio (RCR) (D, E & F) by L6 myotubes as measured by Extracellular Flux Analysis. Cells were cultured in fully supplemented medium and were incubated in KRPH without glucose for 90 minutes before XF analysis. Glucose was not injected during the assay. Cells were assayed without (grey bars: controls) or with exposure to either 1µM $NaNO_2$ (blue bars) or 100nM human insulin (red bars). The control-normalised rates obtained in the presence of 1µM $NaNO_2$ (G) and 100nM insulin (H) are also shown. All rates were obtained in the same manner as described by the oxygen consumption traces reported in Chapter 3 and were calculated as described in the Methods. Rates represent the mean and standard error of the mean of 4 biological repeats, each containing 3-5 technical repeats. Significance was tested using an unpaired T-test. * = p <0.05, ** = p <0.01, *** = p <0.001, **** = p <0.0001.*

5.3 Discussion

The application of nitrite and insulin together significantly and synergistically enhanced glucose uptake by L6 myocytes (Figure 5.1, A). The lack of bioenergetic synergy when nitrite and insulin are applied together in myoblasts, and the notion that nitrite and insulin alone stimulate glycolytic ATP supply (Figure 5.1, B) but not glucose uptake (Figure 5.1, A), demonstrate a mechanistic disconnection between the bioenergetic and glucose uptake phenotypes. Such disconnection is supported by the finding that glycolytic ATP supply is stimulated irrespective of nutrient availability, both in myoblasts (Figures 5.1, B and 5.2, G & H) and myotubes (Figure 5.3, G & H). Taken together, it can be concluded that increases in glycolytic ATP supply in response to nitrite and insulin are not the result of increased glucose availability, neither in myoblasts nor myotubes.

Nitrite and insulin applied together, but not alone, increases glucose uptake in L6 cells

The application of nitrite and insulin together significantly enhanced glucose uptake in L6 myocytes (Figure 5.1, A & C), while alone neither compound had a significant effect. This is an interesting and novel finding. The mechanism behind the apparent synergism is unclear at present but warrants some speculation. Insulin promotes glucose uptake into skeletal muscle cells through an intracellular signalling pathway that ultimately leads to the insertion of GLUT4 into the plasma membrane (Richter *et al.*, 2013). Furthermore, studies have shown increased GLUT4 gene and protein expression (Vaughan *et al.*, 2016), and translocation to the plasma membrane (Jiang *et al.*, 2014) in response to nitrogen species. Thus, nitrite and insulin applied together may increase glucose uptake through increased glucose transport via GLUT4. However, measurement

of glucose uptake as an endpoint does not allow discrimination between glucose transport via GLUT4, or GLUT1, GLUT3, and GLUT12, which are also expressed by L6 cells and can transport glucose (Niu *et al.*, 2003; Stuart *et al.*, 2009; Matsuzaka *et al.*, 2012; Thorens *et al.*, 2014). Thus, future research should aim to assess these effects using GLUT4 knockout cells, or selective GLUT4 inhibitors, such as HIV protease inhibitors; although these inhibitors may also have a degree of affinity for GLUT1 (Hresko *et al.*, 2011). Such experiments will provide a deeper understanding of the mechanistic action behind the observations made within this experiment.

It is also plausible that nitrogen species interact with upstream substrates involved in the insulin signalling cascade. Increased GLUT4 translocation in response to nitrite was attributed to a nitric oxide-driven nitrosylation of 2 cysteine residues present on GLUT4, which affected GLUT4 localisation and translocation (Jiang *et al.*, 2014). Nitrite has also been found to slightly increase the phosphorylation of the regulatory subunit present on phosphatidylinositol-3-kinase, and significantly increases subsequent phosphorylation of protein kinase B, resulting in increased GLUT4 translocation within skeletal muscle (Ohtake *et al.*, 2015). Others have demonstrated that the production of nitric oxide inhibits protein-tyrosine phosphatases, resulting in higher rates of phosphorylation of the tyrosine residues on the insulin receptor, which also remain phosphorylated for a longer length of time (Hsu *et al.*, 2010). These studies provide some insight as to how nitrite could increase GLUT4 translocation in tandem with insulin, which could account for the increased glucose transport seen within the present study.

Insulin applied alone did not affect glucose uptake in myoblasts or myotubes (Figure 5.1, A). Insulin sensitivity and glucose uptake are not necessarily expected to occur in myoblasts (Tong *et al.*, 2001; Cui *et al.*, 2009). Nevertheless, the lack of

insulin-induced glucose uptake in myoblasts reported here is at odds with previously published work, where L6 myoblasts exposed to 100nM human insulin significantly increase their uptake of 2DG (Nisr *et al.*, 2014, 2016). However, as discussed in Chapter 4, the relatively high confluence expected from the previous cell culture regime (Nisr *et al.*, 2014, 2016) may have provoked some myoblast differentiation, as L6 cells differentiate on confluence (Pinset *et al.*, 1982). The lack of insulin-sensitive glucose uptake in myotubes (Figure 5.1, A), however, is unexpected. Myotubes show increased insulin-stimulated glucose uptake compared to myoblasts (Ueyama *et al.*, 1999) and actin remodelling plays a crucial role in GLUT4 insertion into the membrane (Tong *et al.*, 2001). The components for actin are expressed to a higher degree in myotubes compared to myoblasts (Cui *et al.*, 2009). Thus, it is expected that glucose uptake increases in response to insulin when cells are differentiated. It remains to be determined why the myotubes used here are unresponsive to insulin-stimulated glucose uptake but are insulin-sensitive in terms of bioenergetics when glucose is available (Chapter 4, Figure 4.4, H) and when it is not (Figure 5.3, H). Regardless, the lack of insulin sensitivity to glucose uptake shown here may indicate that the significant effects of nitrite and insulin when applied together on glucose uptake occur in a manner that does not involve GLUT4.

Nitrite applied alone did not impact glucose uptake in myoblasts and was significantly lower in myotubes (Figure 5.1, A). Increased GLUT4 mRNA (Lira *et al.*, 2007) and protein expression (Vaughan *et al.*, 2016), along with increased GLUT4 translocation into the membrane (Jiang *et al.*, 2014) imply that nitrogen species may increase glucose uptake. However, these experiments were all executed in myotubes, which may account for the lack of effect of nitrite on glucose uptake in myoblasts seen here. Increased GLUT4 translocation into the cellular membrane of L6 myotubes

occurred after 30 minutes in response to higher concentrations of sodium nitrite (10 and 100μM) (Jiang *et al.*, 2014). Thus, it may be that a higher concentration of nitrite is needed to provoke increased glucose uptake when nitrite is applied alone. Increased GLUT4 mRNA expression occurred in L6 myotubes following a 16-hour exposure to a nitric oxide donor (Lira *et al.*, 2007), and increased GLUT4 gene and protein expression were seen following a 24-hour exposure to beetroot juice, applied to C2C12 myocytes (Vaughan *et al.*, 2016). Thus, the lack of effect of nitrite on glucose uptake in myotubes seen here could be explained by differences in exposure times, the type of nitrogen species applied, and the cell type used.

Nutrient deprivation amplifies the stimulation of glycolytic ATP supply by nitrite and insulin in myoblasts but not in myotubes

The data presented in this chapter show that nutrient deprivation does not notably change how nitrite and insulin affect the respiratory activity of L6 myotubes (Figure 5.5). In the absence of glucose, nitrite does not affect proton-leak-linked respiration or the coupling efficiency in myotubes (Figure 5.5, G) and significantly lowers the coupling efficiency in glucose-deprived myoblasts (Figure 5.4, G), which further confirms that nitrite does not improve mitochondrial efficiency (Chapter 4, Figures 4.1 & 4.2, G) (Whitfield *et al.*, 2016; Ivarsson *et al.*, 2017). In response to insulin, proton leak is decreased, resulting in increases in coupling efficiency and slight increases in respiratory control in myotubes (Figure 5.5, H). These data show that the effect of insulin on proton leak is not dependent on glucose availability in myotubes. However, following nutrient deprivation, insulin provokes significant decreases in proton leak and increases in coupling efficiency in myoblasts (Figure 5.4, H), which differs from the

results obtained in 'fed' myoblasts (Chapter 4, Figure 4.1, H) and likely arises due to the reduction in FBS.

Overnight FBS reductions and glucose deprivation before XF analysis amplifies the stimulatory effect of nitrite and insulin on glycolytic ATP supply in myoblasts (Figure 5.2, G & H). Nitrite and insulin increase glycolytic ATP supply by 60% and 147%, respectively, when glucose is present throughout the assay (Chapter 4, Figure 4.3, G & H), versus increases of 94% and 192%, respectively, in the nutrient-deprived state (Figure 5.2, G & H). When glucose is initially deprived and then reintroduced during the experiment, these increases from the control decrease to 26% for nitrite and 60% for insulin (Figure 5.1, C), which is lower than when glucose is present throughout the assay. However, during glucose deprivation, myoblasts suffer a significant starvation-induced decrease of glycolytic ATP supply, which is reversed and stimulated to a higher level than that seen when glucose is present throughout the experiment by the addition of glucose (Chapter 3, Figure 3.5, B). Thus, the stimulatory effect that nitrite and insulin have on glycolytic ATP supply could be more visible when glucose is removed and masked following glucose injection.

Stimulation of glycolytic ATP supply by nitrite and insulin in myotubes also occurs regardless of nutritional state (Figure 5.3, G & H) (Chapter 4, Figure 4.4, G & H). However, here, the effect moves in the opposite direction, with nitrite and insulin provoking 60% and 45% increases in glycolytic ATP supply, respectively, when glucose is available (Chapter 4, Figure 4.4, G & H) but only 35% increases when glucose is restricted (Figure 5.3, G & H). However, myotubes do not suffer from a starvation-induced decrease of glycolytic ATP supply (Chapter 3, Figure 3.6, B), and the differentiation state of myocytes may impact cellular response to nitrite and insulin.

5.4 Conclusion

The data presented in this chapter rule out the possibility that nitrite and insulin stimulate glycolytic ATP supply in L6 myocytes by increasing glucose uptake. Exactly how these molecules increase ATP supply is yet to be determined. Because both nitrite and insulin impact cellular activities that require large amounts of ATP (Hernández *et al.*, 2012; Haider *et al.*, 2014; Affourtit, 2016; Ivarsson *et al.*, 2017), it is conceivable that increased glycolytic ATP supply occurs in response to an increase in ATP demand. This possibility is explored in the next chapter.

6 Nitrite and insulin increase glycolytic ATP supply both directly and indirectly in L6 myocytes

6.1 Introduction

The data reported in chapters 4 and 5 demonstrate that nitrite and insulin stimulate glycolytic ATP supply irrespective of glucose availability. Continuing the search for the mechanism underlying this finding, I next assessed the effects of nitrite and insulin on L6 bioenergetics in the combined presence of oligomycin (to inhibit mitochondrial ATP synthesis) and BAM15 (to uncouple oxidative phosphorylation). The cells' phosphorylation potential is greatly diminished under these experimental conditions (Affourtit *et al.*, 2018), which means that control over ATP flux is largely shifted from ATP demand to (glycolytic) ATP supply. ATP flux is less controlled by ATP demand because uncouplers, like BAM15, provoke artificial ATP demand by dissipating the proton-motive force (Brand *et al.*, 2011). Thus, if glycolytic stimulation by nitrite and insulin is still evident in the presence of oligomycin and BAM15, stimulation is likely direct. However, if glycolytic stimulation is abolished by oligomycin and BAM15, stimulation is likely the indirect result of increased ATP demand. The data reported in this chapter reveal that stimulation of glycolytic ATP supply by nitrite and insulin is predominantly direct in myotubes and indirect in myoblasts. Probing the indirect stimulation of glycolytic ATP supply further, I first established how ATP supply in myoblasts is allocated to a range of ATP demanding processes. I then determined if nitrite and insulin affected the proportion of ATP supply used for protein synthesis. Neither nitrite nor insulin increased glycolytic ATP supply reserved for protein synthesis in myoblasts, ruling out protein synthesis as possible source of the enhanced ATP demand.

6.2 Results

Nitrite and insulin increase glycolytic ATP supply directly in myotubes and indirectly in myoblasts

In the combined presence of oligomycin and BAM15, mitochondrial ATP supply is relatively low in both myoblasts and myotubes (Figure 6.1, A & D). However, mitochondrial ATP supply is not inhibited entirely, as substrate-level phosphorylation still occurs during (uncoupled) TCA cycle turnover. Under these conditions, both myoblasts and myotubes increase the rate of glycolytic ATP supply to compensate for inhibited oxidative phosphorylation (Figure 6.1, A & D). This compensation is incomplete, however, as total ATP supply is slightly lower in the presence (Figure 6.1, A & D) than in the absence of oligomycin and BAM15 (Chapter 3, Figure 3.2, A). This small difference implies that glycolytic ATP supply in the presence of oligomycin and uncoupler reflects the glycolytic capacity of the myocytes. Consistent with the shift from mitochondrial to glycolytic ATP supply, the glycolytic index increases from just below 30% (Chapter 3, Figure 3.2, B) to 89% in myoblasts (Figure 6.1, B) and 75% in myotubes (Figure 6.1, E). This high glycolytic index does not increase the ATP/O_2 ratio (Figure 6.1, C & F), because oxygen consumption (that is not coupled to ATP synthesis) significantly increases in response to BAM15 (Chapter 3, Figure 3.1, A).

The previously observed stimulation of glycolytic ATP supply by nitrite and insulin is significantly attenuated by oligomycin and uncoupler in myoblasts (Figure 6.1, A, G, H & I), which suggests this stimulation is an indirect result of increased ATP demand. Accordingly, oligomycin and uncoupler render ATP/O_2 ratio effects of nitrite and insulin less significant in myoblasts (Figure 6.1, C, G & H). In myotubes, on the other hand, stimulation of glycolytic ATP supply by nitrite and insulin is unaffected by oligomycin and BAM15, or even somewhat enhanced (Figure 6.1, D, G, H & I).

Therefore, the effects of these molecules on glycolytic ATP supply in myotubes are likely due to direct stimulation of glycolysis. Overall, these XF data demonstrate that nitrite and insulin acutely increase basal glycolytic activity *and* capacity in myotubes, but only basal glycolytic activity in myoblasts.

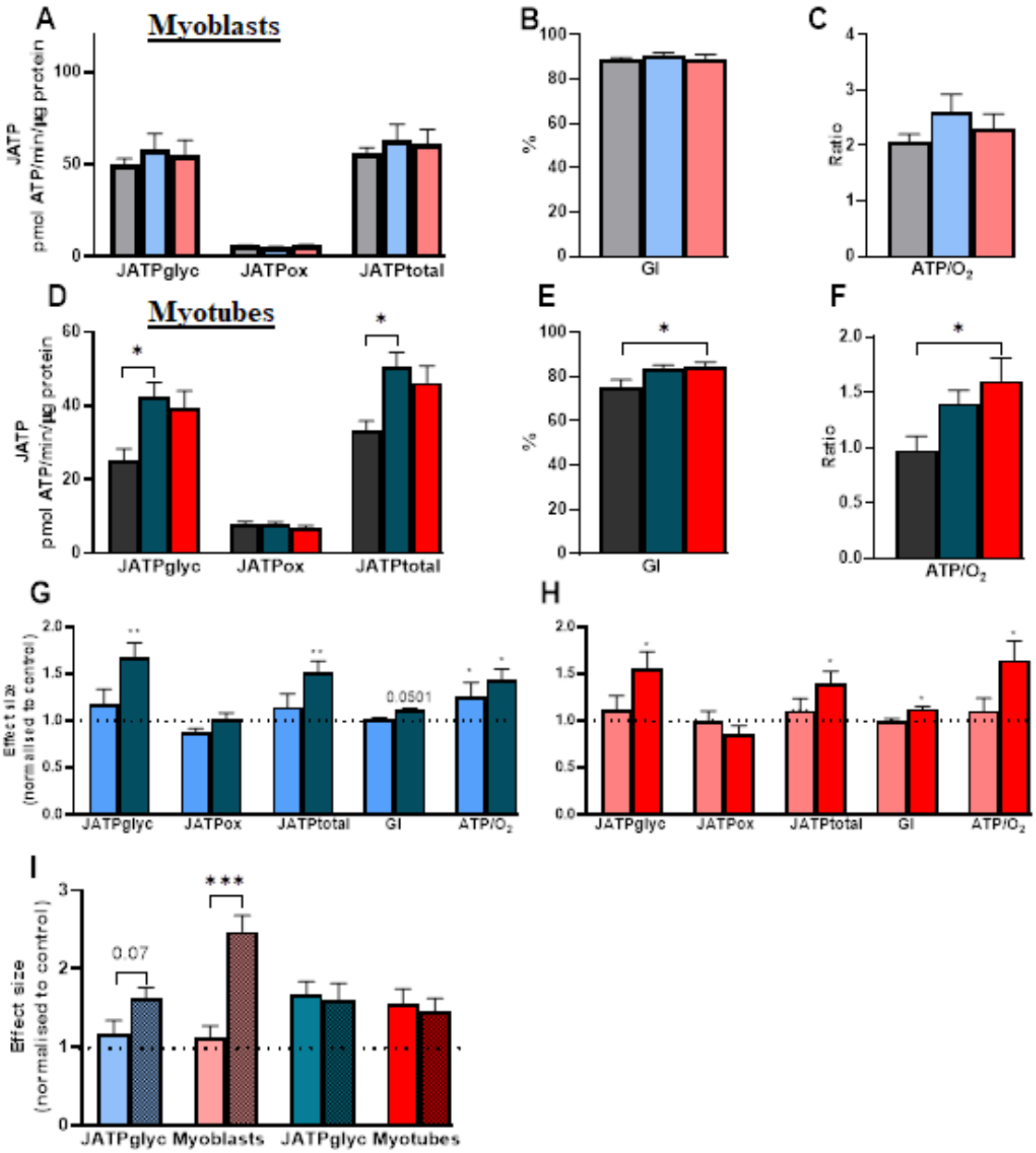

Figure 6.1 – The ATP supply rates in the combined presence of glucose, oligomycin and uncoupler, in response to nitrite and insulin, in myoblasts and myotubes.
Calculation of ATP supply rates (A & D), the glycolytic index (B & E) and the ATP/O_2 ratio (C & F) in the combined presence of oligomycin and BAM15. Calculations occurred in the same manner as basal ATP supply rates given previously, but basal OCR and ECAR rates were substituted with OCR and ECAR rates in the combined presence of oligomycin and BAM15. Cells were assayed in the presence of 5mM glucose for the control (grey), where 1µM $NaNO_2$ was applied (blue), and where 100nM human insulin was applied (red) (myoblasts in the lighter colours and myotubes in the darker colours). Control-normalised glycolytic ATP supply rates obtained in the presence of oligomycin and BAM15 are compared with control-normalised glycolytic ATP supply rates obtained under basal conditions (hatched bars, as shown in Figures 4.3 & 4.4) (I). Data are given as absolute (panels A-F) and control-normalised (panels G-I) values and are means ± SEM of 2-5 biological repeats, each containing 3-5 technical repeats. Differences between absolute values were evaluated for statistical significance by one-way ANOVA with Tukey's post-hoc analysis. Significance of normalised effects were assessed by unpaired T-tests (P < 0.05, ** P < 0.01, *** P < 0.001, **** P < 0.0001).*

Nutrient deprivation reverses the nitrite and insulin effect on glycolytic ATP supply in the combined presence of oligomycin and uncoupler

The effects of nitrite and insulin on glycolytic ATP supply in the combined presence of oligomycin and uncoupler were also assessed in nutrient-deprived myocytes (Figure 6.2) to determine whether nutrient availability affects the results. Similar to when glucose is available (Figure 6.1), in the combined presence of oligomycin and BAM15, mitochondrial ATP supply is low, with increased glycolytic ATP supply to compensate for this decrease (Figure 6.2, A & D). During nutrient deprivation, glycolytic compensation is severely incomplete as total ATP supply decreases to less than half seen in glucose-deprived basal conditions (50-11 pmol/min/µg protein in myoblasts and 37-15 pmol/min/µg protein in myotubes) (Chapter 5, Figures 5.2 & 5.3, A) (Figure 6.2, A & D). The glycolytic index increases from 15% and 23% (myoblasts and myotubes, respectively) (Chapter 5, Figures 5.2 & 5.3, D) to 79% and 85% in the combined presence of oligomycin and uncoupler (myoblasts and myotubes, respectively) (Figure 6.2, B & E). However, this high glycolytic index does not increase the ATP/O_2 ratio (Figure 6.2, C & F) because oxygen consumption does not increase in response to uncoupler when glucose is deprived (Chapter 5, Figures 5.4 & 5.5, A) and total ATP supply is much lower under these circumstances (Figure 6.2, A & D).

During nutrient deprivation, stimulation of glycolytic ATP supply is slightly increased in the combined presence of oligomycin and uncoupler in myoblasts in response to nitrite and insulin compared to the control (Figure 6.2, A, G & H). Nitrite and insulin also increase the glycolytic index under these conditions in myoblasts, which approaches significance (Figure 6.2, B, G & H). In response to nitrite, the increase in glycolytic ATP supply with no impact on mitochondrial or total ATP supply causes a variable increase in the ATP/O_2 ratio (Figure 6.2, C & G). Insulin significantly

increases the ATP/O_2 ratio in myoblasts (Figure 6.2, C & H). This increase is driven by significantly lower oxygen consumption during uncoupled respiration in the nutrient-deprived state in response to insulin (Chapter 5, Figure 5.4, H), which is reflected by significantly lower mitochondrial ATP supply under these conditions (Figure 6.2, H). In myotubes, there is no effect of nitrite or insulin on any of the parameters (Figure 6.2, D, E, F, G & H). The previously observed enhanced stimulation of glycolytic ATP supply by nitrite and insulin in the presence of glucose, oligomycin and uncoupler (Figure 6.1, D, G, H & I) is not observed when glucose is removed from the experiment (Figure 6.2, D, G & H).

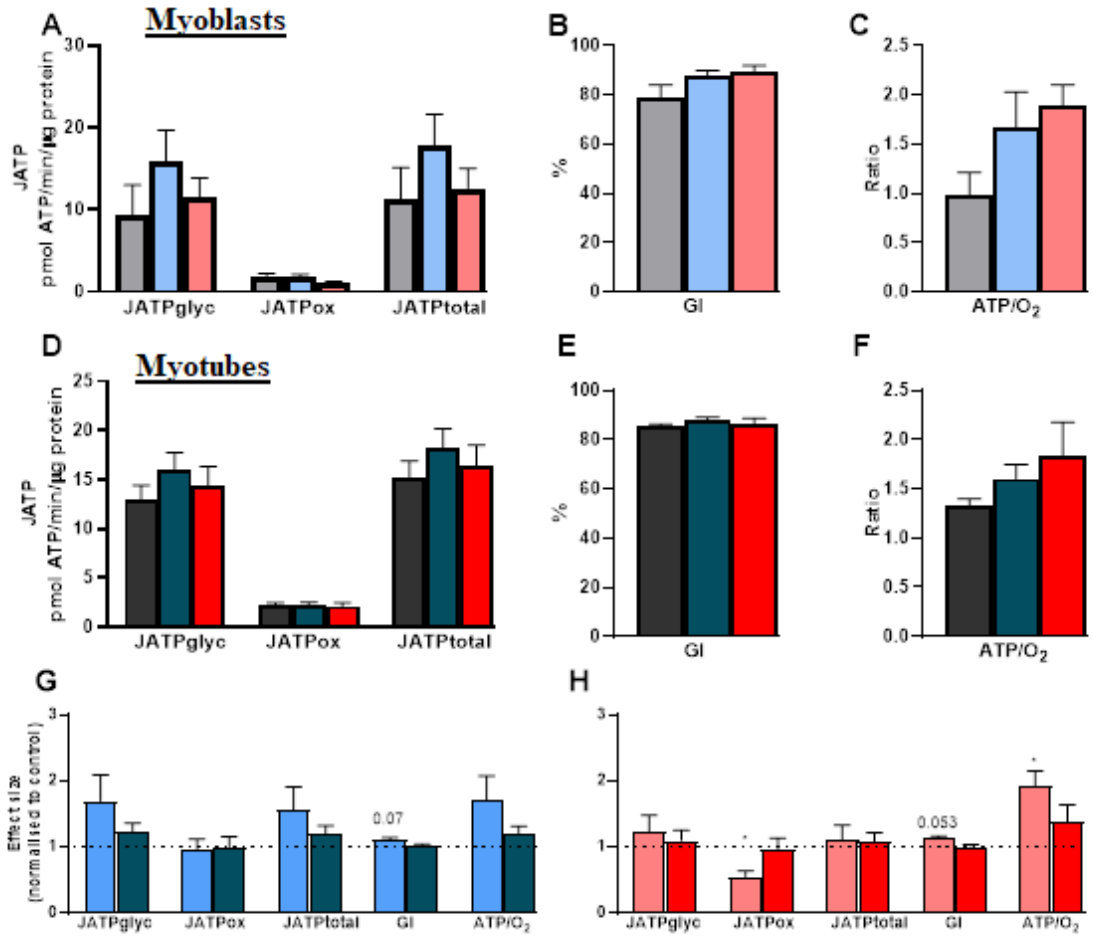

Figure 6.2 – The ATP supply fluxes of glucose-deprived myoblasts and myotubes in the combined presence of oligomycin and uncoupler in response to nitrite and insulin.
Calculation of ATP supply rates (A & D), the glycolytic index (B & E) and the ATP/O_2 ratio (C & F) in the combined presence of oligomycin and BAM15. Calculations were made as described in the legend of Figure 6.1. Cells were cultured in fully supplemented medium but myoblasts underwent a reduction in FBS from 10% to 2% overnight. Cells were incubated in KRPH without glucose for 90 minutes before XF analysis and glucose was not injected during the assay for the control (grey), where 1µM $NaNO_2$ was applied (blue), and where 100nM human insulin was applied (red) (myoblasts in the lighter colours and myotubes in the darker colours). Data are given as absolute (panels A-F) and control-normalised (panels G-H) values and are means ± SEM of 3-4 biological repeats, each containing 3-5 technical repeats. Differences between absolute values were evaluated for statistical significance by one-way ANOVA with Tukey's post-hoc analysis. Significance of normalised effects were assessed by unpaired T-tests (P < 0.05, ** P < 0.01, *** P < 0.001, **** P < 0.0001).*

XF analysis to determine the activity of ATP-consuming processes

The nitrite and insulin stimulation of glycolytic ATP supply is abolished in the presence of oligomycin and uncoupler in myoblasts (Figure 6.1, I), which suggests that these effects are the indirect consequence of changes in ATP demand. To explore this possibility, XF analysis was used to (indirectly) determine the activity of ATP-consuming processes (Divakaruni *et al.*, 2014; Nisr *et al.*, 2016; Mookerjee *et al.*, 2017). Because ATP flux in fully fed skeletal muscle cells is largely controlled by ATP demand (Affourtit, 2016), specific inhibition of any ATP-consuming process will cause immediate inhibition of ATP supply. Changes in glycolytic, mitochondrial and total ATP supply in response to a specific inhibitor of an ATP-consuming process thus reflect the proportions of the respective ATP supply rates that are allocated to the inhibited process.

Titrations of various ATP demand inhibitors were carried out in duplicate and used to calculate the appropriate concentration of each inhibitor to apply to the cells. An example of an inhibitor titration carried out using XF Analysis in myoblasts can be seen in Figure 6.3. This titration was carried out using thapsigargin, which is an inhibitor of SERCA. In this example, cells were exposed to 0.3 – 1μM thapsigargin and the OCR decreases seen after 4 measuring cycles (Figure 6.3, A) were expressed as a fraction of the total oligomycin-sensitive OCR (Figure 6.3, B). The percentage inhibition of oxidative ATP supply is ~30% in response to all concentrations of thapsigargin, with no significant differences between concentrations (Figure 6.3, B). The uncoupled OCR (Figure 6.3, C) is not significantly affected by thapsigargin, demonstrating inhibition of the basal OCR was not due to non-specific interaction with respiratory complexes. Figure 6.3 demonstrates that 300nM is the lowest thapsigargin concentration that inhibits basal OCR maximally without off-target respiratory effects. This method for

determining appropriate ATP demand inhibitor concentrations was applied for a range of ATP-consuming processes, including the sodium-potassium ATPase, tubulin polymerisation, protein synthesis, and actin dynamics.

Myoblasts

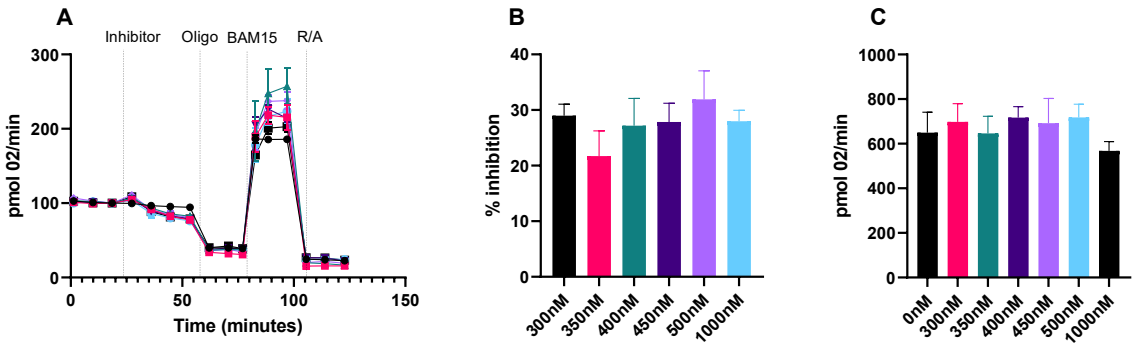

Figure 6.3 - Determining the correct concentration of specific inhibitors of ATP demand in myoblasts.

Myoblasts were grown and assayed in the presence of 5mM glucose as detailed previously. The oxygen consumption rate in response to a range of concentrations of Thapsigargin (colours) or KRPH (black) in myoblasts (A). The percentage of inhibition of oxidative ATP supply (B) and uncoupled rate (C) in response to Thapsigargin. Data are presented as the mean and standard error of the mean of 2-3 technical repeats per concentration. Differences between absolute values were evaluated for statistical significance by one-way ANOVA with Tukey's post-hoc analysis.

The effects of several ATP demand inhibitors on ATP supply by myoblasts are summarised in Figure 6.4. The application of thapsigargin, which inhibits SERCA, shows that 23%, 31%, and 29% of glycolytic, mitochondrial and total ATP supply, respectively, are used to fuel SERCA activity (Figure 6.4, light purple). Thus, myoblasts use most of their ATP supply toward this ATP consuming process. Protein synthesis is the second-largest consumer of ATP in myoblasts, as the application of cycloheximide shows that 14%, 32%, and 26% of glycolytic, mitochondrial, and total ATP supply are used toward this process (Figure 6.4, pink). ATP supplied toward Na^+ cycling via the sodium-potassium ATPase occupies the next largest ATP consumer in myoblasts, with 14%, 19%, and 15% of glycolytic, mitochondrial, and total ATP supply used (Figure 6.4, blue). Finally, tubulin (orange) and actin (green) dynamics each account for smaller percentages of ATP supply (Figure 6.4). In total, 68%, 98% and 89% of glycolytic, mitochondrial and total ATP supply were covered by this range of inhibitors.

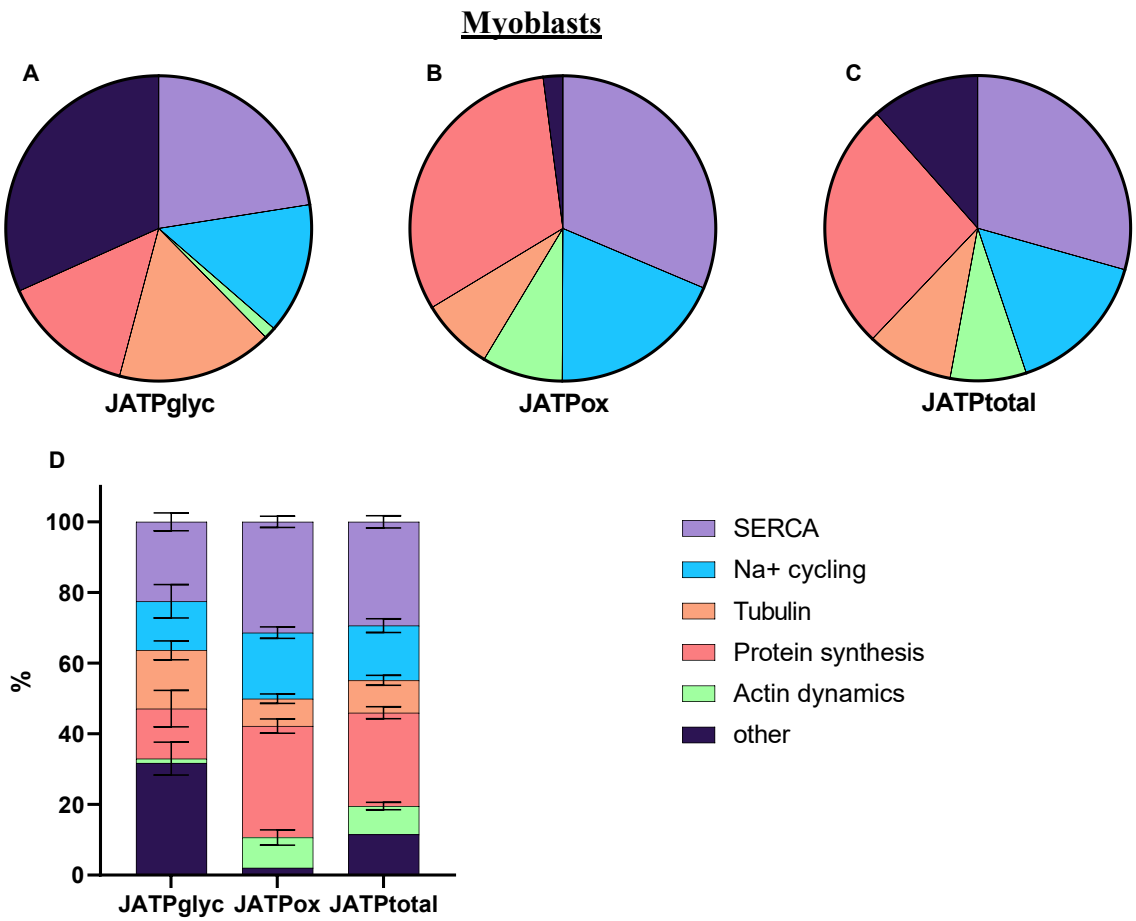

Figure 6.4 – The percentage of glycolytic, mitochondrial and total ATP supply used toward a variety of ATP demanding processes in myoblasts.
The percentage of ATP used toward a variety of ATP demanding processes was estimated in myoblasts that were grown and assayed in 5mM glucose. The activity of an ATP-demanding process was estimated from the response of ATP supply to a specific inhibitor of that process. These responses were expressed as a percentage of uninhibited glycolytic (JATPglyc), mitochondrial (JATPox) or total (JATPtotal) ATP supply, and are shown as pie charts (A-C) and stacked columns (D). Protein normalisation was not carried out in this set of experiments, as the rates were internally normalised. Inhibitor effects were corrected for addition artefacts by subtracting buffer effects. The data are presented as the mean and standard error of the mean (D) of 3-7 technical repeats per inhibitor. The data presented here formed part of inhibitor titrations discussed above (example shown in Figure 6.3) but only the final, chosen, concentration is shown here. The chemical, the process inhibited, and the concentration used (and tested) are as follows: Thapsigargin, SERCA (light purple), 300nM applied (100-1000nM tested). Ouabain, Na+ cycling (blue), 400µM applied (300-2000µM tested). Nocodazole, tubulin polymerisation (orange), 730nM applied (730-3000nM tested). Cycloheximide, protein synthesis (pink), 900nM applied (500-2500nM tested). Latrunculin A, actin dynamics (green), 135nM applied (50-500nM tested). The percentage of ATP supply unaccounted for is shown in dark purple.

Nitrite and insulin decrease the percentage of ATP supply used for protein synthesis

Under conditions when glucose is available, nitrite and insulin stimulation of glycolytic ATP supply is likely indirect in myoblasts, as effects are attenuated by oligomycin and BAM15 (Figure 6.1, G, H & I). This indirect stimulation could be due to enhanced energy demand from any of the ATP-consuming processes described above, or indeed from processes that were not covered by the applied range of inhibitors. Since myoblasts allocate a significant proportion of their ATP supply to make protein, I determined the possible effects of nitrite and insulin on the cycloheximide sensitivity of glycolytic, mitochondrial and total ATP synthesis (Figure 6.5). Such sensitivity is expected to rise if the rate of protein synthesis is indeed increased by nitrite or insulin.

Consistent with previous experiments (Chapter 4, Figure 4.3), both nitrite and insulin stimulate glycolytic ATP supply (Figure 6.5, A and D). Nitrite decreases mitochondrial ATP supply compared to the control, which approaches significance, and insulin significantly increases total ATP supply (Figure 6.5, A & D). The proportions of glycolytic (10%), mitochondrial (32%) and total (25%) ATP supply allocated to protein synthesis in the control condition are comparable to those shown in Figure 6.4. Notably, however, the cycloheximide sensitivity of ATP supply is *not* increased by nitrite or insulin (Figure 6.5, B-D). Instead, cycloheximide sensitivity of glycolytic ATP supply, in particular, tends to be decreased by nitrite and insulin. Experiments with other ATP demand inhibitors should reveal which ATP-consuming processes are increased by nitrite and insulin to explain the indirect stimulation of glycolytic ATP supply in myoblasts.

Myoblasts

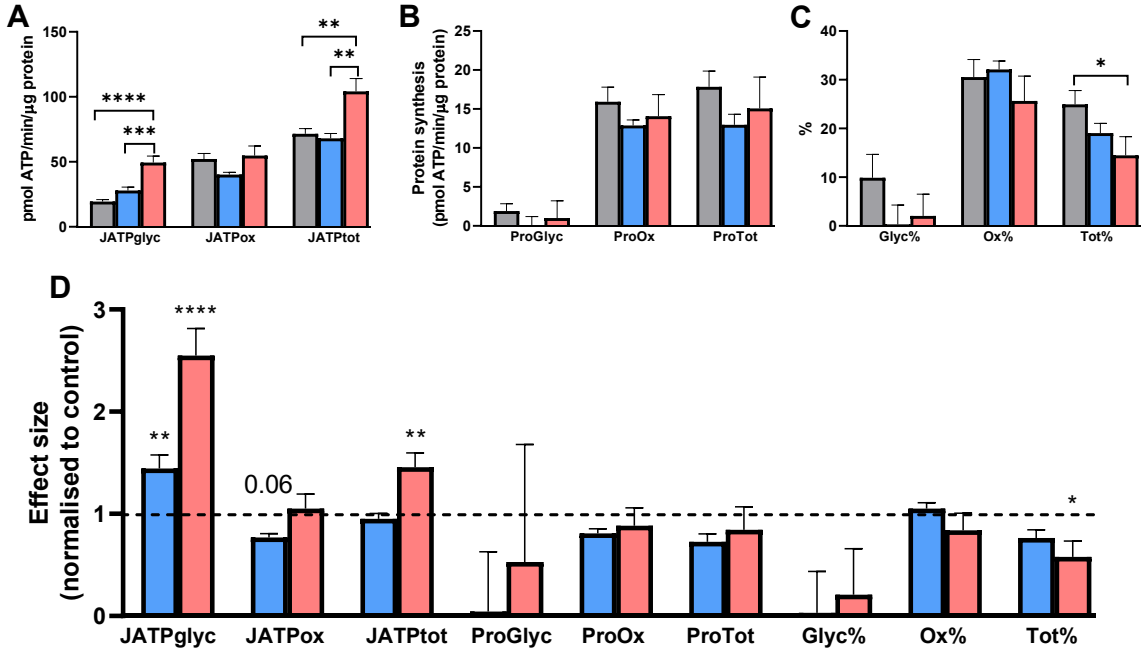

Figure 6.5 – The effect of nitrite and insulin on ATP supplied to protein synthesis in myoblasts.

L6 myoblasts were grown and assayed in 5mM glucose and were exposed to nitrite (blue bars) or insulin (red bars) as stated in previous figure legends. Panel A shows basal ATP supply rates (JATP). Panel B shows the ATP supply rates devoted to protein synthesis for glycolytic (ProGlyc), mitochondrial (ProOx) and total (ProTot) ATP supply. Panel C shows the percentage (%) of the total glycolytic (Glyc%), mitochondrial (Ox%), and total (Tot%) ATP supply devoted to protein synthesis. Inhibitor effects were corrected for addition artefacts by subtracting buffer effects. Panel D shows all rates normalised to the control condition. Data are means ± SEM of 2-3 independent XF runs, containing 3-4 technical repeats. Differences between absolute values were evaluated for statistical significance by one-way ANOVA with Tukey's post-hoc analysis. Significance of normalised effects was assessed by unpaired T-tests ($P < 0.05$, ** $P < 0.01$, *** $P < 0.001$, **** $P < 0.0001$).*

6.3 Discussion

The data presented in this chapter demonstrate that nitrite and insulin stimulation of glycolytic ATP supply is abolished by oligomycin and uncoupler in myoblasts, but persists in myotubes (Figure 6.1, G & H). This finding implies that stimulation of glycolysis is direct in myotubes and indirect in myoblasts. Increased glycolysis in myotubes may be due to direct stimulation of the activity of one or more of the enzymes involved in glycolysis. In myoblasts, however, stimulation of glycolytic ATP supply occurs indirectly, likely due to increased ATP demand. Neither nitrite nor insulin increases the cycloheximide sensitivity of glycolytic ATP supply, ruling out protein synthesis as a possible origin of the enhanced ATP demand.

Nitrite and insulin increase the glycolytic capacity of myotubes, thus stimulating glycolysis directly

The mechanism by which nitrite and insulin stimulate glycolytic ATP supply in myotubes is yet to be revealed, but the data shown in this chapter offers some room for speculation. A mechanistic distinction between glycolytic stimulation in myoblasts and myotubes is evident, as Figure 6.1 demonstrates that nitrite and insulin acutely increase basal glycolytic activity *and* capacity in myotubes, but only basal glycolytic activity in myoblasts. Because the effect of nitrite and insulin on glycolytic ATP supply remains in the presence of glucose and uncoupler, the stimulation likely direct (Figure 6.1). As this is not due to increased glucose uptake (Chapter 5, figure 5.1), it is likely that these molecules directly stimulate one or more of the enzymes involved in glycolysis. Insulin is known to increase the expression of phosphofructokinase and pyruvate kinase, 2 key glycolytic enzymes (Berg *et al.*, 2002). Furthermore, as well as increasing lactate release during high-intensity exercise (Wylie *et al.*, 2016; Domínguez, Garnacho-

Castaño, *et al.*, 2017; Shannon *et al.*, 2017), sodium nitrate and sodium nitrite treatment in zebrafish significantly increase the abundance of several glycolytic intermediates and lactate at rest (Axton *et al.*, 2019), which could suggest increased activity of glycolytic enzymes. Thus, it is conceivable that nitrite and insulin both increase glycolytic ATP supply by directly influencing the expression and/or activity of enzymes involved in this pathway. Given the timescale of the nitrite and insulin effects reported here, post-translational activation is likely.

Stimulation of glycolysis by nitrite and insulin in myotubes may also be due to enhanced glycogen mobilisation, potentially through direct effects on glycogenolytic enzymes, thus increasing fuel availability and flux through glycolysis. The ability of L6 cells to store and utilise glycogen increases significantly upon differentiation (Wahrmann *et al.*, 1977), which may explain why there are apparent mechanistic differences in the way nitrite and insulin stimulate glycolytic ATP supply between myoblasts and myotubes. In favour of increased glycogen mobilisation, glycolytic stimulation by nitrite and insulin in myotubes decreases when myotubes are starved from glucose and glycogen stores are gradually emptied (Chapter 5, Figure 5.3), compared to glycolytic stimulation when glucose is available (Chapter 4, Figure 4.4). The disappearance of glycolytic stimulation by nitrite and insulin in myotubes in the combined presence of oligomycin and uncoupler during glucose deprivation (Figure 6.2, G & H) could signify that the glycogen stores are depleted, and therefore increased flux through glycolysis could not occur. However, insulin promotes glycogen synthesis (Gaster *et al.*, 2004) and beetroot juice supplementation in healthy males during submaximal exercise either had no effect (Betteridge *et al.*, 2016) or significantly decreased (Tan *et al.*, 2018) the decline in muscle glycogen content compared to a control.

Nitrite and insulin stimulate glycolytic ATP supply through multiple targets

The data reveal that nitrite and insulin stimulate glycolytic ATP supply by acting on multiple targets. The relative importance of direct and indirect stimulatory effects will likely depend on the distribution of bioenergetic control between ATP supply and ATP demand. The glycolytic stimulation phenotype is apparent in myoblasts assayed in 5mM glucose (Chapter 4, Figure 4.3). This glycolytic stimulation in response to nitrite and insulin is likely an effect of increased ATP demand in the presence of glucose, as stimulation is abolished by oligomycin and uncoupler (Figure 6.1, G & H). Notably, such indirect stimulation will only be apparent under conditions in which ATP flux is largely controlled by energy expenditure. However, under conditions that shift ATP flux control from ATP demand to ATP supply, direct effects may be expected to dominate the glycolytic stimulation phenotype instead. For instance, when nutrient deprivation moves control to ATP supply (discussed in Chapter 3), one would expect that this indirect stimulation of glycolysis would disappear. However, stimulation is more prominent, although more variable, in the glucose-deprived state in myoblasts (Chapter 5, Figure 5.2), and glycolytic stimulation remains somewhat evident by nitrite and insulin in the absence of glucose but the presence of uncoupler (Figure 6.2, G & H).

Overall, nitrite and insulin likely have a plethora of effects on myocyte energy metabolism, potentially stimulating both ATP supply and ATP demand. The nutritional background, and bioenergetic control structure, determines which of these effects dominate the glycolytic stimulation phenotype. A formal control analysis could establish the distribution of bioenergetic control between ATP supply and ATP demand in myocytes (Brand, 1996) and would give insight as to how the control of energy metabolism changes in response to different nutritional backgrounds.

Nitrite and insulin stimulation of ATP demand is not due to enhanced protein synthesis

The allocation of mitochondrial ATP supply in the control was 32% for protein synthesis and 19% for Na^+ cycling via the sodium-potassium ATPase (Figure 6.4). These results are comparable with L6 myoblasts assayed under slightly different conditions, where 31% and 21% of mitochondrial ATP supply was used for protein synthesis and Na^+ cycling, respectively (Nisr *et al.*, 2016). C2C12 myoblasts, however, have a different ATP consumption profile compared to the L6 myoblasts assayed here, allocating approximately 25% to protein synthesis and only 8% to Na^+ cycling (Mookerjee *et al.*, 2017). Furthermore, C2C12 myoblasts only allocate approximately 7% of their oxidative ATP consumption to calcium handling via SERCA (Mookerjee *et al.*, 2017). Calcium handling was the largest ATP consumer in the L6 myoblasts assessed here, attracting 23%, 32%, and 29% of glycolytic, mitochondrial and total ATP supply, respectively (Figure 6.4).

The effect of nitrite and insulin on ATP allocation to SERCA was not assessed because, although calcium handling occupies a large portion of glycolytic ATP supply, and contractile force production is increased in response to sodium nitrate (Hernández *et al.*, 2012; Ivarsson *et al.*, 2017), the effects of nitrogen species on SERCA are likely inhibitory (Ishii *et al.*, 1998). Furthermore, myoblasts likely face higher demand for ATP than myotubes, which is evident from their comparatively high production of ATP (Chapter 3, Figure 3.2). This difference in demand between differentiation states likely arises because following differentiation the cells are no longer actively dividing, which is expected to require large amounts of protein synthesis. Thus, protein synthesis, which is known to be stimulated by insulin (Stump *et al.*, 2003; Barazzoni *et al.*, 2012;

Robinson *et al.*, 2014), was chosen first to explore how these molecules stimulate glycolytic ATP supply (Figure 6.5).

Overall, insulin slightly decreased the amount of ATP supply used toward protein synthesis in myoblasts (Figure 6.5 C & D), which goes against textbook knowledge of the anabolic actions of insulin (as discussed in the Introduction). One explanation for this is that these myoblasts are not responsive to insulin, as evident from the lack of insulin-stimulated decrease in proton leak (Chapter 4, Figure 4.1) and the lack of glucose uptake (Chapter 5, Figure 5.1). When cells are differentiated, they are responsive to insulin (Chapter 4, Figure 4.2). Furthermore, the presence of amino acids may be required to induce increased mitochondrial protein synthesis in response to insulin (Barazzoni *et al.*, 2012; Robinson *et al.*, 2014). Amino acids did not form part of the KRPH used here (Methods). Overall, the percentage of total ATP supply used toward protein synthesis significantly decreases in response to insulin (Figure 6.5, C & D). Thus, another energy-requiring process must be stimulated because total ATP supply is stimulated by insulin (Figure 6.5, A). Nitrite also provoked decreases in the percentage of total ATP supply used toward protein synthesis compared to the control (Figure 6.5, C & D). Because total ATP supply remains constant when nitrite is applied (Figure 6.5, A) (Chapter 4, Figure 4.3), another ATP demanding process must be stimulated. These observations suggest that ATP allocation to ATP-demanding processes is acutely re-arranged by nitrite. However, why this rearrangement or increase in ATP demand is met by glycolytic, rather than mitochondrial, ATP supply requires explanation.

6.4 Conclusion

When glucose is freely available, glycolytic capacity is increased in myotubes exposed to nitrite and insulin. This finding indicates that these molecules can affect glycolytic ATP supply directly. Previously, nitrite and insulin were shown to not affect glucose uptake by myotubes (Chapter 5, Figure 5.1), thus ruling out the possibility that this stimulation occurs secondary to glucose uptake. Therefore, glycolytic ATP supply is likely stimulated in myotubes through direct stimulation of glycolytic and/or glycogenolytic enzymes, thus increasing fuel availability and flux through glycolysis. In myoblasts, the effects of nitrite and insulin on glycolysis are likely indirect, occurring through changes in ATP demand. Although it remains to be established which ATP-consuming processes are affected, stimulation of protein synthesis can be ruled out. Overall, the data reveal that nitrite and insulin stimulate glycolytic ATP supply by acting on multiple targets. The relative importance of direct and indirect stimulatory effects will likely depend on the distribution of bioenergetic control between ATP supply and ATP demand.

7 General discussion

The findings reported in this thesis inform ongoing debate on the mechanism that underpins the exercise benefits of dietary nitrate. Detailed extracellular flux analysis reveals that nitrite (i.e., the reduction intermediate between nitrate and nitric oxide) acutely stimulates the rate of glycolytic ATP supply in L6 muscle cells. With much less pronounced effects on mitochondrial ATP supply, such stimulation shifts the myocytes towards a more glycolytic phenotype and thus lowers the apparent oxygen cost of ATP synthesis. This acute nitrite effect is also achieved by insulin but appears not to be related to glucose uptake or availability. Instead, it is demonstrated that nitrite and insulin stimulate glycolysis through multiple targets, either directly by activating glycolytic and/or glycogenolytic enzymes, or indirectly by enhancing the activity of ATP-consuming processes. These findings offer an alternative model for the mechanism by which dietary nitrate lowers the oxygen cost of exercise. In this chapter, I will discuss the implications of my work in a wider context, highlight the strengths and limitations of the adopted experimental approach, and make suggestions for future research.

7.1 XF analysis

Simultaneous measurement of oxygen consumption and medium acidification by cultured cells using a Seahorse Extracellular Flux Analyser offers valuable insight into cellular energy metabolism. This technology is used in a wealth of studies exploring immune responses (Garzorz-Stark *et al.*, 2018; Seim *et al.*, 2019), neurological investigations (Polyzos *et al.*, 2019; Vandoorne *et al.*, 2019), and the bioenergetics of cancer (Pan *et al.*, 2019; Panina *et al.*, 2019). Combined OCR and ECAR data offer rich information on intracellular ATP synthesis when such data are analysed through the

application of textbook knowledge on bioenergetics and biochemistry (Mookerjee *et al.*, 2017) (see Chapter 2). Using this approach enables full quantification of ATP supply fluxes, as it accounts for both glycolytic and mitochondrial ATP supply (Mookerjee *et al.*, 2017). This analysis gives a complete view of myocyte energy metabolism and can reveal phenomena that are not evident from the "raw" OCR and ECAR data. Moreover, this technique and analysis can be utilised to develop an ATP consumption profile of cultured cells (Mookerjee *et al.*, 2017). This approach was applied throughout this thesis, allowing for full bioenergetic phenotyping of cells exposed to nitrite and insulin. This is one of the main strengths and novelties of this thesis. Indeed, without such analysis, it would not have been apparent that nitrite and insulin acutely shifted myocytes to a more glycolytic phenotype.

Oxygen consumption, and rates derived from this measurement, are considered reliably calculated. The application of mitochondrial effectors, which activate or inhibit specific processes involved in mitochondrial respiration, allows for the reliable calculation of several parameters pertinent to mitochondrial function (Brand *et al.*, 2011). Thus, respiration linked to oxidative ATP synthesis can be calculated. Medium acidification is more ambiguous and is often misinterpreted as an exclusive reflection of glycolytic ATP supply (Divakaruni *et al.*, 2014). This misinterpretation of ECAR as glycolysis ignores the notion that lactate production *and* CO_2 generated from TCA cycle turnover contribute to medium acidification (Mookerjee *et al.*, 2015). Thus, to fully quantify ATP supply rates and add depth to the information generated from the XF Analyser, certain assumptions and corrections must be made (Mookerjee *et al.*, 2017), which weakens the approach to some extent.

For example, an assumption was made regarding the contributions of the shuttles that move NADH formed by glycolysis from the cytosol and into the

mitochondria, which affects the P/O ratio for oxidative phosphorylation. Within this thesis, it was assumed that NADH shuttling contributions were performed 90% by the malate-aspartate shuttle and 10% by the glycerol-3-phosphate shuttle, which follows previously published logic (Mookerjee *et al.*, 2017). Another fundamental assumption made when assessing ATP supply rates throughout this thesis was that the dominant carbon fuel used by cells was glucose. This assumption was made because cells were incubated in KRPH containing glucose as the only fuel for approximately 1.5 hours before XF analysis. However, when myocytes were deprived of nutrients (Chapters 3 & 5), it was unknown which fuel dominates the signal, which is a limitation for the analysis. It is likely that when glucose is deprived, endogenous substrates, such as glycogen, are mobilised. Therefore, the amount of ATP produced via glycolysis would be underestimated under these conditions, as the P/O ratio for glycolysis during glycogen metabolism is 1.5 times that of glucose (Mookerjee *et al.*, 2017). Regardless of the limitations of the analysis, the pattern of changes in ATP supply rates in response to nitrite and insulin would have been the same, giving confidence in the results presented herein.

7.2 Nutritional background

Chapter 3 provides a detailed characterisation of the bioenergetic behaviour of undifferentiated and differentiated L6 myocytes under different nutritional backgrounds. The findings revealed that the nutritional background in which cells are maintained and the differentiation status of cells impacted the results, which highlights the importance of differences in the nutritional background when drawing conclusions. The importance of nutritional background when drawing conclusions is also highlighted by the use of the XF analysis in cancer research. The use of 25mM glucose within the culture and

assay medium resulted in suppressed mitochondrial respiration and increased aerobic glycolysis in cancer cell lines, which was said to be a hallmark of cancer (Potter *et al.*, 2016). However, assaying the same cell lines in 5mM glucose, a more physiologically relevant concentration, reduces aerobic glycolysis and increases mitochondrial respiration (Potter *et al.*, 2016). Overall, care should be taken when comparing data from XF analysis, and data from any other analysis, when nutrient availability and differentiation status differ.

7.3 Oxygen cost of ATP synthesis

The main novel finding of this thesis was that nitrite increases glycolytic ATP supply in both L6 myoblasts and myotubes, regardless of glucose availability (Chapter 4, Figures 4.3 & 4.4 & Chapter 5, Figures 5.2 & 5.3). Stimulation of glycolytic ATP supply was sufficient to cause rises in the ATP/O_2 ratio, meaning that nitrite significantly decreased the oxygen cost of ATP synthesis in L6 myocytes. Therefore, this thesis adds to the body of knowledge surrounding the effects of nitrogen species by uncovering an alternative explanation as to how nitrogen species lower the oxygen cost of sub-maximal exercise (Larsen *et al.*, 2007).

One school of thought regarding how nitrogen species lower the oxygen cost of exercise poses that dietary nitrate improves the efficiency of oxidative phosphorylation (Larsen *et al.*, 2011). In contrast, recent human trials suggest that nitrogen species-driven decreases in oxygen uptake occur without mitochondrial efficiency changes (Whitfield *et al.*, 2016). This finding is supported by rodent studies, which show either a lack of (Ntessalen *et al.*, 2020) or diminishing (Ivarsson *et al.*, 2017) effect of nitrogen species on coupling efficiency in isolated skeletal muscle mitochondria. My observations further weaken the argument that nitrogen species lower the oxygen cost of

exercise by improving coupling efficiency because no change in ATP-linked or proton leak-linked respiration were observed in response to nitrite (Chapters 4 & 5). On the other hand, insulin provoked improvements in mitochondrial efficiency, which demonstrates that the XF assay is sufficiently sensitive to pick up acute effects on coupling efficiency, giving confidence in the lack of observed effect of nitrite on this parameter. XF analysis of mitochondria isolated from sodium nitrite supplemented mice resulted in a decrease of all respiratory parameters compared to the control (Ntessalen *et al.*, 2020), which mirrors the results for intact myoblasts shown here (Chapter 4, Figure 4.1). Furthermore, primary rat aortic smooth muscle cells assayed under normoxic conditions via XF analysis show no effect of 25μM nitrite on any oxygen consumption related parameter (Mo *et al.*, 2012), again agreeing with the results presented in this thesis. These similarities further strengthen the reliability of the observations made in this thesis.

My data provide an alternative mechanism for how nitrogen species lower the oxygen cost of exercise. Nitrite was shown to provoke significant increases in glycolytic ATP supply, which lowered the overall oxygen cost of ATP synthesis (Chapter 4, Figures 4.3 & 4.4). This effect could account for the lowered oxygen cost of exercise in humans (Larsen *et al.*, 2007) as a larger proportion of ATP supplied during exercise could be fulfilled by ATP from glycolytic, rather than oxidative, origin, thus lowering the overall oxygen cost of skeletal muscle work. The increases in glycolytic ATP supply in response to nitrite also may explain why endurance athletes (Bescós *et al.*, 2012) and the highly aerobically fit (Carriker *et al.*, 2016) do not benefit from ingestion of nitrogen species. These populations are more likely to have a higher composition of slow-twitch muscle fibres, which are predominantly oxidative and have a higher abundance of mitochondria (Westerblad *et al.*, 2010). Indeed, it has been suggested that

nitrogen species preferentially exert their effects on skeletal muscle by impacting fast, glycolytic skeletal muscle fibres (Jones *et al.*, 2016), which, along with the data presented here, provides insights as to why these populations are unaffected by the beneficial effects of nitrogen species on exercise.

7.4 Lactate production

Glycolytic stimulation by nitrite is a robust observation, which occurs irrespective of nutrient availability or differentiation status (Chapters 4 & 5). Many of the studies discussed above do not provide insight on pH or ECAR measurements for comparison, due to the use of isolated mitochondria or machines that do not measure such parameters (Larsen *et al.*, 2011; Mo *et al.*, 2012; Khoo *et al.*, 2014; Whitfield *et al.*, 2016; Ntessalen *et al.*, 2020). C2C12 myocytes assessed by XF analysis were found to rely more strongly on oxidative ATP supply in response to beetroot juice and showed decreased basal and peak ECAR compared to the control (Vaughan *et al.*, 2016). These data suggest that nitrogen species induce a shift into a more oxidative phenotype, which disagrees with the glycolytic phenotype presented here. However, different cell models may have slightly different physiology, which is highlighted by the difference in ATP consumption profile between C2C12 (Mookerjee *et al.*, 2017) and L6 (Chapter 6, Figure 6.4) myoblasts. Furthermore, this oxidative phenotype occurred in response to beetroot juice of ill-defined composition, which contained protein, carbohydrates, fats and vitamins (Vaughan *et al.*, 2016). Therefore, the results could have been a response to any of these factors, as the study lacked an appropriate nitrate-depleted beetroot juice control (Vaughan *et al.*, 2016). The effects of nitrite and insulin on glycolytic ATP synthesis shown in this thesis are reflected by their effects on lactate release, although more convincingly in myoblasts than in myotubes (Chapter 4, Figure 4.5). However, the

XF glycolytic phenotype is much smaller in myotubes than myoblasts, which may explain why the generally smaller lactate release effects are not apparent (nitrite) or statistically significant (insulin) in myotubes.

The results presented here also seem at odds with the reported lack of nitrogen species' effect on lactate production in humans during submaximal workloads (Larsen *et al.*, 2007; Betteridge *et al.*, 2016). Although, it is worth note that in some human trials, lactate release tended to increase in response to nitrate supplementation, but did not reach significance (Larsen *et al.*, 2007). However, the data agree with a nitrogen-species-driven increase in lactate production as exercise intensity increases (Wylie *et al.*, 2016; Domínguez, Garnacho-Castaño, *et al.*, 2017; Shannon *et al.*, 2017). The type of muscle fibre targeted by nitrogen species may explain how lactate release is increased. Nitrogen species have been shown to increase muscle blood flow (Ferguson *et al.*, 2013) and force production at low stimulation frequencies (Hernández *et al.*, 2012; Ivarsson *et al.*, 2017), specifically in type II muscle fibres. Thus, it has been hypothesised that nitrogen species exert their effects specifically on type II fibres (Jones *et al.*, 2016).

It has been suggested that increased blood lactate in response to nitrogen species may be due to increased blood flow to type II fibres, as the transfer of lactate into the blood increases with increased blood flow (Domínguez, Garnacho-Castaño, *et al.*, 2017). However, in rats injected with sodium nitrite, lactate production increases during exercise, with no change in blood flow to the hind limb's type II fibres (Glean *et al.*, 2015). Studies showing increased lactate release in humans (Wylie *et al.*, 2016; Domínguez, Garnacho-Castaño, *et al.*, 2017; Shannon *et al.*, 2017) support the hypothesis that type II fibres are targeted by nitrogen species (Jones *et al.*, 2016), as type II fibre recruitment is expected in the types of exercise used during these

experiments, which are highly glycolytic (Spangenburg *et al.*, 2003). Nitrogen species may increase engagement of type II fibres during exercise, which may account for the decreased oxygen uptake seen during submaximal workloads (Larsen *et al.*, 2007; Bailey *et al.*, 2009; Vanhatalo *et al.*, 2010; Lansley, Winyard, Fulford, *et al.*, 2011). However, why increased lactate production is not observed during submaximal workloads in response to nitrogen species requires explanation.

Lactate production and clearance involves many organs. For example, as skeletal muscle produces lactate, the liver removes around 70% from circulation and metabolises it via gluconeogenesis (Phypers *et al.*, 2006). During submaximal exercise, lactate is efficiently cleared by this and other processes, such that there is a balance between production and removal (Billat *et al.*, 2003) and lactate concentration remains constant (Moxnes *et al.*, 2012; Jones *et al.*, 2019). However, as exercise intensity increases, blood lactate increases (Goodwin *et al.*, 2007; Jones *et al.*, 2019), reflecting increased lactate production or decreased lactate removal (Moxnes *et al.*, 2012). The point at which lactate accumulation begins to increase with increasing work rate is known as the lactate threshold or the maximal lactate steady state (Goodwin *et al.*, 2007; Jones *et al.*, 2019). Thus, an increase in lactate production in response to nitrogen species may go undetected in the blood or plasma during submaximal workloads, as it is under the lactate threshold and within the capacity of the liver and other organs to efficiently clear it. However, the lactate threshold is surpassed during higher exercise intensities, potentially enabling an environment that allows the effect of nitrogen species on lactate production to be detected.

Hepatic recycling of lactate results in an oxygen debt because lactate is oxidised to provide the ATP and GTP required to allow gluconeogenesis from lactate (Bender, 2003). Thus, additional lactate production, seen during higher intensity exercise in

response to nitrogen species (Wylie *et al.*, 2016; Domínguez, Garnacho-Castaño, *et al.*, 2017; Shannon *et al.*, 2017), may augment this oxygen debt and could explain why oxygen consumption is not lowered during severe and maximal intensity exercise by nitrogen species (Pawlak-Chaouch *et al.*, 2016). The cells used in this thesis were at rest, and therefore the exercise intensities used in the above studies were not mimicked. However, evidence suggests that nitrogen species increase lactate accumulation at rest (Domínguez, Garnacho-Castaño, *et al.*, 2017; Axton *et al.*, 2019), which agrees with the data presented here. Finally, my experiments were performed in a system that does not have other organs present. Thus, the only mechanism by which lactate production, or better the pH changes that the XF analyser measures, can be "removed" is by the buffering power of the medium used during experimentation. In such a system, the stimulatory effect of nitrogen species, specifically nitrite, on glycolytic ATP supply, therefore, becomes apparent.

7.5 How do nitrite and insulin stimulate glycolytic ATP supply?

The results presented in this thesis do not conclusively reveal the underlying mechanism by which nitrite and insulin increase glycolytic ATP supply, but they exclude some possibilities and demonstrate that multiple targets are involved.

Glucose uptake

Glycolytic stimulation in response to nitrite was not the result of increased glucose uptake (Chapter 5, Figure 5.1). This assertion was strengthened by the observation that nitrite-driven stimulation of glycolysis occurred even when myocytes were deprived of glucose (Chapter 5, Figures 5.2 and 5.3). This finding is at odds with observations that nitrogen species improve murine glucose homeostasis (Jiang *et al.*, 2014; Singamsetty

et al., 2015), and increase GLUT4 gene and protein expression (Vaughan *et al.*, 2016), but agrees with the lack of effect of nitrogen species on glucose homeostasis in humans (Ashor *et al.*, 2016; Beals *et al.*, 2017).

Interestingly, when nitrite and insulin were applied together to L6 myocytes, glucose uptake was significantly increased (Chapter 5, Figure 5.1). Evidence suggests that sodium nitrite benefits both insulin secretion and glucose disposal. In response to sodium nitrite, insulin secretion is significantly increased at basal (Nyström *et al.*, 2012) and stimulatory (Gheibi *et al.*, 2017) concentrations of glucose. This improvement in insulin output, and potential improvement in glucose disposal (Jiang *et al.*, 2014; Vaughan *et al.*, 2016), could account for improvements in the diabetic phenotype seen in response to nitrogen species (Jiang *et al.*, 2014; Singamsetty *et al.*, 2015). Overall, nitrogen species have positive effects on several parameters related to insulin, from its release and its cellular action, which could indicate that nitrogen species require the presence of insulin to exert their effects on glucose disposal. Indeed, the results presented here show that glucose uptake improvements only occur when nitrite and insulin are applied together, suggesting that these molecules may work in tandem to improve insulin sensitivity.

Direct and indirect stimulation of glycolytic ATP supply

Exploring the ATP supply rates in the presence of oligomycin and uncoupler revealed that in myotubes, nitrite stimulation of glycolysis likely occurs directly, as this stimulation persisted under conditions where control over ATP flux is shifted from demand to supply (Chapter 6, Figure 6.1). Plausible ways in which nitrite stimulates glycolysis directly include direct interaction with glycolytic or glycogenolytic enzymes. Differentiation provokes an increased ability of L6 cells to store and utilise glycogen

(Wahrmann *et al.*, 1977), which may explain the differences in the way nitrite stimulates glycolytic ATP supply between myoblasts and myotubes. However, human trials suggest that glycogen storage at rest and following exercise tends to increase compared to a control group in response to beetroot juice supplementation (Betteridge *et al.*, 2016).

ATP flux is predominately driven by ATP demand in skeletal muscle (Nisr *et al.*, 2016; Mookerjee *et al.*, 2017). Thus, any changes in ATP supply could result from changed ATP consumption. Interestingly, the nitrite and insulin stimulation of glycolytic ATP supply in myoblasts indeed appears to follow from changes in energy expenditure (Chapter 6, Figure 6.1). My data do not conclusively show which ATP-consuming process is stimulated by nitrite or insulin but protein synthesis can be ruled out as a possibility (Chapter 6, Figure 6.5). Why the nitrite and insulin-driven change in ATP demand is met by glycolytic, rather than mitochondrial, ATP supply requires explanation.

Glucose metabolism is thought to be governed by oxygen concentrations, such that the default source of ATP for consuming processes in normoxia was thought to be high-ATP-yielding oxidative phosphorylation, rather than lower-yielding glycolysis, which was thought to be reserved for when oxygen is low (Webster, 2003). However, glycolytic ATP supply resulting in lactate production is observed in cells at ambient oxygen tensions (Chapters 3, 4 & 5). Cancer cells also exhibit higher rates of aerobic glycolysis, which is known as the Warburg effect and is often reported to be due to mitochondrial dysfunction (Hsu *et al.*, 2016). However, another explanation as to why cells produce ATP via aerobic glycolysis is that cells may use both metabolic pathways in tandem to meet energetic demand (Epstein *et al.*, 2014). Epstein and colleagues propose that both pathways' ATP production speed is balanced against the yield of ATP

(the efficiency of the pathway). In this model, it is proposed that cells use slow but efficient oxidative phosphorylation to maintain baseline energetic demand and use rapid but inefficient glycolytic ATP to fuel short term fluctuations in ATP demand, such as membrane transport (Epstein *et al.*, 2014).

Furthermore, there is evidence to suggest that cells may utilise ATP depending on the location of production and consumption. For example, Na^+ cycling, occurring at the membrane of the cell, in fast-twitch skeletal muscle (Okamoto *et al.*, 2001) and human mammary epithelial cells (Epstein *et al.*, 2014) is preferentially met by glycolytic ATP supply in normoxic conditions. In the latter study, ouabain application, which inhibits the sodium-potassium ATPase, significantly inhibited proton production rates but left oxygen consumption unaffected, indicating that cells preferentially use glycolytic ATP supply to fuel this process (Epstein *et al.*, 2014). This evidence could suggest that the increased glycolytic ATP supply in response to nitrite and insulin seen in this thesis may be in response to rapid, short term fluctuations in energy demand, through increases in processes that preferentially consume glycolytic ATP.

7.6 Nitrite or nitric oxide?

It remains to be established whether the acute effects of nitrite reported here are direct nitrite effects or are instead mediated by a nitrite derivative. Nitric oxide is generally held responsible for the exercise benefit afforded by dietary nitrate (Jones *et al.*, 2018). Nitrate reduction to nitrite and then nitric oxide has recently been suggested possible in human muscle cells (Srihirun *et al.*, 2020), but experimental support is indirect. When exposed to nitrate, cells indeed contain increased amounts of nitrate and, to some extent, nitrite (Srihirun *et al.*, 2020). When exposed to 1mM nitrite, the cGMP concentration is increased too (Srihirun *et al.*, 2020), which indicates a raised nitric oxide level. It has

been reported that nitric oxide inhibits cytochrome *c* oxidase, competing with oxygen, thus lowering mitochondrial respiration and ATP production (Brown *et al.*, 2007). Cytochrome *c* oxidase may have been inhibited in myoblasts, as nitrite indeed decreased mitochondrial respiration (Chapter 4, Figure 4.1). However, nitrite did not lower respiration in myotubes (Chapter 4, Figure 4.2), which suggests cytochrome *c* oxidase was not inhibited in this system. The potential generation of nitric oxide in one cell system but not the other weakens the idea that nitric oxide is responsible for the observed nitrite effects. Furthermore, the data show stimulation of glycolytic ATP supply by nitrite at low-micromolar concentrations, at neutral pH and under an oxygen atmosphere (21%) that is hyperoxic from a physiological perspective. Under these conditions, it is unlikely that nitrite is reduced to nitric oxide (Pereira *et al.*, 2013). Thus, nitric oxide generation is unlikely responsible for the nitrite effects reported in this thesis.

7.7 Physiological relevance

At present, it is not known how translatable the findings presented in this thesis are to a human system. Nitrogen species lower the oxygen cost of sub-maximal exercise (Larsen *et al.*, 2007) but it is important to note that submaximal workloads are unlikely to be mimicked in the static L6 cells used here. However, nitrite-driven stimulation of glycolytic ATP supply was observed in spontaneously contracting L6 myotubes (Wynne and Affourtit, unpublished). Regardless, using a cell model limits the ability to discuss these findings in line with those found in human studies. However, L6 cells have proven a reliable model of skeletal muscle bioenergetics, with behaviour that is highly reproducible in primary human myocytes (Nisr *et al.*, 2014, 2016). Importantly, L6 cells and the Seahorse XF Analyser have been used extensively to explore skeletal

muscle bioenergetics, for example, to understand the effect of Bisphenol A, an environmental pollutant, on mitochondrial function and insulin sensitivity (Ahmed *et al.*, 2020). L6 cells have also been used to understand the effect of exercise-induced decreases in pH on skeletal muscle mitochondrial function (Genders *et al.*, 2019). The beneficial bioenergetic effects of insulin on skeletal muscle metabolism and how palmitate annuls these benefits have been explored using L6 cells (Nisr *et al.*, 2014). Finally, L6 cells have been used to explore obesity-related insulin resistance and mitochondrial dysfunction, using a Seahorse XF analyser to determine how fatty acids affect skeletal muscle bioenergetics and the distribution of oxidative ATP supply to ATP demanding processes (Nisr *et al.*, 2016). Thus, this cell line is a reliable model of skeletal muscle.

7.8 What is needed to identify the molecular targets of nitrite and insulin?

Nitrate supplementation has a wealth of effects on human skeletal muscle and exercise (Larsen *et al.*, 2007, 2011; Bailey *et al.*, 2010; Lansley, Winyard, Bailey, *et al.*, 2011; Whitfield *et al.*, 2017). Therefore, it is likely that nitrite has diverse effects on myocyte metabolism by affecting multiple molecular targets and pathways. Initially, the effect of nitrite and insulin on the bioenergetic behaviour of L6 myocytes should be explored using human skeletal muscle cells through their isolation from *vastus lateralis* biopsies (Nisr *et al.*, 2014), to improve the translational meaning of the findings presented here.

To add depth and mechanistic insight into the results presented in this thesis, the following experiments should be considered. Glucose deprivation had several detrimental effects on myocyte metabolism, such as reducing respiratory capacity and increasing proton leak (Chapter 3). To test whether starvation-induced ROS production and UCP activation plays a role in starvation-induced proton leak, measurements of

ROS production by fluorescent probes, such as dihydroethidum (Scherz-Shouval *et al.*, 2007) should occur. Assessment of UCP activation should also occur by subjecting the cells to XF analysis during starvation in the presence of UCP inhibitors or by using UCP knockdown cells. The detrimental effects of glucose deprivation on these parameters were partially rescued through the reintroduction of glucose during the XF assay (Chapter 3). Furthermore, glucose addition following glucose deprivation stimulated glycolytic ATP supply to rates that exceeded those seen when cells were maintained in glucose throughout the assay. Therefore, assessment of the impact of glucose resupply in the presence of non-competitive GLUT inhibitors, such as HIV protease inhibitors (Hresko *et al.*, 2011), or GLUT knockout cells, may shed light on the mechanism behind such results. Importantly, as discussed in section 7.2, the nutritional background in which cells are assayed may impact the results. Thus, future experiments should include assessment of the effects of nitrite and insulin using different metabolic fuels and at different concentrations. Finally, in an effort to understand how glycolytic ATP supply was stimulated indirectly by nitrite and insulin, assessment of the amount of ATP supply used toward protein synthesis occurred. Nitrite and insulin provoked decreases in the percentage of total ATP supply used toward protein synthesis compared to the control (Chapter 6). In order to confirm these results, the rate of de novo protein synthesis should be measured by tagging and measuring newly synthesised proteins with L-azidohomoalanine (Dieterich *et al.*, 2006).

The data presented in this thesis reveal that nitrite and insulin stimulate glycolytic ATP supply by acting on multiple targets. As discussed in Chapter 6, the relative importance of direct and indirect stimulatory effects will depend on the distribution of bioenergetic control between ATP supply and ATP demand. Therefore, establishing the distribution of bioenergetic control between ATP supply and ATP

demand under different nutritional states would give insight as to how the control of energy metabolism changes in response to different nutritional backgrounds. This approach can also be used to identify how nitrite and insulin carry out their effects on metabolism and whether nutritional background impacts these effects. The distribution of bioenergetic control can be calculated using Functional Systems Analysis, which involves conceptually simplifying complex systems into large modules, which contain various reactions (Brand, 1998), that communicate via a common metabolic intermediate (Brand, 1996). Here, the system could be simplified in terms of energy metabolism, by grouping processes that, respectively, supply and demand ATP, which interact via the cytosolic ATP/ADP ratio. Assessing the bioenergetic control structure in this way would add depth to our understanding, by showing the impact of nitrite and insulin on bioenergetics in the whole system.

Nitrite and insulin may influence the mobilisation and metabolism of glycogen. Therefore, glycogen storage and usage should be assessed under the different nutritional states applied throughout this thesis. It is also conceivable that nitrite and insulin increase glycolytic ATP supply by directly influencing glycolytic or glycogenolytic enzyme expression and activity. The activity of glycolytic and glycogenolytic enzymes in L6 cells in response to nitrite and insulin can be tested spectrophotometrically using commercially available assays (Teslaa *et al.*, 2014). This approach, which can be executed with cell lysates that have been incubated with nitrite and insulin, will test whether the glycolytic phenotype is secondary to increased glycogenolysis and glycolysis. Furthermore, possible increased gene expression of glycolytic and glycogenolytic targets in response to nitrite can be explored using quantitative polymerase chain reaction. Western analysis can then be used to confirm whether potential increases in mRNA expression are reflected at the protein level.

To assess how nitrite and insulin impact energy demand, a range of energy-requiring processes should be assessed in the presence of nitrite and insulin using the technique applied in Chapter 6. If an energy-requiring process is found to be enhanced by nitrite, further exploration of that pathway should occur by using the same techniques described above to understand how nitrite impacts that pathway. Once these approaches identify nitrite and insulin targets, potential posttranslational modifications by nitrite to the enzymes and proteins of interest can then be established to increase understanding of how nitrite impacts that pathway. Once the targets of nitrite on metabolism are identified, the physiological relevance of these findings can be further evaluated through analysis of nitrite targets in human skeletal muscle biopsies from control and nitrate-supplemented individuals. For example, healthy participants could be supplemented with beetroot juice or an appropriate control for several days. Skeletal muscle biopsies could be taken at rest and following exercise for enzyme analysis of predicted nitrite targets as discussed above. Furthermore, to confirm whether lactate release is increased in human populations supplemented with nitrate or nitrite, continuous blood lactate monitoring through microdialysis (Schierenbeck *et al.*, 2014) during rest and exercise may provide a more accurate way of measuring glycolytic ATP supply in human populations. Overall, these experiments will add depth to the findings presented within this thesis.

7.9 Prospect

Nitrate supplementation has a clear benefit on skeletal muscle and exercise, such as lowering the oxygen cost of submaximal exercise (Larsen *et al.*, 2007; Lansley, Winyard, Fulford, *et al.*, 2011), increasing exercise tolerance by ~22% (Breese *et al.*, 2013; Bailey *et al.*, 2015) and improving power output and performance (Lansley,

Winyard, Bailey, *et al.*, 2011; Murphy *et al.*, 2012). However, there is variation seen in the physiological benefits of dietary nitrate among healthy and diseased human populations. For example, individuals with chronic illnesses (Pawlak-Chaouch *et al.*, 2016), the highly aerobically fit (Carriker *et al.*, 2016), and elite and endurance athletes (Bescós *et al.*, 2012; Peacock *et al.*, 2012) appear to be non-responsive to the exercise benefit on dietary nitrate supplementation. Several factors may explain the differences in responsiveness to the exercise benefits exerted by nitrate supplementation between and within populations, such as genetics, muscle oxygenation and the muscle fibre-type composition of the population being studied.

The future work detailed above will help to identify the molecular targets of nitrite on skeletal muscle energy metabolism, and identification of such targets will also likely aid understanding of why the effects of nitrate on exercise are not universal. If molecular targets are identified, a population-wide study assessing the correlation between the expression of the nitrite target(s) and nitrate-responsiveness could be performed, which may shed light on why these targets are not impacted by nitrite in individuals that do not respond to nitrate supplementation. For example, variable nitrate sensitivity amongst human populations might arise from regulatory differences of glycolytic targets. Moreover, perturbed metabolic control in disease could lower the potential of these targets to regulate muscle bioenergetics, which would be reflected by an *apparent* lack of nitrate sensitivity.

In conclusion, the full bioenergetic phenotyping of L6 cells reported in this thesis has offered an alternative mechanistic explanation as to how dietary nitrate lowers the oxygen cost of exercise. The reported data suggest that nitrate-derived nitrite hits multiple molecular targets to increase glycolytic ATP supply directly and indirectly, and thus to lower the oxygen cost of ATP synthesis. Future identification of these targets

should open the way for human trials that may explain why the exercise benefits of nitrate are variable, which will be crucial for achieving the full translational potential of dietary nitrate supplementation.

8 References

Affourtit, C. (2016) 'Mitochondrial involvement in skeletal muscle insulin resistance: A case of imbalanced bioenergetics', *Biochimica et Biophysica Acta - Bioenergetics*, 1857(10), pp. 1678–1693. doi: 10.1016/j.bbabio.2016.07.008.

Affourtit, C., Alberts, B., Barlow, J., Carré, J. E. and Wynne, A. G. (2018) 'Control of pancreatic β -cell bioenergetics', *Biochemical Society Transactions*, (March), pp. 1–10.

Affourtit, C., Bailey, S. J., Jones, A. M., Smallwood, M. J. and Winyard, P. G. (2015) 'On the mechanism by which dietary nitrate improves human skeletal muscle function', *Frontiers in Physiology*, 6(JUL), pp. 1–8. doi: 10.3389/fphys.2015.00211.

Affourtit, C. and Brand, M. D. (2006) 'Stronger control of ATP/ADP by proton leak in pancreatic β-cells than skeletal muscle mitochondria', *Biochemical Journal*, 393(1), pp. 151–159. doi: 10.1042/BJ20051280.

Affourtit, C. and Brand, M. D. (2009) 'Chapter 23 Measuring Mitochondrial Bioenergetics in INS-1E Insulinoma Cells', *Methods in Enzymology*, 457, pp. 405–424. doi: 10.1016/S0076-6879(09)05023-X.

Affourtit, C., Quinlan, C. and Brand, M. (2012) 'Measurement of Proton Leak and Electron Leak in Isolated Mitochondria', *Methods in Molecular Biology*, 810(May 2014), pp. 103–117. doi: 10.1007/978-1-61779-382-0.

Agilent (2018) *Seahorse XFe Analyzer Operating Manual*.

Ahmed, F., Chehadé, L., Garneau, L., Caron, A. and Aguer, C. (2020) 'The effects of acute BPA exposure on skeletal muscle mitochondrial function and glucose metabolism', *Molecular and Cellular Endocrinology*, 499(September 2019), p. 110580. doi: 10.1016/j.mce.2019.110580.

Allen, D. G., Lamb, G. D. and Westerblad, H. (2008) 'Skeletal muscle fatigue: cellular mechanisms', *Physiological reviews*, 88(1), pp. 287–332. doi: 10.1152/physrev.00015.2007.

Archer, S. (1993) 'Measurement of nitric oxide in biological models', *The FASEB Journal*, 7(2), pp. 349–360. doi: 10.1096/fasebj.7.2.8440411.

Arias-Calderón, M., Almarza, G., Díaz-Vegas, A., Contreras-Ferrat, A., Valladares, D., Casas, M., Toledo, H., Jaimovich, E. and Buvinic, S. (2016) 'Characterization of a multiprotein complex involved in excitation-transcription coupling of skeletal muscle', *Skeletal Muscle*, 6(1), pp. 1–16. doi: 10.1186/s13395-016-0087-5.

Ashor, A. W., Chowdhury, S., Oggioni, C., Qadir, O., Brandt, K., Ishaq, A., Mathers, J. C., Saretzki, G. and Siervo, M. (2016) 'Inorganic Nitrate Supplementation in Young and Old Obese Adults Does Not Affect Acute Glucose and Insulin Responses but Lowers Oxidative Stress', *Journal of Nutrition*, 146(11), pp. 2224–2232. doi: 10.3945/jn.116.237529.

Avila-Medina, J., Mayoral-Gonzalez, I., Dominguez-Rodriguez, A., Gallardo-Castillo, I., Ribas, J., Ordoñez, A., Rosado, J. A. and Smani, T. (2018) 'The complex role of store operated calcium entry pathways and related proteins in the function of cardiac,

skeletal and vascular smooth muscle cells', *Frontiers in Physiology*, 9(MAR). doi: 10.3389/fphys.2018.00257.

Axton, E. R., Beaver, L. M., St. Mary, L., Truong, L., Logan, C. R., Spagnoli, S., Prater, M. C., Keller, R. M., Garcia-Jaramillo, M., Ehrlicher, S. E., Stierwalt, H. D., Newsom, S. A., Robinson, M. M., Tanguay, R. L., Stevens, J. F. and Hord, N. G. (2019) 'Treatment with Nitrate, but Not Nitrite, Lowers the Oxygen Cost of Exercise and Decreases Glycolytic Intermediates While Increasing Fatty Acid Metabolites in Exercised Zebrafish', *The Journal of Nutrition*, (3), pp. 1–13. doi: 10.1093/jn/nxz202.

Bailey, S. J., Fulford, J., Vanhatalo, A., Winyard, P. G., Blackwell, J. R., Dimenna, F. J., Wilkerson, D. P., Benjamin, N. and Jones, A. M. (2010) 'Dietary nitrate supplementation enhances muscle contractile efficiency during knee-extensor exercise in humans', *J Appl Physiol*, 109(July), p. 9238. doi: 10.1152/japplphysiol.00046.2010.

Bailey, S. J., Varnham, R. L., DiMenna, F. J., Breese, B. C., Wylie, L. J. and Jones, A. M. (2015) 'Inorganic nitrate supplementation improves muscle oxygenation, O_2 uptake kinetics, and exercise tolerance at high but not low pedal rates', *Journal of Applied Physiology*, 118(11), pp. 1396–1405. doi: 10.1152/japplphysiol.01141.2014.

Bailey, S. J., Winyard, Paul, Vanhatalo, Anni, Blackwell, J. R., Dimenna, F. J., Wilkerson, D. P., Tarr, Joanna, Benjamin, Nigel, Jones, A. M., Sj, B., Winyard, P, Vanhatalo, A, Jr, B., Dp, W., Tarr, J, Benjamin, N and Dietary, J. A. M. (2009) 'Dietary nitrate supplementation reduces the O 2 cost of low-intensity exercise and enhances tolerance to high-intensity exercise in humans', *Journal of applied physiology*, 107, pp. 1144–1155. doi: 10.1152/japplphysiol.00722.2009.

Barazzoni, R., Short, K. R., Asmann, Y., Coenen-Schimke, J. M., Robinson, M. M. and Nair, K. S. (2012) 'Insulin fails to enhance mTOR phosphorylation, mitochondrial protein synthesis, and ATP production in human skeletal muscle without amino acid replacement', *American Journal of Physiology - Endocrinology and Metabolism*, 303(9), pp. 1117–1125. doi: 10.1152/ajpendo.00067.2012.

Barclay, C. J. (2017) 'The basis of differences in thermodynamic efficiency among skeletal muscles', *Clinical and Experimental Pharmacology and Physiology*, 44(12), pp. 1279–1286. doi: 10.1111/1440-1681.12850.

Barclay, C. J., Woledge, R. C. and Curtin, N. A. (2007) 'Energy turnover for Ca2+ cycling in skeletal muscle', *Journal of Muscle Research and Cell Motility*, 28(4–5), pp. 259–274. doi: 10.1007/s10974-007-9116-7.

Baron, A., Brechtel, G., Wallace, P. and Edelman, S. (1988) 'Rates and Tissue Sites of Noninsulin- and Insulin-Mediated Glucose Uptake in Diabetic Rats', *American Journal of Physiology*, 255, pp. 769–774. doi: 10.3181/00379727-199-43333.

Beals, J. W., Binns, S. E., Davis, J. L., Giordano, G. R., Klochak, A. L., Paris, H. L., Schweder, M. M., Peltonen, G. L., Scalzo, R. L. and Bell, C. (2017) 'Concurrent Beet Juice and Carbohydrate Ingestion: Influence on Glucose Tolerance in Obese and Nonobese Adults', *Journal of Nutrition and Metabolism*, 2017. doi: 10.1155/2017/6436783.

Bender, D. (2003) 'GLUCOSE | Function and Metabolism', in Caballero, B. (ed.) *Encyclopedia of Food Sciences and Nutrition (Second Edition)*. 2nd edn. Academic Press, pp. 2904–2911.

Berg, J., Tymoczko, J. and Stryer, L. (2002) *Biochemistry*. 5th edn. New York: W H Freeman.

Bescós, R., Ferrer-Roca, V., Galilea, P. A., Roig, A., Drobnic, F., Sureda, A., Martorell, M., Cordova, A., Tur, J. A. and Pons, A. (2012) 'Sodium nitrate supplementation does not enhance performance of endurance athletes', *Medicine and Science in Sports and Exercise*, 44(12), pp. 2400–2409. doi: 10.1249/MSS.0b013e3182687e5c.

Betteridge, S., Bescós, R., Martorell, M., Pons, A., Garnham, A. P., Stathis, C. C. and McConell, G. K. (2016) 'No effect of acute beetroot juice ingestion on oxygen consumption, glucose kinetics, or skeletal muscle metabolism during submaximal exercise in males', *Journal of Applied Physiology*, 120(4), pp. 391–398. doi: 10.1152/japplphysiol.00658.2015.

Billat, V. L., Sirvent, P., Py, G., Koralsztein, J. P. and Mercier, J. (2003) 'The concept of maximal lactate steady state: a bridge between biochemistry, physiology and sport science', *Sports medicine (Auckland, N.Z.)*, 33(6), pp. 407–426.

Boirie, Y., Short, K. R., Ahlman, B., Charlton, M. and Nair, K. S. (2001) 'Tissue-specific regulation of mitochondrial and cytoplasmic protein synthesis rates by insulin', *Diabetes*, 50(12), pp. 2652–2658. doi: 10.2337/diabetes.50.12.2652.

Brand, M. D. (1996) 'Top down metabolic control analysis', *Journal of Theoretical Biology*, 182(3), pp. 351–360. doi: 10.1006/jtbi.1996.0174.

Brand, M. D. (1998) 'Top-down elasticity analysis and its application to energy metabolism in isolated mitochondria and intact cells', *Mol Cell Biochem*, 184(1–2), pp. 13–20. Available at: http://www.biomednet.com/db/medline/98417391.

Brand, M. D. (2000) 'Uncoupling to survive? The role of mitochondrial inefficiency in ageing', *Experimental Gerontology*, 35(6–7), pp. 811–820. doi: 10.1016/S0531-5565(00)00135-2.

Brand, M. D. (2005) 'The efficiency and plasticity of mitochondrial energy transduction', *Biochemical Society Transactions*, 33(5), p. 897. doi: 10.1042/BST20050897.

Brand, M. D. (2016) 'Mitochondrial generation of superoxide and hydrogen peroxide as the source of mitochondrial redox signaling', *Free Radical Biology and Medicine,* 100(2016), pp. 14-31. doi: 10.1016/j.freeradbiomed.2016.04.001

Brand, M. D. and Nicholls, D. G. (2011) 'Assessing mitochondrial dysfunction in cells', *Biochemical Journal*, 437(3), pp. 575.1-575. doi: 10.1042/BJ4370575u.

Brand, M. D., Pakay, J. L., Ocloo, A., Kokoszka, J., Wallace, D. C., Brookes, P. S. and Cornwall, E. J. (2005) 'The basal proton conductance of mitochondria depends on adenine nucleotide translocase content', *Biochemical Journal*, 392(2), pp. 353–362. doi: 10.1042/BJ20050890.

Brand, M., Pamplona, R., Portero-Otiyn, M., Requena, J., Roebuck, S., Buckingham, J., Clapham, J. and Cadenas, s (2002) 'Oxidative damage and phospholipid fatty acyl composition in skeletal muscle mitochondria from mice underexpressing or overexpressing uncoupling protein 3', *Biochemical Journal*, 368, pp. 597–603. doi: 10.1016/B978-0-12-378630-2.00162-6.

Breese, B. C., McNarry, M. A., Marwood, S., Blackwell, J. R., Bailey, S. J. and Jones,

A. M. (2013) ‘Beetroot juice supplementation speeds O2 uptake kinetics and improves exercise tolerance during severe-intensity exercise initiated from an elevated metabolic rate’, *AJP: Regulatory, Integrative and Comparative Physiology*, 305(12), pp. R1441–R1450. doi: 10.1152/ajpregu.00295.2013.

Breitwieser (2008) ‘Extracellular calcium as an integrator of tissue function Gerda’, *The International Journal of Biochemistry & Cell Biology*, 40(8), pp. 1467–1480. doi: 10.1038/jid.2014.371.

Brown, G. C. and Borutaite, V. (2007) ‘Nitric oxide and mitochondrial respiration in the heart’, *Cardiovascular Research*, 75(2), pp. 283–290. doi: 10.1016/j.cardiores.2007.03.022.

Buttgereit, F. and Brand, M. D. (1995) ‘A hierarchy of ATP-consuming processes in mammalian cells’, *Biochemical Journal*, 312, pp. 163–167.

Cadenasa, S., Buckinghama, J., Samec, S., Seydoux, J., Din, N., Dulloo, A. and Brand, M. (1999) ‘UCP2 and UCP3 rise in starved rat skeletal muscle but mitochondrial proton conductance is unchanged’, *FEBS Letters*, 462(3), pp. 257–260. doi: 10.1016/S0014-5793(99)01540-9.

Carlström, M., Larsen, F. J., Nyström, T., Hezel, M., Borniquel, S. and Weitzberg, E. (2010) ‘Dietary inorganic nitrate reverses features of metabolic syndrome in endothelial nitric oxide synthase-de fi cient mice’. doi: 10.1073/pnas.1008872107/-/DCSupplemental.www.pnas.org/cgi/doi/10.1073/pnas.1008872107.

Carriker, C. R., Vaughan, R. A., VanDusseldorp, T. A., Johnson, K. E., Beltz, N. M., McCormick, J. J., Cole, N. H. and Gibson, A. L. (2016) ‘Nitrate-containing beetroot juice reduces oxygen consumption during submaximal exercise in low but not high aerobically fit male runners’, *J Exerc Nutrition Biochem*, 20(4), pp. 27–34. doi: 10.20463/jenb.2016.0029.

Cheng, Z., Tseng, Y. and White, M. F. (2010) ‘Insulin signaling meets mitochondria in metabolism’, *Trends in Endocrinology and Metabolism*, 21(10), pp. 589–598. doi: 10.1016/j.tem.2010.06.005.

Ching, J. K., Rajguru, P., Marupudi, N., Banerjee, S. and Fisher, J. S. (2010) ‘A role for AMPK in increased insulin action after serum starvation’, *American Journal of Physiology - Cell Physiology*, 299(5), pp. 1171–1179. doi: 10.1152/ajpcell.00514.2009.

Christensen, P. M., Nyberg, M. and Bangsbo, J. (2013) ‘Influence of nitrate supplementation on VO2 kinetics and endurance of elite cyclists’, *Scandinavian Journal of Medicine and Science in Sports*, 23(1), pp. 21–31. doi: 10.1111/sms.12005.

Clerc, P., Rigoulet, M., Leverve, X. and Fontaine, E. (2007) ‘Nitric oxide increases oxidative phosphorylation efficiency’, *Journal of Bioenergetics and Biomembranes*, 39(2), pp. 158–166. doi: 10.1007/s10863-007-9074-1.

Cui, Z., Chen, X., Lu, B., Sung, K. P., Xu, T., Xie, Z., Xue, P., Hou, J., Hang, H., Yates, J. R. and Yang, F. (2009) *Preliminary quantitative profile of differential protein expression between rat L6 myoblasts and myotubes by stable isotope labeling with amino acids in cell culture*, *Proteomics*. doi: 10.1002/pmic.200800354.

DeFronzo, R. A., Ferrannini, E., Sato, Y., Felig, P. and Wahren, J. (1981) ‘Synergistic interaction between exercise and insulin on peripheral glucose uptake’, *Journal of*

Clinical Investigation, 68(6), pp. 1468–1474. doi: 10.1172/JCI110399.

Dieterich, D. C., Link, A. J., Graumann, J., Tirrell, D. A. and Schuman, E. M. (2006) 'Selective identification of newly synthesized proteins in mammalian cells using bioorthogonal noncanonical amino acid tagging (BONCAT)', *Proceedings of the National Academy of Sciences of the United States of America*, 103(25), pp. 9482–9487. doi: 10.1073/pnas.0601637103.

Divakaruni, A. S. and Brand, M. D. (2011) 'The regulation and physiology of mitochondrial proton leak.', *Physiology (Bethesda, Md.)*, 26(3), pp. 192–205. doi: 10.1152/physiol.00046.2010.

Divakaruni, A. S., Paradyse, A., Ferrick, D. A. and Jastroch, M. (2014) 'Analysis and Interpretation of Microplate-Based Oxygen Consumption and pH Data', *Methods in Enzymology*, 547, pp. 309–354. doi: 10.1016/B978-0-12-801415-8.00016-3.

Doel, J. J., Benjamin, N., Hector, M. P., Rogers, M. and Allaker, R. P. (2005) 'Evaluation of bacterial nitrate reduction in the human oral cavity', *Eur J Oral Sci*, 113(1), pp. 14–19. doi: 10.1111/j.1600-0722.2004.00184.x.

Domínguez, R., Cuenca, E., Maté-Muñoz, J. L., García-Fernández, P., Serra-Paya, N., Estevan, M. C. L., Herreros, P. V. and Garnacho-Castaño, M. V. (2017) 'Effects of beetroot juice supplementation on cardiorespiratory endurance in athletes. A systematic review', *Nutrients*, 9(1), pp. 1–18. doi: 10.3390/nu9010043.

Domínguez, R., Garnacho-Castaño, M., Cuenca, E., García-Fernández, P., Muñoz-González, A., de Jesús, F., Lozano-Estevan, M., Fernandes da Silva, S., Veiga-Herreros, P. and Maté-Muñoz, J. (2017) 'Effects of Beetroot Juice Supplementation on a 30-s High-Intensity Inertial Cycle Ergometer Test', *Nutrients*, 9(12), p. 1360. doi: 10.3390/nu9121360.

Domínguez, R., Maté-Muñoz, J. L., Cuenca, E., García-Fernández, P., Mata-Ordoñez, F., Lozano-Estevan, M. C., Veiga-Herreros, P., da Silva, S. F. and Garnacho-Castaño, M. V. (2018) 'Effects of beetroot juice supplementation on intermittent high-intensity exercise efforts', *Journal of the International Society of Sports Nutrition*, 15(1), p. 2. doi: 10.1186/s12970-017-0204-9.

Egan, B. and Zierath, J. R. (2013) 'Exercise metabolism and the molecular regulation of skeletal muscle adaptation', *Cell Metabolism*, 17(2), pp. 162–184. doi: 10.1016/j.cmet.2012.12.012.

Epstein, T., Xu, L., Gillies, R. J. and Gatenby, R. A. (2014) 'Separation of metabolic supply and demand: Aerobic glycolysis as a normal physiological response to fluctuating energetic demands in the membrane', *Cancer and Metabolism*, 2(1), pp. 1–9. doi: 10.1186/2049-3002-2-7.

Fawcett, J., Hamel, F. G., Bennett, R. G., Vajo, Z. and Duckworth, W. C. (2001) 'Insulin and analogue effects on protein degradation in different cell types. Dissociation between binding and activity', *Journal of Biological Chemistry*, 276(15), pp. 11552–11558. doi: 10.1074/jbc.M007988200.

Feher, J. (2017) 'ATP Production I', *Quantitative Human Physiology*, pp. 218–226. doi: 10.1016/b978-0-12-800883-6.00020-3.

Ferguson, S. K., Hirai, D. M., Copp, S. W., Holdsworth, C. T., Allen, J. D., Jones, A.

M., Musch, T. I. and Poole, D. C. (2013) 'Impact of dietary nitrate supplementation via beetroot juice on exercising muscle vascular control in rats', *Journal of Physiology*, 591(2), pp. 547–557. doi: 10.1113/jphysiol.2012.243121.

Fiedler, G. B., Schmid, A. I., Goluch, S., Schewzow, K., Laistler, E., Niess, F., Unger, E., Wolzt, M., Mirzahosseini, A., Kemp, G. J., Moser, E. and Meyerspeer, M. (2016) 'Skeletal muscle ATP synthesis and cellular H+ handling measured by localized 31P-MRS during exercise and recovery', *Scientific Reports*, 6(1), p. 32037. doi: 10.1038/srep32037.

Garzorz-Stark, N. *et al.* (2018) 'Toll-like receptor 7/8 agonists stimulate plasmacytoid dendritic cells to initiate TH17-deviated acute contact dermatitis in human subjects', *Journal of Allergy and Clinical Immunology*, 141(4), pp. 1320-1333.e11. doi: 10.1016/j.jaci.2017.07.045.

Gaster, M. and Beck-Nielsen, H. (2004) 'The reduced insulin-mediated glucose oxidation in skeletal muscle from type 2 diabetic subjects may be of genetic origin - Evidence from cultured myotubes', *Biochimica et Biophysica Acta - Molecular Basis of Disease*, 1690(1), pp. 85–91. doi: 10.1016/j.bbadis.2004.05.006.

Genders, A. J., Martin, S. D., McGee, S. L. and Bishop, D. J. (2019) 'A physiological drop in ph decreases mitochondrial respiration, and HDAC and Akt signaling, in l6 myocytes', *American Journal of Physiology - Cell Physiology*, 316(3), pp. C404–C414. doi: 10.1152/ajpcell.00214.2018.

Gerencser, A. A., Neilson, A., Choi, S. W., Edman, U., Yadava, N., Oh, R. J., Ferrick, D. A., Nicholls, D. G. and Brand, M. D. (2009) 'Quantitative microplate-based respirometry with correction for oxygen diffusion', *Analytical Chemistry*, 81(16), pp. 6868–6878. doi: 10.1021/ac900881z.

Gheibi, S., Bakhtiarzadeh, F., Jeddi, S., Farrokhfall, K., Zardooz, H. and Ghasemi, A. (2017) 'Nitrite increases glucose-stimulated insulin secretion and islet insulin content in obese type 2 diabetic male rats', *Nitric Oxide - Biology and Chemistry*, 64, pp. 39–51. doi: 10.1016/j.niox.2017.01.003.

Glean, A. A., Ferguson, S. K., Holdsworth, C. T., Colburn, T. D., Wright, J. L., Fees, A. J., Hageman, K. S., Poole, D. C. and Musch, T. I. (2015) 'Effects of nitrite infusion on skeletal muscle vascular control during exercise in rats with chronic heart failure', *American Journal of Physiology - Heart and Circulatory Physiology*, 309(8), pp. H1354–H1360. doi: 10.1152/ajpheart.00421.2015.

Goodwin, M. L., Harris, J. E., Hernández, A. and Gladden, L. B. (2007) 'Blood lactate measurements and analysis during exercise: A guide for clinicians', *Journal of Diabetes Science and Technology*, 1(4), pp. 558–569. doi: 10.1177/193229680700100414.

Govoni, M., Jansson, E. A., Weitzberg, E. and Lundberg, J. O. (2008) 'The increase in plasma nitrite after a dietary nitrate load is markedly attenuated by an antibacterial mouthwash', *Nitric Oxide - Biology and Chemistry*, 19(4), pp. 333–337. doi: 10.1016/j.niox.2008.08.003.

Haider, G. and Folland, J. P. (2014) 'Nitrate supplementation enhances the contractile properties of human skeletal muscle', *Medicine and Science in Sports and Exercise*, 46(12), pp. 2234–2243. doi: 10.1249/MSS.0000000000000351.

Haseler, L. J. *et al.* (1999) 'Skeletal muscle phosphocreatine recovery in exercise-

trained humans is dependent on O 2 availability Skeletal muscle phosphocreatine recovery in exercise-trained humans is dependent on O 2 availability', *Journal of Applied Physiology*, pp. 2013–2018. doi: 10.1097/00005768-199905001-01364.

Heldt, H. W. and Klingenberg, M. (1972) 'and in the Extramitochondrial Space', 440, pp. 434–440.

Hernández, A., Schiffer, T. A., Ivarsson, N., Cheng, A. J., Bruton, J. D., Lundberg, J. O., Weitzberg, E. and Westerblad, H. (2012) 'Dietary nitrate increases tetanic [Ca 2+] i and contractile force in mouse fast-twitch muscle', *Journal of Physiology*, 590(15), pp. 3575–3583. doi: 10.1113/jphysiol.2012.232777.

Ho, K. (2011) 'A critically swift response: Insulin-stimulated potassium and glucose transport in Skeletal Muscle', *Clinical Journal of the American Society of Nephrology*, 6(7), pp. 1513–1516. doi: 10.2215/CJN.04540511.

Hong, S. and Pedersen, P. L. (2008) 'ATP Synthase and the Actions of Inhibitors Utilized To Study Its Roles in Human Health, Disease, and Other Scientific Areas', *Microbiology and Molecular Biology Reviews*, 72(4), pp. 590–641. doi: 10.1128/mmbr.00016-08.

Hoon, M. W., Fornusek, C., Chapman, P. G. and Johnson, N. A. (2015) 'The effect of nitrate supplementation on muscle contraction in healthy adults', *European Journal of Sport Science*, 15(8), pp. 712–719. doi: 10.1080/17461391.2015.1053418.

Hresko, R. C. and Hruz, P. W. (2011) 'HIV protease inhibitors act as competitive inhibitors of the cytoplasmic glucose binding site of GLUTs with differing affinities for GLUT1 and GLUT4', *PLoS ONE*, 6(9). doi: 10.1371/journal.pone.0025237.

Hsu, C. C., Tseng, L. M. and Lee, H. C. (2016) 'Role of mitochondrial dysfunction in cancer progression', *Experimental Biology and Medicine*, 241(12), pp. 1281–1295. doi: 10.1177/1535370216641787.

Hsu, M. F. and Meng, T. C. (2010) 'Enhancement of insulin responsiveness by nitric oxide-mediated inactivation of protein-tyrosine phosphatases', *Journal of Biological Chemistry*, 285(11), pp. 7919–7928. doi: 10.1074/jbc.M109.057513.

Hyde, E. R., Andrade, F., Vaksman, Z., Parthasarathy, K., Jiang, H., Parthasarathy, D. K., Torregrossa, A. C., Tribble, G., Kaplan, H. B., Petrosino, J. F. and Bryan, N. S. (2014) 'Metagenomic analysis of nitrate-reducing bacteria in the oral cavity: Implications for nitric oxide homeostasis', *PLoS ONE*, 9(3). doi: 10.1371/journal.pone.0088645.

Ishii, T., Sunami, O., Saitoh, N., Nishio, H., Takeuchi, T. and Hata, F. (1998) 'Inhibition of skeletal muscle sarcoplasmic reticulum Ca $^{2+}$ -ATPase by nitric oxide', *FEBS Letters*, 440(1–2), pp. 218–222. doi: 10.1016/S0014-5793(98)01460-4.

Ivarsson, N., Schiffer, T. A., Hernández, A., Lanner, J. T., Weitzberg, E., Lundberg, J. O. and Westerblad, H. (2017) 'Dietary nitrate markedly improves voluntary running in mice', *Physiology and Behavior*, 168, pp. 55–61. doi: 10.1016/j.physbeh.2016.10.018.

Jastroch, M., Divakaruni, A. S., Mookerjee, S., Treberg, J. R. and Brand, M. D. (2010) 'Mitochondrial proton and electron leaks', *Essays in Biochemistry*, 47, pp. 53–67. doi: 10.1042/BSE0470053.

Jiang, H., Torregrossa, A. C., Potts, A., Pierini, D., Aranke, M., Garg, H. K. and Bryan,

N. S. (2014) ‘Dietary nitrite improves insulin signaling through GLUT4 translocation’, *Free Radical Biology and Medicine*, 67, pp. 51–57. doi: 10.1016/j.freeradbiomed.2013.10.809.

Jones, A. M. (2014) ‘Dietary nitrate supplementation and exercise performance’, *Sports Medicine*, 44(SUPPL.1). doi: 10.1007/s40279-014-0149-y.

Jones, A. M., Burnley, M., Black, M. I., Poole, D. C. and Vanhatalo, A. (2019) ‘The maximal metabolic steady state: redefining the “gold standard”’, *Physiological Reports*, 7(10), pp. 1–16. doi: 10.14814/phy2.14098.

Jones, A. M., Ferguson, S. K., Bailey, S. J., Vanhatalo, A. and Poole, D. C. (2016) ‘Fiber Type-Specific Effects of Dietary Nitrate’, *Exercise and Sport Sciences Reviews*, 44(2), pp. 53–60. doi: 10.1249/JES.0000000000000074.

Jones, A. M., Thompson, C., Wylie, L. J. and Vanhatalo, A. (2018) ‘Dietary Nitrate and Physical Performance’, *Annual Review of Nutrition*, 38(1), pp. 303–328. doi: 10.1146/annurev-nutr-082117-051622.

Keller-Ross, M. L., Larson, M. and Johnson, B. D. (2019) ‘Skeletal muscle fatigability in heart failure’, *Frontiers in Physiology*, 10(FEB), pp. 1–8. doi: 10.3389/fphys.2019.00129.

Kemp, G. J. and Brindle, K. M. (2012) ‘What do magnetic resonance-based measurements of Pi→ATP flux tell us about skeletal muscle metabolism?’, *Diabetes*, 61(8), pp. 1927–1934. doi: 10.2337/db11-1725.

Kenwood, B. M. *et al.* (2014) ‘Identification of a novel mitochondrial uncoupler that does not depolarize the plasma membrane’, *Molecular Metabolism*, 3(2), pp. 114–123. doi: 10.1016/j.molmet.2013.11.005.

Khoo, N. K. H., Mo, L., Zharikov, S., Kamga-Pride, C., Quesnelle, K., Golin-Bisello, F., Li, L., Wang, Y. and Shiva, S. (2014) ‘Nitrite augments glucose uptake in adipocytes through the protein kinase A-dependent stimulation of mitochondrial fusion’, *Free Radical Biology and Medicine*, 70, pp. 45–53. doi: 10.1016/j.freeradbiomed.2014.02.009.

Kim, K. M., Jang, H. C. and Lim, S. (2016) ‘Differences among skeletal muscle mass indices derived from height-, weight-, and body mass index-adjusted models in assessing sarcopenia’, *Korean Journal of Internal Medicine*, 31(4), pp. 643–650. doi: 10.3904/kjim.2016.015.

Klip, L., Logan, W. and Li G. (1982) ‘Hexose transport in L6 muscle cells. Kinetic properties and the number of [3H]cytochalasin B binding sites’, *Biochimica et Biophysica Acta (BBA) - Biomembranes*, 2(687), pp. 265-280. doi: 10.1016/0005-2736(82)90555-7.

Koenig, X., Choi, R. H. and Launikonis, B. S. (2018) ‘Store-operated Ca2+ entry is activated by every action potential in skeletal muscle’, *Communications Biology*, 1(1). doi: 10.1038/s42003-018-0033-7.

Kolomeisky, A. (2014) ‘Motor Proteins and Molecular Motors: How to Operate Machines at Nanoscale’, *Journal of Physics: Condensed Matter*, 25(46), pp. 1–25. doi: 10.1038/jid.2014.371.

Kuo, I. Y. and Ehrlich, B. E. (2015) ‘Signaling in muscle contraction’, *Cold Spring*

Harbor Perspectives in Biology, 7(2), pp. 1–14. doi: 10.1101/cshperspect.a006023.

Lansley, K., Winyard, P., Bailey, S., Vanhatalo, A., Wilkerson, D., Blackwell, J., Gilchrist, M., Benjamin, N. and Jones, A. (2011) 'Acute dietary nitrate supplementation improves cycling time trial performance', *Medicine and Science in Sports and Exercise*, 43(6), pp. 1125–1131. doi: 10.1249/MSS.0b013e31821597b4.

Lansley, K., Winyard, P., Fulford, J., Vanhatalo, A., Bailey, S., Blackwell, J. R., DiMenna, F. J., Gilchrist, M., Benjamin, N. and Jones, A. M. (2011) 'Dietary nitrate supplementation reduces the O2 cost of walking and running: a placebo-controlled study', *Journal of Applied Physiology*, 110(3), p. 591. doi: 10.1152/japplphysiol.01070.2010.

Larsen, F. J., Schiffer, T. A., Borniquel, S., Sahlin, K., Ekblom, B., Lundberg, J. O. and Weitzberg, E. (2011) 'Dietary inorganic nitrate improves mitochondrial efficiency in humans', *Cell Metabolism*, 13(2), pp. 149–159. doi: 10.1016/j.cmet.2011.01.004.

Larsen, F. J., Weitzberg, E., Lundberg, J. O. and Ekblom, B. (2007) 'Effects of dietary nitrate on oxygen cost during exercise', *Acta Physiologica*, 191(1), pp. 59–66. doi: 10.1111/j.1748-1716.2007.01713.x.

Li, Q., Zhu, X., Ishikura, S., Zhang, D., Gao, J., Sun, Y., Contreras-Ferrat, A., Foley, K. P., Lavandero, S., Yao, Z., Bilan, P. J., Klip, A. and Niu, W. (2014) 'Ca2+ signals promote GLUT4 exocytosis and reduce its endocytosis in muscle cells', *American Journal of Physiology - Endocrinology and Metabolism*, 307(2), pp. 209–224. doi: 10.1152/ajpendo.00045.2014.

Li, W. Y., Song, Y. L., Xiong, C. J., Lu, P. Q., Xue, L. X., Yao, C. X., Wang, W. P., Zhang, Shu Feng, Zhang, Shan Feng, Wei, Q. X., Zhang, Y. Y., Zhao, J. M. and Zang, M. X. (2013) 'Insulin induces proliferation and cardiac differentiation of P19CL6 cells in a dose-dependent manner', *Development Growth and Differentiation*, 55(7), pp. 676–686. doi: 10.1111/dgd.12075.

Lidder, S. and Webb, A. J. (2013) 'Vascular effects of dietary nitrate (as found in green leafy vegetables and beetroot) via the nitrate-nitrite-nitric oxide pathway', *British Journal of Clinical Pharmacology*, 75(3), pp. 677–696. doi: 10.1111/j.1365-2125.2012.04420.x.

Lira, V. A., Soltow, Q. A., Long, J. H. D., Betters, J. L., Sellman, J. E. and Criswell, D. S. (2007) 'Nitric oxide increases GLUT4 expression and regulates AMPK signaling in skeletal muscle', *American Journal of Physiology - Endocrinology and Metabolism*, 293(4), pp. 1062–1068. doi: 10.1152/ajpendo.00045.2007.

Lundberg, J., Weitzberg, E. and Gladwin, M. T. (2008) 'The nitrate–nitrite–nitric oxide pathway in physiology and therapeutics', *Nature Reviews Drug Discovery*, 7(2008), pp. 156–167.

Mador, M. and Bozkanat, E. (2001) 'Skeletal muscle dysfunction in chronic obstructive pulmonary disease', *Respiratory Research*, 2, pp. 216–224. doi: 10.1164/ajrccm.159.supplement_1.15945.

Matsuzaka, T. and Shimano, H. (2012) 'GLUT12: A second insulin-responsive glucose transporters as an emerging target for type 2 diabetes', *Journal of Diabetes Investigation*, 3(2), pp. 130–131. doi: 10.1111/j.2040-1124.2011.00177.x.

Minetto, M. A., Giannini, A., McConnell, R., Busso, C. and Massazza, G. (2019) 'Effects of exercise on skeletal muscles and tendons', *Current Opinion in Endocrine and Metabolic Research*, 9, pp. 90–95. doi: 10.1016/j.coemr.2019.09.001.

Mo, L., Wang, Y., Geary, L., Corey, C., Alef, M. J., Beer-Stolz, D., Zuckerbraun, B. S. and Shiva, S. (2012) 'Nitrite activates AMP kinase to stimulate mitochondrial biogenesis independent of soluble guanylate cyclase', *Free Radical Biology and Medicine*, 53(7), pp. 1440–1450. doi: 10.1016/j.freeradbiomed.2012.07.080.

Moncada, S. and Higgs, E. (1993) 'The L-arginine-nitric oxide pathway', *The New England Journal of Medicine*, 329(27), pp. 2002–2012.

Moncada, S. and Higgs, E. A. (2006) 'The discovery of nitric oxide and its role in vascular biology', *British Journal of Pharmacology*, 147(SUPPL. 1), pp. 193–201. doi: 10.1038/sj.bjp.0706458.

Mookerjee, Shona A and Brand, M. D. (2015) 'Measurement and Analysis of Extracellular Acid Production to Determine Glycolytic Rate', *Journal of Visualized Experiments*, 2(December), pp. 1–9. doi: 10.3791/53464.

Mookerjee, S. A., Gerencser, A. A., Nicholls, D. G. and Brand, M. D. (2017) 'Quantifying intracellular rates of glycolytic and oxidative ATP production and consumption using extracellular flux measurements', *Journal of Biological Chemistry*, 292(17), pp. 7189–7207. doi: 10.1074/jbc.M116.774471.

Mookerjee, Shona A., Goncalves, R. L. S., Gerencser, A. A., Nicholls, D. G. and Brand, M. D. (2015) 'The contributions of respiration and glycolysis to extracellular acid production', *Biochimica et Biophysica Acta - Bioenergetics*, 1847(2), pp. 171–181. doi: 10.1016/j.bbabio.2014.10.005.

Moxnes, J. F. and Sandbakk, Ø. (2012) 'The kinetics of lactate production and removal during whole-body exercise', *Theoretical Biology and Medical Modelling*, 9(1), p. 7. doi: 10.1186/1742-4682-9-7.

Murphy, M., Eliot, K., Heuertz, R. M. and Weiss, E. (2012) 'Whole Beetroot Consumption Acutely Improves Running Performance', *Journal of the Academy of Nutrition and Dietetics*, 112(4), pp. 548–552. doi: 10.1016/j.jand.2011.12.002.

Nair, K. S. (2005) 'Aging muscle', *American Journal of Clinical Nutrition*, 81(5), pp. 953–963. doi: 10.1097/00013614-198510000-00004.

Nisr, R. B. and Affourtit, C. (2014) 'Insulin acutely improves mitochondrial function of rat and human skeletal muscle by increasing coupling efficiency of oxidative phosphorylation', *Biochimica et Biophysica Acta - Bioenergetics*, 1837(2), pp. 270–276. doi: 10.1016/j.bbabio.2013.10.012.

Nisr, R. B. and Affourtit, C. (2016) 'Palmitate-induced changes in energy demand cause reallocation of ATP supply in rat and human skeletal muscle cells', *Biochimica et Biophysica Acta - Bioenergetics*, 1857(9), pp. 1403–1411. doi: 10.1016/j.bbabio.2016.04.286.

Niu, W., Huang, C., Nawaz, Z., Levy, M., Somwar, R., Li, D., Bilan, P. J. and Klip, A. (2003) 'Maturation of the regulation of GLUT4 activity by p38 MAPK during L6 cell myogenesis', *Journal of Biological Chemistry*, 278(20), pp. 17953–17962. doi: 10.1074/jbc.M211136200.

Ntessalen, M., Procter, N. E. K., Schwarz, K., Loudon, B. L., Minnion, M., Fernandez, B. O., Vassiliou, V. S., Vauzour, D., Madhani, M., Constantin-Teodosiu, D., Horowitz, J. D., Feelisch, M., Dawson, D., Crichton, P. G. and Frenneaux, M. P. (2020) 'Inorganic nitrate and nitrite supplementation fails to improve skeletal muscle mitochondrial efficiency in mice and humans', *American Journal of Clinical Nutrition*, 111(1), pp. 79–89. doi: 10.1093/ajcn/nqz245.

Nyakayiru, J., Kouw, I. W. K., Cermak, N. M., Senden, J. M., Van Loon, L. J. C. and Verdijk, L. B. (2017) 'Sodium nitrate ingestion increases skeletal muscle nitrate content in humans', *Journal of Applied Physiology*, 123(3), pp. 637–644. doi: 10.1152/japplphysiol.01036.2016.

Nyakayiru, J., van Loon, L. J. C. and Verdijk, L. B. (2020) 'Could intramuscular storage of dietary nitrate contribute to its ergogenic effect? A mini-review', *Free Radical Biology and Medicine*, 152(March), pp. 295–300. doi: 10.1016/j.freeradbiomed.2020.03.025.

Nyström, T., Ortsäter, H., Huang, Z., Zhang, F., Larsen, F. J., Weitzberg, E., Lundberg, J. O. and Sjöholm, Å. (2012) 'Inorganic nitrite stimulates pancreatic islet blood flow and insulin secretion', *Free Radical Biology and Medicine*, 53(5), pp. 1017–1023. doi: 10.1016/j.freeradbiomed.2012.06.031.

Ohtake, K., Nakano, G., Ehara, N., Sonoda, K., Ito, J., Uchida, H. and Kobayashi, J. (2015) 'Dietary nitrite supplementation improves insulin resistance in type 2 diabetic KKAy mice', *Nitric Oxide - Biology and Chemistry*, 44, pp. 31–38. doi: 10.1016/j.niox.2014.11.009.

Okamoto, K. E. N., Wang, W., Rounds, J. A. N., Chambers, E. A. and Jacobs, D. O. (2001) 'ATP from glycolysis is required for normal sodium homeostasis in resting fast-twitch rodent skeletal muscle', *American Journal of Physiology - Endocrinology and Metabolism*, 281(3 44-3), pp. 479–488. doi: 10.1152/ajpendo.2001.281.3.e479.

Omar, S. A. and Webb, A. J. (2014) 'Nitrite reduction and cardiovascular protection', *Journal of Molecular and Cellular Cardiology*, 73, pp. 57–69. doi: 10.1016/j.yjmcc.2014.01.012.

Omata, W., Shibata, H., Li, L., Takata, K. and Kojima, I. (2000) 'Actin filaments play a critical role in insulin-induced exocytotic recruitment but not in endocytosis of GLUT4 in isolated rat adipocytes', *Biochemical Journal*, 346(2), pp. 321–328. doi: 10.1042/0264-6021:3460321.

Pan, Y., Wang, W., Huang, Shuai, Ni, W., Wei, Z., Cao, Y., Yu, S., Jia, Q., Wu, Y., Chai, C., Zheng, Q., Zhang, L., Wang, A., Sun, Z., Huang, Shile, Wang, S., Chen, W. and Lu, Y. (2019) 'Beta-elemene inhibits breast cancer metastasis through blocking pyruvate kinase M2 dimerization and nuclear translocation', *Journal of Cellular and Molecular Medicine*, 23(10), pp. 6846–6858. doi: 10.1111/jcmm.14568.

Panina, S. B., Baran, N., Brasil da Costa, F. H., Konopleva, M. and Kirienko, N. V. (2019) 'A mechanism for increased sensitivity of acute myeloid leukemia to mitotoxic drugs', *Cell Death and Disease*, 10(8). doi: 10.1038/s41419-019-1851-3.

Pawlak-Chaouch, M., Boissière, J., Gamelin, F. X., Cuvelier, G., Berthoin, S. and Aucouturier, J. (2016) 'Effect of dietary nitrate supplementation on metabolic rate during rest and exercise in human: A systematic review and a meta-analysis', *Nitric*

Oxide - Biology and Chemistry, 53, pp. 65–76. doi: 10.1016/j.niox.2016.01.001.

Peacock, O., TjØnna, A. E., James, P., WislØff, U., Welde, B., Böhlke, N., Smith, A., Stokes, K., Cook, C. and Sandbakk, Ø. (2012) 'Dietary nitrate does not enhance running performance in elite cross-country skiers', *Medicine and Science in Sports and Exercise*, 44(11), pp. 2213–2219. doi: 10.1249/MSS.0b013e3182640f48.

Penna, F., Ballarò, R., Beltrà, M., De Lucia, S., Castillo, L. G. and Costelli, P. (2019) 'The skeletal muscle as an active player against cancer cachexia', *Frontiers in Physiology*, 10(FEB), pp. 1–15. doi: 10.3389/fphys.2019.00041.

Pereira, C., Ferreira, N. R., Rocha, B. S., Barbosa, R. M. and Laranjinha, J. (2013) 'The redox interplay between nitrite and nitric oxide: From the gut to the brain', *Redox Biology*, 1(1), pp. 276–284. doi: 10.1016/j.redox.2013.04.004.

Periasamy, M., Herrera, J. L. and Reis, F. C. G. (2017) 'Skeletal muscle thermogenesis and its role in whole body energy metabolism', *Diabetes and Metabolism Journal*, 41(5), pp. 327–336. doi: 10.4093/dmj.2017.41.5.327.

Perry, B., Caldow, M., Brennan-Speranza, T., Sbaraglia, M., Jerums, G., Garnham, A., Wong, C., Levinger, P., Haq, M., Hare, D., Price, S. and Levinger, I. (2016) 'Muscle atrophy in patients with T2DM role of inflammatory pathways, physical activity and exercise', *Exerc Immunol Rev*, 22, pp. 94–109.

Petersen, K. F., Dufour, S. and Shulman, G. I. (2005) 'Decreased insulin-stimulated ATP synthesis and phosphate transport in muscle of insulin-resistant offspring of type 2 diabetic parents', *PLoS Medicine*, 2(9), pp. 0879–0884. doi: 10.1371/journal.pmed.0020233.

Phypers, B. and Pierce, J. M. T. (2006) 'Lactate physiology in health and disease', *Continuing Education in Anaesthesia, Critical Care and Pain*, 6(3), pp. 128–132. doi: 10.1093/bjaceaccp/mkl018.

Piknova, B., Park, J. W., Swanson, K. M., Dey, S., Noguchi, C. T. and Schechter, A. N. (2015) 'Skeletal muscle as an endogenous nitrate reservoir', *Nitric Oxide - Biology and Chemistry*, 47, pp. 10–16. doi: 10.1016/j.niox.2015.02.145.

Pillon, N. J., Li, Y. E., Fink, L. N., Brozinick, J. T., Nikolayev, A., Kuo, M. S., Bilan, P. J. and Klip, A. (2014) 'Nucleotides released from palmitate-challenged muscle cells through pannexin-3 attract monocytes', *Diabetes*, 63(11), pp. 3815–3826. doi: 10.2337/db14-0150.

Pinset, C. and Whalen, R. G. (1982) 'Control of Cell Proliferation and Differentiation in the Myogenic Cell Line L6 by Manipulation of Culture Conditions', in Fischer, G. and Wieser, R. (eds) *Hormonally Defined Media: A Tool in Cell Biology Lectures and Posters Presented at the First European Conference on Serum-Free Cell Culture Heidelberg*. Springer Science & Business Media, p. 398.

Polyzos, A. A., Lee, D. Y., Datta, R., Hauser, M., Budworth, H., Holt, A., Mihalik, S., Goldschmidt, P., Frankel, K., Trego, K., Bennett, M. J., Vockley, J., Xu, K., Gratton, E. and McMurray, C. T. (2019) 'Metabolic Reprogramming in Astrocytes Distinguishes Region-Specific Neuronal Susceptibility in Huntington Mice', *Cell Metabolism*, 29(6), pp. 1258-1273.e11. doi: 10.1016/j.cmet.2019.03.004.

Poole and Richardson (1997) 'Determinants of oxygen uptake: Implications for exercise

testing', *Sports Medicine*, 24(5), pp. 308–320.

Potter, M., Newport, E. and Morten, K. J. (2016) 'The Warburg effect: 80 years on', *Biochemical Society Transactions*, 44(5), pp. 1499–1505. doi: 10.1042/BST20160094.

Pride, C. K., Mo, L., Quesnelle, K., Dagda, R. K., Murillo, D., Geary, L., Corey, C., Portella, R., Zharikov, S., St Croix, C., Maniar, S., Chu, C. T., K. H. Khoo, N. and Shiva, S. (2014) 'Nitrite activates protein kinase A in normoxia to mediate mitochondrial fusion and tolerance to ischaemia/reperfusion', *Cardiovascular Research*, 101(1), pp. 57–68. doi: 10.1093/cvr/cvt224.

Qin, L., Liu, X., Sun, Q., Fan, Z., Xia, D., Ding, G., Ong, H. L., Adams, D., Gahl, W. A., Zheng, C., Qi, S., Jin, L., Zhang, C., Gu, L., He, J., Deng, D., Ambudkar, I. S. and Wang, S. (2012) 'Sialin (SLC17A5) functions as a nitrate transporter in the plasma membrane', *Proceedings of the National Academy of Sciences*, 109(33), pp. 13434–13439. doi: 10.1073/pnas.1116633109.

Rahmatabady, M. (2013) 'A quick look at biochemistry: Carbohydrate metabolism', *Clinical Biochemistry*, 46(15), pp. 1339–1352. doi: 10.1016/j.clinbiochem.2013.04.027.

Richter, E. A. and Hargreaves, M. (2013) 'Exercise, GLUT4, and Skeletal Muscle Glucose Uptake', *Physiological Reviews*, 93(3), pp. 993–1017. doi: 10.1152/physrev.00038.2012.

Robinson, M. M., Soop, M., Sohn, T. S., Morse, D. M., Schimke, J. M., Klaus, K. A. and Nair, K. S. (2014) 'High insulin combined with essential amino acids stimulates skeletal muscle mitochondrial protein synthesis while decreasing insulin sensitivity in healthy humans', *Journal of Clinical Endocrinology and Metabolism*, 99(12), pp. E2574–E2583. doi: 10.1210/jc.2014-2736.

Rodriguez, L. P., López-Rego, J., Calbet, J. A. L., Valero, R., Varela, E. and Ponce, J. (2002) 'Effects of training status on fibers of the musculus vastus lateralis in professional road cyclists', *American Journal of Physical Medicine and Rehabilitation*, 81(9), pp. 651–660. doi: 10.1097/00002060-200209000-00004.

Rooyackers, O. and Nair, K. (1997) 'Hormonal regulation of human protein metabolism', *Annual Review of Nutrition*, 17, pp. 457–485. doi: 10.1530/eje.0.1350007.

Rowland, A. F., Fazakerley, D. J. and James, D. E. (2011) 'Mapping Insulin/GLUT4 Circuitry', *Traffic*, 12(6), pp. 672–681. doi: 10.1111/j.1600-0854.2011.01178.x.

Rutter, G. A., Pullen, T. J., Hodson, D. J. and Martinez-Sanchez, A. (2015) 'Pancreatic β-cell identity, glucose sensing and the control of insulin secretion', *Biochemical Journal*, 466, pp. 203–218. doi: 10.1042/BJ20141384.

Scherz-Shouval, R., Shvets, E., Fass, E., Shorer, H., Gil, L. and Elazar, Z. (2007) 'Reactive oxygen species are essential for autophagy and specifically regulate the activity of Atg4', *EMBO Journal*, 26(7), pp. 1749–1760. doi: 10.1038/sj.emboj.7601623.

Schierenbeck, F., Nijsten, M. W. N., Franco-Cereceda, A. and Liska, J. (2014) 'Introducing intravascular microdialysis for continuous lactate monitoring in patients undergoing cardiac surgery: A prospective observational study', *Critical Care*, 18(2), pp. 1–8. doi: 10.1186/cc13808.

Seim, G. L., Britt, E. C., John, S. V., Yeo, F. J., Johnson, A. R., Eisenstein, R. S.,

Pagliarini, D. J. and Fan, J. (2019) 'Two-stage metabolic remodelling in macrophages in response to lipopolysaccharide and interferon-γ stimulation', *Nature Metabolism*, 1(7), pp. 731–742. doi: 10.1038/s42255-019-0083-2.

Shannon, O. M., Barlow, M. J., Duckworth, L., Williams, E., Wort, G., Woods, D., Siervo, M. and O'Hara, J. P. (2017) 'Dietary nitrate supplementation enhances short but not longer duration running time-trial performance', *European Journal of Applied Physiology*, 117(4), pp. 775–785. doi: 10.1007/s00421-017-3580-6.

Shiav, S. (2013) 'Nitrite: A physiological store of nitric oxide and modulator of mitochondrial function', *Redox Biology*, 1(1), pp. 40–44. doi: 10.1016/j.redox.2012.11.005.

Singamsetty, S., Watanabe, Y., Guo, L., Corey, C., Wang, Y., Tejero, J., Mcverry, B. J., Gladwin, M. T., Shiva, S. and O'Donnell, C. P. (2015) 'Inorganic nitrite improves components of the metabolic syndrome independent of weight change in a murine model of obesity and insulin resistance', *Journal of Physiology*, 593(14), pp. 3135–3145. doi: 10.1113/JP270386.

Spangenburg, E. E. and Booth, F. W. (2003) 'Molecular regulation of individual skeletal muscle fibre types', *Acta Physiologica Scandinavica*, 178(4), pp. 413–424. doi: 10.1046/j.1365-201X.2003.01158.x.

Srihirun, S., Park, J. W., Teng, R., Sawaengdee, W., Piknova, B. and Schechter, A. N. (2020) 'Nitrate uptake and metabolism in human skeletal muscle cell cultures', *Nitric Oxide - Biology and Chemistry*, 94(October 2019), pp. 1–8. doi: 10.1016/j.niox.2019.10.005.

Stossel, T. P., Fenteany, G. and Hartwig, J. H. (2006) 'Cell surface actin remodeling', *Journal of Cell Science*, 119(16), pp. 3261–3264. doi: 10.1242/jcs.02994.

Stuart, C. A., Howell, M. E. A., Zhang, Y. and Yin, D. (2009) 'Insulin-stimulated translocation of glucose transporter (GLUT) 12 parallels that of GLUT4 in normal muscle', *Journal of Clinical Endocrinology and Metabolism*, 94(9), pp. 3535–3542. doi: 10.1210/jc.2009-0162.

Stump, C. S., Short, K. R., Bigelow, M. L., Schimke, J. M. and Nair, K. S. (2003) 'Effect of insulin on human skeletal muscle mitochondrial ATP production, protein synthesis, and mRNA transcripts', *Proceedings of the National Academy of Sciences of the United States of America*, 100(13), pp. 7996–8001. doi: 10.1073/pnas.1332551100.

Szendroedi, J., Schmid, A. I., Chmelik, M., Toth, C., Brehm, A., Krssak, M., Nowotny, P., Wolzt, M., Waldhausl, W. and Roden, M. (2007) 'Muscle mitochondrial ATP synthesis and glucose transport/phosphorylation in type 2 diabetes', *PLoS Medicine*, 4(5), pp. 0858–0867. doi: 10.1371/journal.pmed.0040154.

Takahama, U., Ansai, T. and Hirota, S. (2013) *Advances in Molecular Toxicology: Nitrogen Oxides Toxicology of the Aerodigestive Tract.* 7th edn. Elsevier Inc.

Tan, R., Wylie, L. J., Thompson, C., Blackwell, J. R., Bailey, S. J., Vanhatalo, A. and Jones, A. M. (2018) 'Beetroot juice ingestion during prolonged moderate-intensity exercise attenuates progressive rise in O2 uptake', *Journal of Applied Physiology*, 124(5), pp. 1254–1263. doi: 10.1152/japplphysiol.01006.2017.

Technologies, A. (2018) 'Agilent Seahorse XF Buffer Factor Protocol Quick Reference

Guide'.

Teslaa, T. and Teitell, M. A. (2014) 'Techniques to monitor glycolysis', *Methods in Enzymology*, 542, pp. 91–114. doi: 10.1016/B978-0-12-416618-9.00005-4.

Thompson, C., Vanhatalo, A., Jell, H., Fulford, J., Carter, J., Nyman, L., Bailey, S. J. and Jones, A. M. (2016) 'Dietary nitrate supplementation improves sprint and high-intensity intermittent running performance', *Nitric Oxide - Biology and Chemistry*, 61(3), pp. 55–61. doi: 10.1016/j.niox.2016.10.006.

Thompson, C., Wylie, L. J., Blackwell, J. R., Fulford, J., Black, M. I., Kelly, J., McDonagh, S. T. J., Carter, J., Bailey, S. J., Vanhatalo, A. and Jones, A. M. (2017) 'Influence of dietary nitrate supplementation on physiological and muscle metabolic adaptations to sprint interval training', *Journal of Applied Physiology*, 122(3), pp. 642–652. doi: 10.1152/japplphysiol.00909.2016.

Thorens, B. and Mueckler, M. (2014) 'The SLC2 (GLUT) Family of Membrane Transporters', *Molecular Aspects of Medicine*, 34(0), pp. 121–138. doi: 10.1016/j.biotechadv.2011.08.021.Secreted.

Toime, L. J. and Brand, M. D. (2010) 'Uncoupling protein-3 lowers reactive oxygen species production in isolated mitochondria', *Free Radical Biology and Medicine*, 49(4), pp. 606–611. doi: 10.1016/j.freeradbiomed.2010.05.010.

Tong, P., Khayat, Z. A., Huang, C., Patel, N., Ueyama, A. and Klip, A. (2001) 'Insulin-induced cortical actin remodeling promotes GLUT4 insertion at muscle cell membrane ruffles', 108(3), pp. 371–381. doi: 10.1172/JCI200112348.Introduction.

Totzeck, M., Schicho, A., Stock, P., Kelm, M., Rassaf, T. and Hendgen-Cotta, U. B. (2014) 'Nitrite circumvents canonical cGMP signaling to enhance proliferation of myocyte precursor cells', *Molecular and Cellular Biochemistry*, 401(1–2), pp. 175–183. doi: 10.1007/s11010-014-2305-y.

Tripathi, Parul, Tripathi, Prashant, Kashyap, L. and Singh, V. (2007) 'The role of nitric oxide in inflammatory reactions', *FEMS Immunology and Medical Microbiology*, 51(3), pp. 443–452. doi: 10.1111/j.1574-695X.2007.00329.x.

Tsakiridis, T., Vranic, M. and Klip, A. (1994) 'Disassembly of the actin network inhibits insulin-dependent stimulation of glucose transport and prevents recruitment of glucose transporters to the plasma membrane', *Journal of Biological Chemistry*, 269(47), pp. 29934–29942.

Tunduguru, R. and Thurmond, D. C. (2017) 'Promoting glucose transporter-4 vesicle trafficking along cytoskeletal tracks: PAK-ing them out', *Frontiers in Endocrinology*, 8(NOV), pp. 1–15. doi: 10.3389/fendo.2017.00329.

Ueyama, A., Yaworsky, K. L., Wang, Q., Ebina, Y., Klip, A., Yaworsky, K. L., Wang, Q., Ebina, Y. and Glut-myc, A. K. (1999) 'GLUT-4myc ectopic expression in L6 myoblasts generates a GLUT-4-specific pool conferring insulin sensitivity', *The American Journal of Physiology: Endocrinology and Metabolism*, 277, pp. 572–578.

Vandoorne, T. *et al.* (2019) 'Differentiation but not ALS mutations in FUS rewires motor neuron metabolism', *Nature Communications*, 10(1). doi: 10.1038/s41467-019-12099-4.

Vanhatalo, A., Bailey, S., Blackwell, J., DiMenna, F., Pavey, T., Wilkerson, D.,

Benjamin, N., Winyard, P. and Jones, A. (2010) 'Acute and chronic effects of dietary nitrate supplementation on blood pressure and the physiological responses to moderate-intensity and incremental exercise .', *Am J Physiol Regul Integr Comp Physiol.*, 299(4), pp. R1121-31. doi: 10.1152/ajpregu.00206.2010.

Vanhatalo, A., Fulford, J., Bailey, S. J., Blackwell, J. R., Winyard, P. G. and Jones, A. M. (2011) 'Dietary nitrate reduces muscle metabolic perturbation and improves exercise tolerance in hypoxia', *Journal of Physiology*, 589(22), pp. 5517–5528. doi: 10.1113/jphysiol.2011.216341.

Vaughan, R. A., Gannon, N. P. and Carriker, C. R. (2016) 'Nitrate-containing beetroot enhances myocyte metabolism and mitochondrial content', *Journal of Traditional and Complementary Medicine*, 6(1), pp. 17–22. doi: 10.1016/j.jtcme.2014.11.033.

Veech, R. L., Lawson, J. W., Cornell, N. W. and Krebs, H. A. (1979) 'Cytosolic phosphorylation potential.', *Journal of Biological Chemistry*, 254(14), pp. 6538–6547.

Wahrmann, J. P., Recouvreur, M. and Favard-Sereno, C. (1977) 'Development and regulation of the phosphorylase-glycogen complex in myogenic cells of the L6 line', *Journal of Cell Science*, Vol. 26, pp. 77–91.

Webster, K. A. (2003) 'Evolution of the coordinate regulation of glycolytic enzyme genes by hypoxia', *Journal of Experimental Biology*, 206(17), pp. 2911–2922. doi: 10.1242/jeb.00516.

Westerblad, H., Bruton, J. D. and Katz, A. (2010) 'Skeletal muscle: Energy metabolism, fiber types, fatigue and adaptability', *Experimental Cell Research*, 316(18), pp. 3093–3099. doi: 10.1016/j.yexcr.2010.05.019.

Whitfield, J., Gamu, D., Heigenhauser, G. J. F., Van Loon, L. J. C., Spriet, L. L., Tupling, A. R. and Holloway, G. P. (2017) 'Beetroot juice increases human muscle force without changing Ca2+-handling proteins', *Medicine and Science in Sports and Exercise*, 49(10), pp. 2016–2024. doi: 10.1249/MSS.0000000000001321.

Whitfield, J., Ludzki, A., Heigenhauser, G. J. F., Senden, J. M. G., Verdijk, L. B., van Loon, L. J. C., Spriet, L. L. and Holloway, G. P. (2016) 'Beetroot juice supplementation reduces whole body oxygen consumption but does not improve indices of mitochondrial efficiency in human skeletal muscle', *Journal of Physiology*, 594(2), pp. 421–435. doi: 10.1113/JP270844.

Wickham, K. A., McCarthy, D. G., Pereira, J. M., Cervone, D. T., Verdijk, L. B., van Loon, L. J. C., Power, G. A. and Spriet, L. L. (2019) 'No effect of beetroot juice supplementation on exercise economy and performance in recreationally active females despite increased torque production', *Physiological Reports*, 7(2), pp. 1–14. doi: 10.14814/phy2.13982.

Wylie, L. J., Bailey, S. J., Kelly, J., Blackwell, J. R., Vanhatalo, A. and Jones, A. M. (2016) 'Influence of beetroot juice supplementation on intermittent exercise performance', *European Journal of Applied Physiology*, 116(2), pp. 415–425. doi: 10.1007/s00421-015-3296-4.

Wylie, L. J., Park, J. W., Vanhatalo, A., Kadach, S., Black, M. I., Stoyanov, Z., Schechter, A. N., Jones, A. M. and Piknova, B. (2019) 'Human skeletal muscle nitrate store: influence of dietary nitrate supplementation and exercise', *Journal of Physiology*, 597(23), pp. 5565–5576. doi: 10.1113/JP278076.

Yamamoto, N., Kawasaki, K., Kawabata, K. and Ashida, H. (2010) 'An enzymatic fluorimetric assay to quantitate 2-deoxyglucose and 2-deoxyglucose-6-phosphate for in vitro and in vivo use', *Analytical Biochemistry*, 404(2), pp. 238–240. doi: 10.1016/j.ab.2010.05.012.

Yamamoto, N., Sato, T., Kawasaki, K., Murosaki, S. and Yamamoto, Y. (2006) 'A nonradioisotope, enzymatic assay for 2-deoxyglucose uptake in L6 skeletal muscle cells cultured in a 96-well microplate', *Analytical Biochemistry*, 351(1), pp. 139–145. doi: 10.1016/j.ab.2005.12.011.

Yang, C., Aye, C. C., Li, X., Diaz Ramos, A., Zorzano, A. and Mora, S. (2012) 'Mitochondrial dysfunction in insulin resistance: Differential contributions of chronic insulin and saturated fatty acid exposure in muscle cells', *Bioscience Reports*, 32(5), pp. 465–478. doi: 10.1042/BSR20120034.

Ziman, A. P., Ward, C. W., Rodney, G. G., Lederer, W. J. and Bloch, R. J. (2010) 'Quantitative measurement of Ca2+ in the sarcoplasmic reticulum lumen of mammalian skeletal muscle', *Biophysical Journal*, 99(8), pp. 2705–2714. doi: 10.1016/j.bpj.2010.08.032.